



Conference Series
Advances in Nonlinear Science

Scientific Heritage of Sergey A. Chaplygin

*Nonholonomic Mechanics,
Vortex Structures and Hydrodynamics*

Book of Abstracts

2–6 June 2019
Cheboksary, Russia

Chuvash State University
Moscow Institute of Physics and Technology
Steklov Mathematical Institute of RAS
University Innopolis
Russian Foundation for Basic Research
Institute of Computer Science
Journal “Regular and Chaotic Dynamics”
Russian Journal of Nonlinear Dynamics

The International Conference “Scientific Heritage of Sergey A. Chaplygin (Nonholonomic Mechanics, Vortex Structures and Hydrodynamics)” is being held under the auspices of the Russian Foundation for Basic Research (project No. 19-01-20086).

ANS Conference Series: Scientific Heritage of Sergey A. Chaplygin (Nonholonomic Mechanics, Vortex Structures and Hydrodynamics) : Book of Abstracts. — Moscow–Izhevsk : Institute of Computer Science, 2019. — 212 p.

SCIENTIFIC COMMITTEE

Chair: *Valery Kozlov*, Steklov Mathematical Institute of RAS, Russia

Vice-chair: *Alexey Borisov*, Moscow Institute of Physics and Technology, Russia

Jan Awrejcewicz, Lodz University of Technology, Poland

Luis García Naranjo, Institute for Research in Applied Mathematics and Systems, UNAM, Mexico

Alexander Ivanitsky, Chuvash State University, Cheboksary, Russia

Alexandr Klimchik, Innopolis University, Russia

Viktor Kazantsev, Lobachevski State University, Nizhni Novgorod, Russia

Ivan Mamaev, Udmurt State University, Izhevsk, Russia

Andrzej Maciejewski, University of Zielona Góra, Poland

Sergey Kuznetsov, Kotel'nikov's Institute of Radio-Engineering and Electronics of RAS, Russia

Grigory Osipov, Lobachevski State University, Nizhni Novgorod, Russia

Yuri Sachkov, Program Systems Institute of RAS, Russia

Iskander Taimanov, Novosibirsk State University, Russia

Alexey Terentyev, Chuvash State University, Cheboksary, Russia

Dmitry Treschev, V. A. Steklov Mathematical Institute of RAS, Russia

Andrey Tsiganov, Saint Petersburg State University, Russia

ORGANIZING COMMITTEE

Chair: *Andrey Alexandrov*, Chuvash State University, Cheboksary, Russia

Alexey Borisov, Moscow Institute of Physics and Technology, Russia

Ivan Mamaev, Izhevsk Technical State University, Izhevsk, Russia

Alexander Ivanitsky, Chuvash State University, Cheboksary, Russia

Daria Troeshestova, Chuvash State University, Cheboksary, Russia

CONTACTS OF PERSON IN CHARGE

Daria Troeshestova, chapconf@yandex.ru

Tel.: +7 (8352) 45-00-91

Tel./WhatsApp: +7 (917) 650-04-33

Telegram: +7 (919) 976-92-88



Sergey A. Chaplygin (1869–1942)

CONTENTS

Anani Adabrah, Vladimir Dragovic, Milena Radnovic Elliptical Billiards in the Minkowski plane and Extremal Polynomials	13
Alain Albouy Transformation of the equations of dynamics	14
Виктор В. Алексеев, Сергей А. Васильев, Сергей И. Чучкалов Движение плоскости в вязкой высокодисперсной среде, не насыщенной жидкостью	15
Anna I. Allilueva Evolution of Lagrangian manifolds and asymptotic solutions to the linearized equations of gas dynamics	16
Vsevolod V. Andreev Study of the boundary layer near outer surface of the porous catalyst pellet during the reaction-diffusion process in it	17
Дарья А. Ануфриева, Виктор С. Абриков, Александр Н. Лукин, Charlie Oommen, V. R. Sanalkumar and Nichith Chandrasekaran Обобщенные многофакторные вычислительные модели детонации конденсированных и газовых систем	18
Andrey A. Ardentov Hidden Maxwell stratum in Euler's elastica problem	20
Elizaveta M. Artemova, Alexander A. Kilin Dynamics of vortex lattices	21
Boris S. Bardin On orbital stability of periodic motions of a heavy rigid body with a fixed point in the Hess case	25
Ivan A. Bizyaev, Alexey V. Borisov and Ivan S. Mamaev Dynamic of nonholonomic Suslov problem under periodic control: unbounded speed-up and strange attractors	26
Sergey V. Bolotin Jumps of energy near a separatrix in slowly time dependent Hamiltonian systems	28
Alexey V. Bolsinov, Jinrong Bao A note about integrable systems on low dimensional Lie groups and Lie algebras	29

Alexey V. Borisov, Tatiana B. Ivanova, Alexander A. Kilin, Ivan S. Mamaev	
Dynamics of a ball on a rotating cone	30
Alexey V. Borisov, Alexander A. Kilin, Ivan S. Mamaev	
Motion of a Particle on the Surface of a Rotating Paraboloid in the Presence of Friction Forces	34
Andrey V. Borisov, Ivan E. Kaspirovich, Robert G. Mukharlyamov	
Dynamics control of nonholonomic system modelling motion of skier and snowboarder	37
Anastasios Bountis, Yannis Kominis, Joniald Shena, Vassilios Kovanis	
Limit cycles and resonances in asymmetric laser dimers: new oscillatory phenomena in photonic arrays	40
Pavol Božek	
Controlling of DC motor robots via INS	42
Evgeniya A. Chekina, Boris S. Bardin	
The orbital stability analysis of planar rotations of a satellite in a circular orbit at the boundaries of a domain of stability in linear approximation	45
Елена Г. Ефимова, Александр Я. Корнилов	
Кавитационное обтекание нескольких пластинок	48
Kirill S. Efremov, Andrey A. Ardentov, Yury L. Karavaev	
Experimental studies of the movement of a mobile wheeled robot along optimal trajectories	49
Gennadiy A. Fedoreyev, Alexander S. Znatkov	
High-speed transport system “Ekranoflot-Chuvashia”	52
Gennadiy A. Fedoreyev, Alexander Yu. Zhurenko, Konstantin V. Gribov, Dmitry V. Nazarov, Sergey M. Krivel, Egor A. Galushko	
WIG – transformer for effective logistics in far east and arctic . . .	53
Sergey D. Glyzin, Andrey Yu. Kolesov, Nikolay K. Rozov	
On some sufficient conditions for hyperbolicity and topological mixing	55
Borislav Gajić, Božidar Jovanović	
Connections and Time Reperametrizations in Nonholonomic Mechanics	58

Luis C. García-Naranjo	
The problem of general multi-dimensional rigid bodies rolling on the plane	61
Rene Hartansky, Jaroslav Hricko, Martin Mierka and Michal Dzuris	
MEMS Sensor of Force	62
Yehor S. Hladkov, Evgeny V. Vetchanin	
Dynamics of toroidal bodies in a fluid	64
Jaroslav Hricko, Stefan Havlik, Rene Hartansky	
Verifying the Performance Characteristics of the (micro) Robotic Devices	66
Alexander Yu. Ivanitskiy, Fedor P. Vasilyev, Vladimir V. Ejov	
The residual method for solving ill-posed system of algebraic inequalities and linear programming problems with approximate data	69
Božidar Jovanović, Borislav Gajić	
Two integrable models of rolling balls over a sphere	71
Alexander A. Karabanov, Albert D. Morozov	
On resonances in Hamiltonian systems with three degrees of freedom	72
Yury L. Karavaev, Alexander A. Kilin	
The dynamics of a spherical robot of the combined type by periodic control actions	73
Yury L. Karavaev, Kirill S. Efremov, Ivan S. Zvonarev	
Experimental evaluation of mobile wheeled robot control using artificial neural network	75
Tatiana V. Kartuzova, Alevtina G. Kulagina, Lyudmila V. Seliverstova	
Numerical research of flow of profiles system near screen	77
Alexandra A. Kashchenko	
Non-rough cycles in a model of two delayed oscillators	78
Iliia S. Kashchenko	
Asymptotic of spatially inhomogeneous solutions of the system with a space deviation	80
Anastasia O. Kazakova	
Generalization of the Joukowski-Chaplygin solution of the plane hydrodynamic problem in eccentric ring	82

Anastasia O. Kazakova, Evgenia A. Mikishanina	
Numerical solution of the boundary value problems for the Poisson's equation in the plane domain	85
Olga V. Kholostova	
Nonlinear stability analysis of relative equilibriums of a solid carrying a movable point mass in the central gravitational field . . .	88
Alexander A. Kilin, Elena N. Pivovarova	
Topological Analysis and Absolute Dynamics of the Nonholonomic Rolling of a Rubber Wheel with Sharp Edges	90
Mikhail V. Kiselev	
Appearance of working memory mechanism in self-organizing liquid state machine	93
Anton V. Klekovkin, Evgeny V. Vetchanin, Ivan S. Mamaev	
A dynamic study of screwless fish-like robot with internal rotor . . .	96
Ivan F. Kobtsev	
Chaplygin parabolic pendulum problem: Liouville equivalence invariants	99
Alexander Ja. Kornilov, Alevtina G. Kulagina, Ildus Ju. Jusupov, Dmitry V. Bobin	
The flow around a thin profile with perforated contour lines	101
Ivan K. Kozlov	
About realization of Jordan-Kronecker invariants of Lie algebras . . .	103
Sergey P. Kuznetsov, Vyacheslav P. Kruglov, Yulia V. Sedova	
Mechanical systems with hyperbolic chaotic attractors based on Froude pendulums	106
Vyacheslav P. Kruglov, Sergey P. Kuznetsov	
Dynamics of phases and chaos in lattices of locally coupled conservative or dissipative oscillators	109
Grzegorz Kudra, Jan Awrejcewicz	
Modelling and dynamics of rigid body systems with 3D frictional and impact contacts	112
Nikolay A. Kudryashov	
Traveling wave solutions of some mathematical models for description of propagation pulses in optical fibers	114

Leonid G. Kurakin, Irina V. Ostrovskaya	
On the stability of discrete vortex structures in two-layer rotating fluid and in homogeneous fluid	115
Leonid G. Kurakin, Irina A. Lysenko	
On stability of orbit and invariant set of Thomson's vortex polygon in two-fluid plasma	117
Leonid G. Kurakin, Aik V. Kurdoglyan	
Semi-invariant form of equilibrium stability criteria for systems with one or two cosymmetries	119
Valentina V. Kuritsyina, Tatiana V. Mitrofanova, Tatiana N. Smirnova	
Application of boundary element techniques to the solution of tasks of hydrodynamics	120
Victor V. Kuzenov, Sergei V. Ryzhkov	
Mathematical modeling of plasma dynamics for processes in capillary discharges	121
Sergey P. Kuznetsov	
Complex dynamics in generalizations of the Chaplygin sleigh	124
Sergey P. Kuznetsov	
Some lattice models with hyperbolic chaotic attractors	127
Nikolay V. Kuznetsov, Timur N. Mokaev	
Theory of hidden oscillations	130
Sergey P. Kuznetsov, Vladimir V. Mochalov, Vasiliy P. Chuev	
On Pauli's theorem in Clifford algebra $R_{p,q}$	133
Dmitry S. Loginov	
Analysis of bifurcations at varying boundary conditions in a logistic equation with delay and diffusion	136
Andrzej J. Maciejewski, Maria Przybylska	
Integrability analysis of constrained Euler equation on six di- mensional Lie algebras	138
Ivan S. Mamaev, Ivan A. Bizyaev, Alexey V. Borisov	
Dynamics of a Chaplygin sleigh with an unbalanced rotor	139
Ivan S. Mamaev, Evgeny V. Vetchanin	
The motion of foils in a fluid due to periodical excitations	142
Anatoly P. Markeev	
On periodic motions of sympathetic pendulums at resonance in forced oscillations	144

Elena A. Marushkina	
Local dynamics of a pair of Hutchinson equations with competitive and diffusion interaction	147
Alexey R. Mashtakov	
Sub-Riemannian Geometry in Image Processing and Modelling of Human Visual System	149
Evgenia A. Mikishanina	
The solution of dynamic problems of filtration consolidation in a rectangular area and the area representing the band, in the formulation of V. A. Florin	151
Alexander A. Nazarov	
Superposition method in computer simulation of multi-agent systems and its supercomputer implementation	153
Vladimir I. Nekorkin	
Cloning of chimera states in a multiplex network of relaxation bistable oscillators	154
Stanislav S. Nikolaienko	
Topological invariants for the Chaplygin-Goryachev integrable case with non-compact Liouville foliations	155
Alexey V. Nozdrin, Yury L. Karavaev, Sergey V. Sokolov	
Design features and control of a Spherical Robot of pendulum-type	156
Alexander G. Petrov	
Saturation free numerical scheme for computing the flow past a lattice of airfoils with sharp edge	158
Vladimir N. Pichugin	
Modeling and analysis of dynamic systems in robotics polygon meshes	161
Alexey V. Podobryaev	
Symmetric extremal trajectories in left-invariant optimal control problems	163
Ivan Yu. Polekhin	
Precession of the Kovalevskaya and Goryachev-Chaplygin tops	166
Maria Przybylska, Stefan Rauch-Wojciechowski	
Dynamics of rolling and sliding rigid bodies	168
Aleksandrina Yu. Rembovskaya	
Symplectic classification of spherical 2-atoms	169

Pavel E. Ryabov, Artemiy A. Shadrin	
Bifurcation Diagram and its Visualization in the One Generalized Integrable Model of Vortex Dynamics	170
Yury L. Sachkov, Elena F. Sachkova	
Abnormal extremals in (2, 3, 5, 8) sub-Riemannian problem	173
Aleksandr V. Sakharov	
Dynamics of a point in the axisymmetric potential of a massive fixed ring and center	174
Andrei I. Shafarevich	
Hamiltonian systems and Lagrangian manifolds, corresponding to linearized equations of relativistic hydrodynamics	176
Vyacheslav A. Shestakov, Kirill S. Efremov, Yury L. Karavaev	
Experimental investigations of the control algorithm of a mobile manipulation robot on a highly maneuverable platform with omniwheels	177
Vyacheslav V. Shumaev	
Estimation of azimuthal instabilities under the joint action of laser radiation and a magnetic field on a plasma	179
Nikolai I. Sidnyaev, Vladimir U. Loginov	
On the Influence of the Pressure Gradient on the Electron Concentration in the Wake of Descent Spacecraft	182
Марина Е. Сироткина, Елена Г. Ефимова, Евгения В. Володина	
Численные исследования предельного сопротивления остроугольного анизотропного клина сдвигу и отрыву	184
Sergei V. Sokolov	
Bifurcation Diagram For Two Vortices of Opposite Signs in Trapped Bose–Einstein Condensate	185
Gennady M. Sorokin, Tatiana G. Terekhova	
The investigation of whirlwind in stability of the plasmoid above the water surface	186
George A. Sukhov	
Bifurcation analysis of periodic motions originating from hyperboloidal precession of a dynamically symmetric satellite	187
Seyed Amir Tafrishi, Mikhail Svinin, Esmaeil Esmaeilzadeh, Motoji Yamamoto	

Modeling and Motion Analysis of a Fluid Actuated Spherical Rolling Robot	190
Alexey G. Terentyev, Nikolay A. Fedorov	
Numerical solution of the problem of flow around flexible arcs . . .	192
Stepan S. Troeshestov, Vladimir A. Aliev, Anton E. Mashikhin, Sergey I. Nikolenko	
AI Driving Olympics challenge: reinforcement learning approach solving line following task	195
Daria A. Troeshestova, Victor S. Abrukov, Michael V. Kiselev, Nichith Chandrasekaran	
Artificial neural networks for creation of energetic materials genome	197
Andrey V. Tsiganov	
Integrable systems with algebraic first integrals	199
Olga V. Vasilyeva, Sergey I. Ksenofontov, Alexander N. Lepaev	
Viscous fluid burning particles	200
Evgeny V. Vetchanin, Evgenia A. Mikishanina	
The dynamics of rigid bodies with internal mechanisms	201
Lyudmila Yu. Vorochaeva, Sergei I. Savin, Andrey V. Malchikov	
An approach moving over obstacles for a wheeled jumping robot . .	204
Lyudmila Yu. Vorochaeva, Sergei I. Savin, Andrey S. Yatsun	
An investigation of motion of a crawling robot with supports with controllable friction	207
Konstantin S. Vorushilov	
Jordan–Kronecker invariants of semidirect sums of Lie algebras . .	210
Hamad M. Yehia	
On Chaplygin’s case of the body in a liquid	211

Elliptical Billiards in the Minkowski plane and Extremal Polynomials

Anani Adabrah¹, Vladimir Dragovic^{1,2}, Milena Radnovic^{2,3}

¹ *The University of Texas at Dallas*

² *MI SANU*

³ *University of Sydney*

We derive necessary and sufficient conditions for periodic and for elliptic periodic trajectories of billiards within an ellipse in the Minkowski plane in terms of an underlining elliptic curve. Equivalent conditions are derived in terms of polynomial-functional equations as well. The corresponding polynomials are related to the classical extremal polynomials. The similarities and differences with respect to previously studied Euclidean case are indicated.

Transformation of the equations of dynamics

Alain Albouy¹

¹ *Observatoire de Paris, Paris, France*

The theory of the “Transformation of the equations of dynamics” was mainly concluded in Painlevé [1] and Thomas [2]. The subject is obviously important: to classify the transformations that send a “natural” mechanical system onto another one, the changes of time being allowed. But this theory was soon misunderstood: Whittaker [3] presents it as an exercise, of which he gives the solution... which is obviously wrong. The theory was then universally forgotten. We claim that the reasons for this bad reception are:

- A hesitation about the hypothesis: “natural” forces are they derived from a potential?
- A too complicated conclusion, unrelated with the classical examples, which are not even recalled.
- The lack of examples.

We will try to improve the situation of the three points, by also discussing a third hypothesis, by relating the conclusion with the examples, and by giving new examples.

References

- [1] Painlevé P. *Sur les transformations des équations de la dynamique*// Comptes Rendus, 1896, vol. 123, pp. 392–395.
- [2] Thomas, T. Y. *On the Transformation of the Equations of Dynamics*// Journal of mathematics and physics, 1946, vol. 25, pp. 191–208.
- [3] Whittaker, E. T. *A Treatise on the Analytical Dynamics of Particles and Rigid Bodies*. Cambridge: at the University Press, 1937, p. 261.

Движение плоскости в вязкой высокодисперсной среде, не насыщенной жидкостью

Виктор В. Алексеев¹, Сергей А. Васильев², Сергей И. Чучкалов³

¹ Чебоксарский кооперативный институт, Чебоксары, Россия

^{2,3} ЧГУ имени И.Н. Ульянова, Чебоксары, Россия

Воздействие почвообрабатывающего орудия на почву представляет собой движение твердого тела в дисперсной многофазной среде и сопровождается рядом сложных физико-механических процессов. При сильно развитой удельной поверхности дисперсной среды наблюдаются существенные отклонения от известных расчетных формул. В связи с этим предлагается решение для описания силы трения, основанное на комплексном учете вкладов, вносимых в силу трения твердой и жидкой фазами. Вклад жидкой фазы, обуславливающий эффекты налипания, определяется по основной гидрофизической характеристике (ОГХ) пористой среды [1], что позволяет учесть как пористость дисперсной среды, так и степень заполнения жидкостью порового пространства. Обобщение экспериментальных и расчетных данных [2] на основе указанного подхода приводит к выражению (1) для коэффициента трения почвы:

$$f = \alpha\Omega w^{2/3}(1 - \beta w)(1 - \Pi_0) + \gamma L, \quad (1)$$

где Ω — удельная (по объему) поверхность почвенных частиц; w — объемная влажность почвы; Π_0 — пористость сухого почвенного образца; L — липкость почвы; α , β и γ — коэффициенты.

Список литературы

- [1] Сысуев В. А. Получение основной гидрофизической характеристики почв на основе идеализированных моделей / В. А. Сысуев, И. И. Максимов, В. В. Алексеев, В. И. Максимов // Доклады Россельхозакадемии. 2013. № 5. С. 63–66.
- [2] Алексеев В. В. Гидрофизика почв в мелиорации: монография / В. В. Алексеев, И. И. Максимов. — Чебоксары: «Новое время», 2017. — 280 с.

Evolution of Lagrangian manifolds and asymptotic solutions to the linearized equations of gas dynamics

Anna I. Allilueva

Institute for Problems in Mechanics, Moscow, Russia

We study evolution of Lagrangian manifolds, corresponding to short-wave solutions of linearized equations of gas dynamics. We discuss also decomposition of the resolving operator for this system and asymptotics of the Cauchy problem with localized initial data.

Study of the boundary layer near outer surface of the porous catalyst pellet during the reaction-diffusion process in it

Vsevolod V. Andreev

Chuvash State University, Cheboksary, Russia

Catalytic reactions of arbitrary type (1), occurring in porous pellets of spherical, cylindrical and slab geometrical forms, are analyzed.

$$0 = \sum_{i=1}^n a_i^p A_i, \quad p = 1, \dots, k. \quad (1)$$

Here A_i are the symbols of substances participated in reactions (1); a_i^p are the stoichiometric coefficients (for the initial substances $a_i^p < 0$ and for the reaction products $a_i^p > 0$); the index p defines stage number in reactions (1). Reaction (1) in porous catalyst pellets is coupled by diffusion of substances A_i in the pores [1, 2]. During catalytic processes of the type (1) reagents A_i are transferred to pellets by moving of outer reaction mixture. At small distance from the pellet the reaction mixture rate decreases to zero on its outer surface. As result, the boundary layer appears. Influence of boundary layer hydrodynamics on the reaction-diffusion processes in the porous pellets is studied. Formulas, linking the reagents concentrations and temperature in the incompressible reaction mixture core with their values on pellet external surface, were obtained.

References

- [1] Andreev V. V., Vozyakov V. I., Kol'tsov N. I. The reaction mixture stream flowing around porous granules of catalyst and chemical reaction on their inner surface // *Chemical Physics Reports*, 1995. Vol. 13. No. 11. P. 1848–1860.
- [2] Andreev V. V. Formation of a “Dead Zone” in Porous Structures During Processes That Proceeding under Steady-State and Unsteady-State Conditions // *Review Journal of Chemistry*, 2013. Vol. 3. No. 3. P. 239–269.

Обобщенные многофакторные вычислительные модели детонации конденсированных и газовых систем

Дарья А. Ануфриева¹, Виктор С. Абруков¹, Александр Н. Лукин²,
Charlie Oommen³, V. R. Sanalkumar⁴ and Nichith Chandrasekaran³

¹ ЧГУ имени И.Н. Ульянова, Чебоксары, Россия

² Западно-Кавказский научный центр, Туапсе, Россия

³ Индийский институт науки, Бангалор, Индия

⁴ Технологический колледж Кумарагуру, Коимбатур, Индия

Показаны возможности применения одного из основных методов интеллектуального анализа данных — искусственных нейронных сетей [1–3] при моделировании детонации конденсированных и газовых систем [4, 5]. Созданы многофакторные вычислительные модели детонации, позволяющие решать разнообразные прямые и обратные задачи: определять зависимость скорости детонации от состава молекулы системы и ее плотности, определять, какой состав молекул систем и плотность обеспечивает требуемую скорость детонации. Показано, что искусственные нейронные сети позволяют обобщать результаты экспериментальных исследований на принципиально новом уровне.

Исполняемые модули представленных в данной работе моделей с инструкцией по их использованию размещены на сайте проекта РФФИ <http://www.wcrc.ru/Indo-Russian-JRP.html> и на страничке проекта на сайте: <https://www.researchgate.net/project/Development-of-the-Multifactorial-Computational-Models-of-the-Energetic-Materials-Combustion-and-Detonation-by-means-of-Data-Science-Methods>. Они доступны также по прямым ссылкам: <http://www.wcrc.ru/INSTRUCTION.pdf>; <http://www.wcrc.ru/DETONATION-1.rar>.

Все заинтересованные лица и организации могут их использовать для знакомства с результатами работы, приобретения опыта работы с методами интеллектуального анализа данных и проведения самостоятельных исследований с помощью данных моделей.

Работа выполнена при поддержке Департамента науки и технологий (DST), Индия и Российского фонда фундаментальных исследований (РФФИ), Россия (проект № 16-53-48010) в рамках междисциплинарного научного исследования DST-РФФИ, программа сотрудничества в рамках Гранта INT/RUS/РФФИ/IDIR/P-3/2016.

Список литературы

- [1] Abrukov V.S. et al. Creation of propellant combustion models by means of data mining tools // International Journal of Energetic Materials and Chemical Propulsion, 2010. Vol. 9, no. 5. P. 385–394.
- [2] Abrukov V.S., Valery Kochakov, Alexander Smirnov, Sergey Abrukov, Darya Anufrieva. Knowledge-Based System is a Goal and a Tool for Basic and Applied Research // Conference Proceedings of 9th International Conference on Application of Information and Communication Technologies — AICT (14–16 October 2015, Rostov-on-Don, Russia), The Institute of Electrical and Electronics Engineers, Inc., 2015, pp. 60–63.
- [3] Абриков В. С., Кочергин А. В., Ануфриева Д. А. Искусственные нейронные сети как средство обобщения экспериментальных данных // Вестник Чувашского университета, 2016, № 3. С. 155–162.
- [4] Stine J.R. On predicting properties of explosives — detonation velocity // Journal of Energetic Materials, 1990. № 8:1-2, p. 41–73.
- [5] Васильев А. А. Характеристики горения и детонации метаноугольных смесей // Физика горения и взрыва, 2013. Т. 49, № 4. С. 48–59.

Hidden Maxwell stratum in Euler's elastica problem

Andrey A. Ardentov¹

¹ *Ailamazyan Program Systems Institute of RAS, Pereslavl-Zalessky, Russia*

This investigation continues study of the classical problem on stationary configurations of an elastic rod on a plane. Length of the rod, ends of the rod and directions at the ends are fixed. The problem was first studied by Leonard Euler in 1744 [1] and it is still an open problem. Euler described a family of curves containing the solutions, which is called Euler elasticae. It is known [2] that sufficiently small pieces of Euler elasticae are optimal, i.e. they have minimum of the potential energy. In theory, the point, where an optimal curve loses its optimality, is called a cut point. Usually several optimal curves arrive to such points, so the points have multiplicity more than 1 and are called Maxwell points. Work [3] studies the symmetric case containing all solutions with multiplicity 3 and 4. An open problem is to describe explicitly solutions with multiplicity 2. This work describes them numerically. Therefore, we numerically describe the set of all cut points for the problem, i.e. the cut locus.

References

- [1] Euler L., *Methodus Inveniendi Lineas Curvas Maximi Minimive Proprietate Gaudentes, sive Solutio Problematis Isoperimetrici Latissimo Sensu Accepti*, Lausanne: Bousquet, 1744.
- [2] Sachkov Yu. L., *Maxwell Strata in the Euler Elastic Problem*, J. Dynam. Control Syst., 2008, Vol. 14, no. 2, pp. 169–234.
- [3] Ardentov A. A., *Multiple Solutions in Euler's Elastic Problem*, Automation and Remote Control, 2018, Vol. 79, Issue 7, pp. 1191–1206.

Dynamics of vortex lattices

Elizaveta M. Artemova¹, Alexander A. Kilin¹

¹ *Udmurt State University, Izhevsk, Russia*

This paper is concerned with the problem of the interaction of squared orthogonal vortex lattices, which is equivalent to the problem of the motion of point vortices on a torus. In [1] it is shown that the Hamiltonian describing N vortex lattices can be represented as

$$H = -\frac{1}{4\pi} \sum'_{k,n=1}^N \Gamma_k \Gamma_n \left(\sum_{m=-\infty}^{\infty} \ln \left(\frac{\cosh(x_k - x_n - 2\pi m) - \cos(y_k - y_n)}{\cosh(2\pi m)} \right) - \frac{(x_k - x_n)^2}{2\pi} \right), \quad (1)$$

where x_k, y_k are the coordinates of the k th vortex, and Γ_k is the strength of the k th vortex. The equations of motion of the system of N vortex lattices can be represented in Hamiltonian form and admit, in addition to the energy integral (1), two first integrals

$$Q = \sum_{k=1}^N \Gamma_k x_k, \quad P = \sum_{k=1}^N \Gamma_k y_k. \quad (2)$$

Let us consider two vortex lattices ($N = 2$) and perform a reduction of the equations of motion using the first integrals (2):

$$Q = \Gamma_1 x_1 + \Gamma_2 x_2, \quad P = \Gamma_1 y_1 + \Gamma_2 y_2, \quad \xi = x_1 - x_2, \quad \eta = y_1 - y_2. \quad (3)$$

The system obtained is 2π -periodic, i.e., the system describes the motion on a torus. The phase portrait of the reduced system taking into account periodicity is represented in Fig. 1 a). To restore the trajectory in absolute space, it is necessary to consider the phase portrait without gluing (see in Fig. 1 b)).

It can be seen from Fig. 1 that the reduced system has three fixed points and separatrix solutions connecting these points.

Further we consider the problem of the motion of three vortex lattices ($N = 3$) in the case of nonzero total strength. This problem in the case of zero total strength is integrable [2].

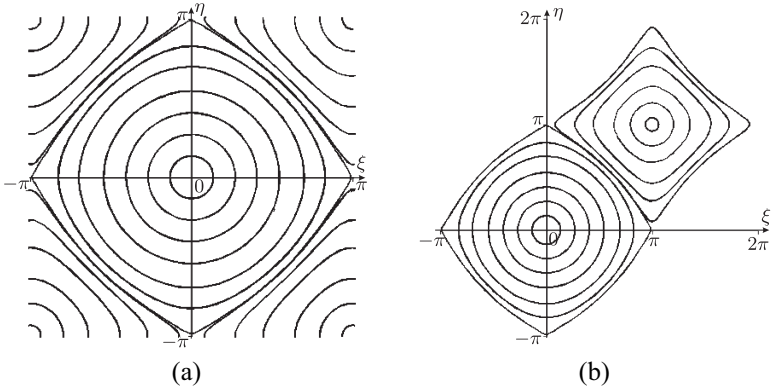


Fig. 1. Phase portrait a) with gluing b) without gluing

We perform reduction of the equations in the case considered on the level set of the first integrals Q, P . To do so, we make the following change of variables:

$$\begin{aligned} Q &= \Gamma_1 x_1 + \Gamma_2 x_2 + \Gamma_3 x_3, & \xi_1 &= x_1 - x_2, & \xi_2 &= x_2 - x_3, \\ P &= \Gamma_1 y_1 + \Gamma_2 y_2 + \Gamma_3 y_3, & \eta_1 &= y_1 - y_2, & \eta_2 &= y_2 - y_3. \end{aligned} \quad (4)$$

The equations of motion on the fixed level set of the first integrals Q, P can be represented in Hamiltonian form $\dot{\xi}_1 = \{\xi_1, H\}$, $\dot{\xi}_2 = \{\xi_2, H\}$, $\dot{\eta}_1 = \{\eta_1, H\}$, $\dot{\eta}_2 = \{\eta_2, H\}$ with the following Poisson brackets

$$\begin{aligned} \{\xi_i, \xi_j\} &= 0, \quad \{\eta_i, \eta_j\} = 0, \quad \{\xi_1, \eta_2\} = \{\xi_2, \eta_1\} = -\frac{1}{\Gamma_2}, \\ \{\xi_1, \eta_1\} &= \frac{1}{\Gamma_1} + \frac{1}{\Gamma_2}, \quad \{\xi_2, \eta_2\} = \frac{1}{\Gamma_2} + \frac{1}{\Gamma_3}. \end{aligned}$$

Poincaré maps at different values of energy $E = H(\xi_1, \xi_2, \eta_1, \eta_2)$ and the secant $\eta_1 = 0$ are shown in Fig. 2. The maps are represented on isoenergetic surfaces $E = H(\xi_1, \xi_2, \eta_1 = 0, \eta_2)$ embedded in three-dimensional space (ξ_1, ξ_2, η_2) . It can be seen from Fig. 2 that as the level set of the energy integral changes, the topological type of the section of isoenergetic surfaces can change. Also, chaotic layers are seen, which confirms non-integrability of the problem under consideration.

Let us consider the problem of the motion of four vortex lattices ($N = 4$) in the case of nonzero total strength. As in [3], it can be shown that the

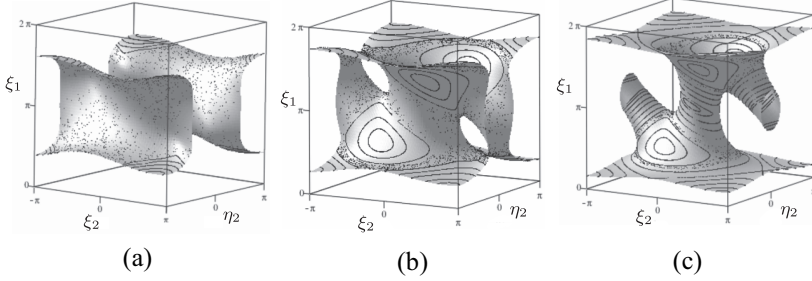


Fig. 2. Maps at a) $E = -0.25$, $\Gamma_1 = \Gamma_2 = \Gamma_3 = 1$, b) $E = -0.15$, $\Gamma_1 = \Gamma_2 = \Gamma_3 = 1$, c) $E = 0$, $\Gamma_1 = \Gamma_2 = \Gamma_3 = 1$.

equations of vortex motion on a torus admit the invariant manifold

$$x_1 - x_4 = x_2 - x_3, \quad y_1 - y_4 = y_2 - y_3. \quad (5)$$

A complete proof and reduction of equations can be found in our paper [4]. The equations in new variables can be represented as

$$\dot{\xi}_i = \{\xi_i, H(\xi_1, \xi_2, \eta_1, \eta_2)\}, \quad \dot{\eta}_i = \{\eta_i, H(\xi_1, \xi_2, \eta_1, \eta_2)\}, \quad i = 1, 2, \quad (6)$$

where H is a restriction of the Hamiltonian (1) to the invariant manifold (5) written in new variables, and the Poisson bracket has form

$$\{\xi_i, \xi_j\} = 0, \quad \{\eta_i, \eta_j\} = 0, \quad \{\xi_i, \eta_j\} = \frac{1}{2} \left(\frac{1}{\Gamma_2} + \frac{2\delta_{ij} - 1}{\Gamma_1} \right).$$

The resulting system depends on two parameters Γ_1, Γ_2 . We assume that $\Gamma_1 = 1$. This follows from an arbitrary choice of time units.

As in the problem of the motion of three vortices, we construct Poincaré maps for different values of energy $E = H(\xi_1, \xi_2, \eta_1, \eta_2)$ and the secant $\eta_1 = 0$ on the isoenergetic surfaces $E = H(\xi_1, \xi_2, \eta_1 = 0, \eta_2)$.

It can be seen from Figs. 3 that the surfaces have complex form and their type changes depending on the values of parameters E and Γ_2 . For example, the surface shown in Fig. 3 b) is a sphere with five handles. On the Poincaré maps the chaotic layers can be seen, so the system is non-integrable.

This work was supported by the RFBR under grants 18-38-00344 mol_a and 17-01-00846-a.

References

- [1] Weiss J.B., McWilliams J.C. *Nonergodicity of point vortices* // Phys. Fluids. A. 1991. V. 3(5). P. 835–844.

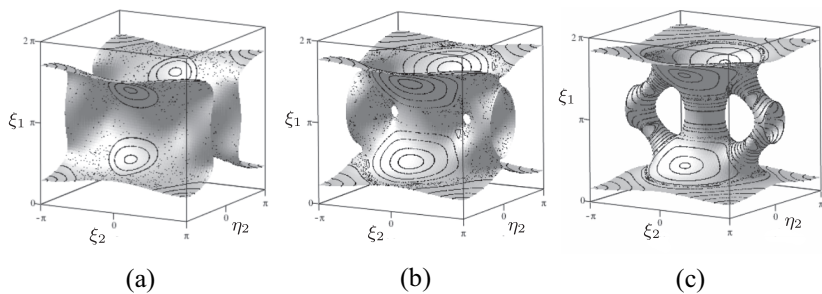


Fig. 3. Maps at a) $E = -0.35$, $\Gamma_2 = 1$, b) $E = -0.21$, $\Gamma_2 = 1$, c) $E = 0$, $\Gamma_2 = 1$

- [2] Stremler M. A., Aref H. *Motion of three point vortices in a periodic parallelogram* // J. Fluid Mech. 1999. V. 392. P. 101–128.
- [3] Borisov A. V., Mamaev I. S. *Mathematical Methods in the Dynamics of Vortex Structures*, Izhevsk: R&C Dynamics, Institute of Computer Science, 2005 (Russian). — 90 p.
- [4] Kilin A. A., Artemova E. M. *Integrability and Chaos in Vortex Lattice Dynamics* // Regular and Chaotic Dynamics, 2019, vol. 24, no. 1, pp. 101–113.

On orbital stability of periodic motions of a heavy rigid body with a fixed point in the Hess case

Boris S. Bardin

*Moscow Aviation Institute (National Research University)
Faculty of Information Technologies and Applied Mathematics
Department of Mechatronics and Theoretical Mechanics, Moscow, Russia*

We study the problem of orbital stability for pendulum-like oscillations and rotations of a rigid body with a fixed point in a uniform gravitational field. The mass geometry of the body corresponds to the Hess case. The Hamiltonian for the canonical system of equations of perturbed motion depends on three parameters. Two of them describe the mass geometry of the body and the third one parameterizes the family of the periodic orbits.

By an analytical study of the linearized system it was shown that pendulum-like rotations are orbitally unstable in the sense of Lyapunov for any values of parameters. The linear analysis of orbital stability for pendulum-like oscillations has shown that in this case the first order identical resonance takes place, that is the characteristic equation of the linearized system always has double root, which is equal to 1 for any values of parameters. It was established that in the three-dimensional space of parameters there exists two-dimensional surface, where the Jordan normal form of the monodromy matrix is diagonal. For parameters values corresponding to the above surface the pendulum-like oscillations are orbitally stable in linear approximation and outside of this surface the pendulum-like oscillations are orbitally unstable in linear approximation. We have also shown that the nonlinear problem of orbital stability for pendulum-like oscillations cannot be solve by taking into account terms of any finite order, that is the so-called transcendental case takes place. To solve the nonlinear problem of orbital stability we use the method developed in [1]. It has allowed us to prove that pendulum-like oscillations are orbitally unstable in the sense of Lyapunov.

This work was carried out at the Moscow Aviation Institute (National Research University) within the framework of the state assignment (project No 3.3858.2017/4.6).

References

- [1] Bardin B.S., *On the Stability of a Periodic Hamiltonian System with One Degree of Freedom in a Transcendental Case* // *Doklady Mathematics*, 2018, vol. 97, no. 2, pp. 161–163.

Dynamic of nonholonomic Suslov problem under periodic control: unbounded speed-up and strange attractors

Ivan A. Bizyaev¹, Alexey V. Borisov¹ and Ivan S. Mamaev²

¹ Udmurt State University,

ul. Universitetskaya 1, Izhevsk, 426034 Russia

² M. T. Kalashnikov Izhevsk State Technical University,

ul. Studencheskaya 7, Izhevsk, 426069 Russia

Consider the motion of a multicomponent mechanical system which includes:

- a *rigid body* with a fixed point, which cannot rotate in a direction e fixed relative to the body:

$$(\boldsymbol{\omega}, e) = 0, \quad (1)$$

where $\boldsymbol{\omega}$ is the angular velocity of the body.

- n *material points*, with each point P_i moving inside the rigid body according to a prescribed law of time $\mathbf{r}_i(t)$.

We make the following assumptions concerning the motion of point masses and parameters of the rigid body:

- Material points move in such a way that the moment of inertia of the system $\mathbf{I} = \text{const}$ does not depend on time and the gyrostatic momentum has the form $\mathbf{k}(t) = (0, k_2(t), k_3(t))$, where $k_2(t), k_3(t)$ are periodic functions of time with the same period T .
- The axis Ox_1 is directed along the principal axis of inertia of the system ($I_{13} = 0$):

$$\mathbf{I} = \begin{pmatrix} I_{11} & 0 & 0 \\ 0 & I_{22} & I_{23} \\ 0 & I_{23} & I_{33} \end{pmatrix}.$$

In other words, the vector e always lies in the principal plane of inertia.

In this case, the problem reduces to investigating the following reduced system, which describes the angular velocity of the rigid body:

$$\begin{aligned} \dot{u} &= -vu - K(t)v - \dot{\Lambda}(t), \\ \dot{v} &= u^2 + K(t)u, \end{aligned} \quad (2)$$

where $K(t)$ and $\Lambda(t)$ are periodic functions of time.

Numerical experiments show that in this case the following statement holds:

If the average is

$$\langle G \rangle = \frac{1}{T} \int_0^T K(t)(\dot{\Lambda}(t) - \dot{K}(t)) dt > 0, \quad (3)$$

then the system (2) exhibits trajectories that are unbounded in v and have the following asymptotics:

$$\begin{aligned} v(t) &= Ct^{\frac{1}{2}} + o(t^{\frac{1}{2}}), & u(t) &= -K(t) + o(t^{-\frac{1}{2}}), \\ C &= \sqrt{2\langle G \rangle}. \end{aligned} \quad (4)$$

If $\langle G \rangle < 0$, then there are no unbounded trajectories. The case $\langle G \rangle = 0$ requires a separate analysis.

If $\langle G \rangle < 0$, then all trajectories of the system (2) are bounded. Indeed, numerical experiments show that in this case the trajectories display the following qualitatively different behavior patterns:

1. *Stability and multistability:* as $t \rightarrow +\infty$, all trajectories tend to one or several periodic solutions of the system (2).
2. *Chaotic oscillations:* the system exhibits a strange attractor.

The work was supported by the RFBR grant no. 18-31-00344 mol_a.

Jumps of energy near a separatrix in slowly time dependent Hamiltonian systems

Sergey V. Bolotin

Moscow Steklov Mathematical Institute and University of Wisconsin

We consider natural Hamiltonian systems slowly depending on time:

$$H(q, p, \tau) = \frac{1}{2} \|p\|^2 + V_\tau(q), \quad \dot{\tau} = \epsilon \ll 1.$$

For small ϵ the energy $E(t) = H(q(t), p(t), \tau(t))$ changes slowly. For one degree of freedom, when level curves $H(\cdot, \cdot, \tau) = E$ of the frozen Hamiltonian are closed curves, there is an adiabatic invariant $I(\tau, E)$ which changes much slower than energy. Then the energy changes gradually with (τ, E) following a level curve of $I(\tau, E)$. Neishtadt [1] showed that the adiabatic invariant is destroyed for trajectories passing near a figure eight separatrix of a hyperbolic equilibrium: generically the energy will have quasi-random jumps of order ϵ with frequency of order $1/|\ln \epsilon|$.

We partly extend Neishtadt's result to multidimensional systems. Suppose that V_τ has a nondegenerate maximum at q_τ . If the configuration space is compact, there always exist homoclinic orbits to q_τ . Under certain conditions we construct trajectories which have prescribed jumps of energy of order ϵ with frequency $1/|\ln \epsilon|$ while staying distance of order ϵ away from the homoclinic set. The proofs are based on a generalization of the method of anti-integrable limit [2].

Gelfreigh and Turayev [3] showed that if the frozen system has compact uniformly hyperbolic chaotic invariant sets on energy levels, then generically there exist trajectories with energy having quasirandom jumps of order ϵ with frequency of order 1. However, this result does not work near a homoclinic set of an equilibrium since there is no uniform hyperbolicity.

References

- [1] Neishtadt A. I. *Passage through a separatrix in a resonance problem with a slowly-varying parameter*. // J. Appl. Math. Mech. 1975, vol. 39, pp. 594–605.
- [2] Bolotin S. V., Treschev D. V. *Anti-integrable limit* // Russian Math. Surveys, 2015, vol. 70, pp. 975–1030.
- [3] Gelfreich V., Turaev D. *Unbounded energy growth in Hamiltonian systems with a slowly varying parameter* // Comm. Math. Phys., 2008, vol. 283, pp. 769–794.

A note about integrable systems on low dimensional Lie groups and Lie algebras

Alexey V. Bolsinov^{1,2}, Jinrong Bao¹

¹ *School of Mathematics, Loughborough University, LE11 3TU, UK*

² *Faculty of Mechanics and Mathematics, Moscow State University, 11992, Russia*

The goal of the paper is to explain why any left-invariant Hamiltonian system on (the cotangent bundle of) a 3-dimensional Lie group G is Liouville integrable. We derive this property from the fact that the coadjoint orbits of G are two-dimensional so that the integrability of left-invariant systems is a common property of all such groups regardless their dimension.

We also give normal forms for left-invariant Riemannian and sub-Riemannian metrics on 3-dimensional Lie groups focusing on the case of solvable groups, as the cases of $SO(3)$ and $SL(2)$ have been already extensively studied. Our description is explicit and is given in global coordinates on G which allows one to easily obtain parametric equations of geodesics in quadratures.

Dynamics of a ball on a rotating cone

Alexey V. Borisov^{1,2}, Tatiana B. Ivanova², Alexander A. Kilin^{1,2},
Ivan S. Mamaev¹

¹ *Moscow Institute of Physics and Technology, Dolgoprudny, Russia*

² *Udmurt State University, Izhevsk, Russia*

This paper investigates the motion of a completely dynamically symmetric (in particular, homogeneous) ball rolling without slipping on a cone. The cone rotates uniformly about its symmetry axis.

The dimensionless equations of motion of the ball relative to the moving coordinate system (which rotates with angular velocity Ω relative to vertical fixed axis) have a following form

$$\begin{aligned} \tilde{\mathbf{J}}\dot{\boldsymbol{\omega}} &= k\boldsymbol{\omega} \times \boldsymbol{\Omega} + (\boldsymbol{\gamma}, \boldsymbol{\omega})\dot{\boldsymbol{\gamma}} - 2(\boldsymbol{\gamma}, \boldsymbol{\Omega})\boldsymbol{\gamma} \times \boldsymbol{\omega} + \Omega^2\boldsymbol{\gamma} \times \mathbf{r} - \\ &\quad - (\boldsymbol{\Omega}, \mathbf{r})\boldsymbol{\gamma} \times \boldsymbol{\Omega} + \boldsymbol{\gamma} \times \mathbf{e}_3 + \mathbf{M}_f, \\ \dot{\rho} &= \sin\theta(\omega_2 \cos\varphi - \omega_1 \sin\varphi), \\ \rho\dot{\varphi} &= -\sin\theta(\omega_1 \cos\varphi + \omega_2 \sin\varphi) - \omega_3 \cos\theta. \end{aligned} \quad (1)$$

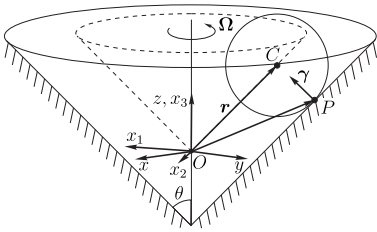


Fig. 1. The ball on a rotating cone

where $\tilde{\mathbf{J}} = (k + 1)\mathbf{E} - \boldsymbol{\gamma} \otimes \boldsymbol{\gamma}$, $k = I/(mR^2)$, m and I are the mass and the moment of inertia of the ball, $\boldsymbol{\Omega} = (0, 0, \Omega)$ is the angular velocity of a cone, $\boldsymbol{\omega}$ is the angular velocity of the ball, R is the radius of the ball, $\boldsymbol{\gamma}$ is the normal at the point of contact, $\mathbf{r} = (\rho \cos\varphi, \rho \sin\varphi, \rho/\tan\theta)$ is the radius vector of the center of mass of the ball, $\mathbf{e}_3 = (0, 0, 1)$, $\theta \in [0, \pi/2)$ is the constant apex angle of the cone.

We investigate two cases of the system (1).

1. In one of cases we assume the existence of a non-holonomic constraint corresponding to the absence of slipping at the point of contact, without friction ($\mathbf{M}_f = 0$).

The system possesses the Jacobi integral [3], which has the meaning of generalized energy:

$$E = \frac{1}{2}(\boldsymbol{\omega}, \tilde{\mathbf{J}}\boldsymbol{\omega}) + V(\mathbf{r}), \quad V(\mathbf{r}) = -\frac{\Omega^2 \rho^2}{2} + \frac{\rho}{\tan\theta}. \quad (2)$$

In [4], two additional integrals linear in angular velocities were found for the system of interest:

$$\begin{aligned} F_1 &= \omega_3 - \frac{\Omega \cos \theta}{k+1} \rho, \\ F_2 &= \rho \left(\omega_1 \cos \varphi + \omega_2 \sin \varphi + \frac{\omega_3}{\tan \theta} \right) - \frac{\rho^2 (k+2)\Omega}{2(k+1) \sin \theta}. \end{aligned} \quad (3)$$

Thus, the rolling of the ball on the surface of the cone is described by a system of five differential equations (1). The system possesses three integrals of motion (2), (3) and an invariant measure. Therefore, in this case *the system is integrable and can be reduced to quadratures* according to the Euler–Jacobi theorem [1].

On the level set of first integrals $F_1 = \kappa_1, F_2 = \kappa_2, E = h + U_0(\kappa_1, \kappa_2)$ quadratures have a following form:

$$\dot{\rho}^2 = \frac{2 \sin^2 \theta}{k+1} (h - U_\kappa(\rho)), \quad \dot{\varphi} = -\frac{(k+2)\Omega}{2(k+1)} - \frac{\kappa_2 \sin \theta}{\rho^2}, \quad (4)$$

where $U_\kappa(\rho)$ is the effective potential energy whose minima (maxima) correspond to stable (unstable) periodic solutions of the system

$$\begin{aligned} U_\kappa(\rho) &= \frac{\Omega^2 k^2 (\sin^2 \theta + k)}{8(k+1)^2 \sin^2 \theta} \rho^2 - \frac{\cos \theta (\Omega k^2 \kappa_1 - 2(k+1) \sin \theta)}{2(k+1) \sin^2 \theta} \rho - \\ &\quad - \frac{k \kappa_1 \kappa_2 \cos \theta}{\rho \sin \theta} + \frac{(\sin^2 \theta + k) \kappa_2^2}{2\rho^2}. \end{aligned} \quad (5)$$

To define possible types of motion we construct the bifurcation surface in the space (κ_1, κ_2, h) (for example, see Fig. 2).

When $\kappa_1 > \kappa_1^*$ (κ_1^* is the bifurcation point), there exist three fixed points, two of which are stable and correspond to minima of $U_\kappa(\rho)$ (see Fig. 2b).

2. In the second case, the ball is acted upon by the rolling friction torque which linearly depends on the velocity:

$$\mathbf{M}_f = -\alpha \boldsymbol{\omega}, \quad \alpha = \text{const.}$$

It was shown in [2] that the trajectory of a ball moving on a plane under the action of a constant external force and the friction torque \mathbf{M}_f is an untwisting spiral. On a cone ball can depending on the initial conditions, either move in an untwisting trajectory (the value of ρ and the height increase in this case) or approach the vertex of the cone (the value of ρ and the height decrease).

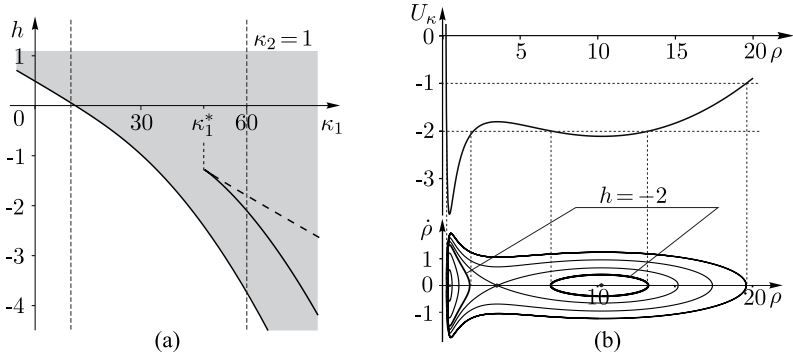


Fig. 2. (a) Section of the bifurcation surface for $\kappa_2 = 1$. (b) Effective potential energy, the relevant phase portraits of the system (4) on a level set of the integrals $\kappa_1 = 60, \kappa_2 = 1, h = -2$

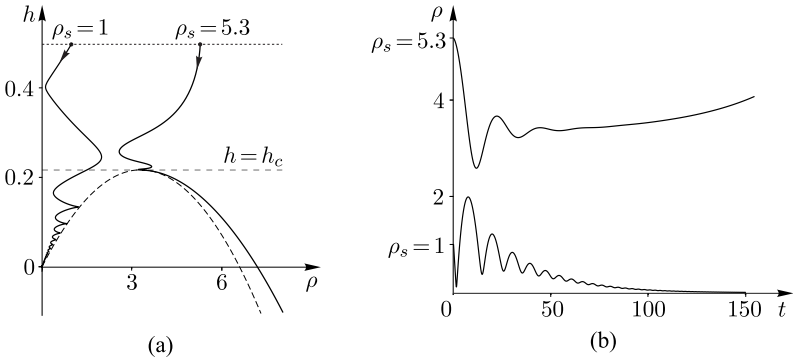


Fig. 3. (a) Projections of the phase trajectories of the system (1) onto the plane (ρ, h) and (b) graphs showing the dependence $\rho(t)$, plotted for parameters $\Omega = 0.2, \alpha = 0.1, h = 0.5, \rho_s = 1$ and $\rho_s = 5.3$

We present an analysis of the dependence of the type of terminal motion of the center of mass of the ball on initial conditions. For example, Figure 3a shows two projections of the phase trajectories of the system (1) onto the plane (ρ, h) which demonstrate different types of terminal motion for the same initial values of the level set of the energy integral. Figure 3b shows the corresponding dependences $\rho(t)$.

The work was carried out at MIPT within the framework of project 5-100 for state support for leading universities of the Russian Federation.

References

- [1] Bolsinov A. V., Borisov A. V., Mamaev I. S., *Hamiltonization of Nonholonomic Systems in the Neighborhood of Invariant Manifolds* // Regul. Chaotic Dyn., 2011, vol. 16, no. 5, pp. 443-464.
- [2] Borisov A. V., Ivanova T. B., Karavaev Y. L., Mamaev I. S., *Theoretical and experimental investigations of the rolling of a ball on a rotating plane (turntable)* // Eur. J. Phys, 2018, vol. 39, no. 6, 065001, 13 pp.
- [3] Borisov A. V., Mamaev I. S., Bizyaev I. A., *The Jacobi Integral in Nonholonomic Mechanics* // Regul. Chaotic Dyn., 2015, vol. 20, no. 3, pp. 383-400.
- [4] Borisov A. V., Mamaev I. S., Kilin A. A. *The rolling motion of a ball on a surface: New integrals and hierarchy of dynamics* // Regul. Chaotic Dyn., 2002, vol. 7, no. 2, pp. 201-219.

Motion of a Particle on the Surface of a Rotating Paraboloid in the Presence of Friction Forces

Alexey V. Borisov^{1,2}, Alexander A. Kilin^{1,3} and Ivan S. Mamaev^{1,4}

¹ *Moscow Institute of Physics and Technology, Dolgoprudny, Russia*

² *A. A. Blagonravov Mechanical Engineering Research Institute of RAS, Moscow, Russia*

³ *Udmurt State University, Izhevsk, Russia*

⁴ *M. T. Kalashnikov Izhevsk State Technical University, Izhevsk, Russia*

Consider the problems of stability and destabilization of motion of a material point in a gravitational field on a rotating paraboloid. Represent the surface equation as

$$x_3 = \frac{1}{2}(x_1^2 + bx_2^2). \quad (1)$$

When $b > 0$, the paraboloid is elliptic, and when $b < 0$, it is hyperbolic.

In a (noninertial) coordinate system $Ox_1x_2x_3$, which rotates together with the surface (1), for a point of unit mass the Lagrangian of the system can be represented as

$$L = \frac{1}{2} \left((\dot{x}_1 - \Omega x_2)^2 + (\dot{x}_2 + \Omega x_1)^2 + (x_1 \dot{x}_1 + bx_2 \dot{x}_2)^2 \right) - \frac{1}{2} g (x_1^2 + bx_2^2),$$

where Ω is the angular velocity of rotation of the paraboloid and g is the free-fall acceleration.

The corresponding equations of motion are

$$\begin{aligned} \left(\frac{\partial L}{\partial \dot{\mathbf{x}}} \right)' - \frac{\partial L}{\partial \mathbf{x}} &= \mathbf{Q}, \\ \mathbf{x} = (x_1, x_2), \quad \mathbf{Q} &= \left(Q_1^{(0)} + Q_3^{(0)} \frac{\partial x_3}{\partial x_1}, Q_2^{(0)} + Q_3^{(0)} \frac{\partial x_3}{\partial x_2} \right), \end{aligned} \quad (2)$$

where $(Q_1^{(0)}, Q_2^{(0)}, Q_3^{(0)})$ is the three-dimensional vector of nonpotential forces acting on the material point in \mathbb{R}^3 ; this vector is assumed to be tangent to the surface (1).

If $\mathbf{Q} = 0$, then the system admits the energy integral

$$E = \frac{1}{2} (\dot{x}_1^2 + \dot{x}_2^2 + (x_1 \dot{x}_1 + bx_2 \dot{x}_2)^2) - \frac{\Omega^2}{2} (x_1^2 + x_2^2) + \frac{g}{2} (x_1^2 + bx_2^2). \quad (3)$$

As we see, for integrability we need another additional integral.

Possible friction forces dealt with in this work are as follows.

1° *Internal viscous friction* (internal damping), for which the drag force opposes the relative velocity of the point:

$$Q_1^{(0)} = -\mu\dot{x}_1, \quad Q_2^{(0)} = -\mu\dot{x}_2, \quad Q_3^{(0)} = -\mu\dot{x}_3,$$

where μ is the coefficient of friction. Substituting into (2) gives

$$\begin{aligned} \mathbf{Q} &= -\hat{\boldsymbol{\mu}}\dot{\mathbf{x}} = -\frac{\partial R^i}{\partial \dot{\mathbf{x}}}, \\ R^i &= \frac{1}{2}(\dot{\mathbf{x}}, \hat{\boldsymbol{\mu}}\dot{\mathbf{x}}), \quad \hat{\boldsymbol{\mu}} = \mu \begin{pmatrix} 1 + x_1^2 & bx_1x_2 \\ bx_1x_2 & 1 + b^2x_2^2 \end{pmatrix}, \end{aligned} \quad (4)$$

where R^i is the Rayleigh function and $\hat{\boldsymbol{\mu}}$ is a positive definite matrix.

2° *External viscous friction* (for example, air drag). In this case, the friction force opposes the velocity of the point in the fixed coordinate system:

$$Q_1^{(0)} = -\mu(\dot{x}_1 - \Omega x_2), \quad Q_2^{(0)} = -\mu(\dot{x}_2 + \Omega x_1), \quad Q_3^{(0)} = -\mu\dot{x}_3.$$

In this case, we find

$$\mathbf{Q} = -\hat{\boldsymbol{\mu}}\dot{\mathbf{x}} + \hat{\mathbf{D}}\mathbf{x}, \quad \hat{\mathbf{D}} = \begin{pmatrix} 0 & \mu\Omega \\ -\mu\Omega & 0 \end{pmatrix},$$

where $\hat{\boldsymbol{\mu}}$ is a 2×2 matrix defined in (4).

3° *Dry friction*:

$$\begin{aligned} Q_1^{(0)} &= -\frac{\mu N}{v}\dot{x}_1, \quad Q_2^{(0)} = -\frac{\mu N}{v}\dot{x}_2, \quad Q_3^{(0)} = -\frac{\mu N}{v}\dot{x}_3 \\ v &= \sqrt{\dot{x}_1^2 + \dot{x}_2^2 + \dot{x}_3^2}, \\ N &= \frac{g + \dot{x}_1^2 + b\dot{x}_2^2 + 2\Omega(x_1\dot{x}_2 - bx_2\dot{x}_1) + \Omega^2(x_1^2 + bx_2^2)}{\sqrt{1 + x_1^2 + b^2x_2^2}}, \end{aligned}$$

where N is the value of the reaction force. Thus, we obtain

$$\mathbf{Q} = -\frac{N}{v}\hat{\boldsymbol{\mu}}\dot{\mathbf{x}}, \quad (5)$$

where $\hat{\boldsymbol{\mu}}$ is also the matrix from (4).

This work presents a detailed analysis of the problem of frictionless motion of a material point on the surface of both a fixed and a rotating paraboloid. A bifurcation diagram is plotted for the case of a fixed paraboloid. We also give a complete bifurcation analysis of the stability of critical solutions and an analysis of regions of possible motion in configuration space (Hill's regions).

For the case of a rotating paraboloid, the linear stability of the equilibrium point at the vertex of the paraboloid is investigated. An analysis of Hill's regions depending on the value of the energy integral and the system parameters is carried out. It is shown that, even in the case of unbounded Hill's regions, in phase space there can exist regions of bounded motion. Regions of existence of bounded motions on the plane of the energy integral and the system parameter are constructed. Using a numerical construction of separatrix splitting, the nonintegrability of the problem is proved for the case of a rotating paraboloid.

Also in this work the problem of a material point moving on the surface of a rotating paraboloid in the presence of viscous friction forces is studied. A linear stability analysis of equilibrium points is carried out. It is shown that, in the case of viscous friction forces acting from the surface, the equilibrium point at the vertex of the hyperbolic paraboloid is always unstable. However, the instability pattern allows an interpretation of the behavior of trajectories near an equilibrium point as a temporal stability.

In this work it is shown that the addition of viscous air drag forces, as opposed to other friction forces, does not destroy the region of bounded motion. The above-mentioned types of behavior are illustrated by constructing three-dimensional Poincaré maps of the system under consideration.

This work is carried out at MIPT under project 5–100 for state support for leading universities of the Russian Federation.

Dynamics control of nonholonomic system modelling motion of skier and snowboarder

Andrey V. Borisov¹, Ivan E. Kaspirovich², Robert G. Mukharlyamov²

¹ *The Branch of National Research University "Moscow Power Engineering Institute" in Smolensk, Smolensk, Russia*

² *Peoples' Friendship University of Russia, RUDN University, Moscow, Russia*

In this paper a problem of dynamics control of nonholonomic Chaplygin systems is considered. A model of a skier or a snowboarder is chosen as an example of these systems. A structure of its Lagrange function and nonholonomic constraint equations allows us to set up the motion equations in the Chaplygin's form. The control is realized by extra forces defined by the constraints that determine a required motion.

In some cases, generalized coordinates and velocities describing a motion of a snowboarder or a skier can be rearranged into dependent and independent parts, so the Lagrange function and the constraint equations do not include the dependent ones. Then the system of motion equations for the considered model can be written in Chaplygin's form thereby reducing its dimension [1,2]. Papers by Borisov A.V. and colleagues [3], Karapetyan A.V. and colleagues [4], Chernousko F.L. and colleagues [5,6], Mukharlyamov and colleagues [7–9] and by a lot of other authors are devoted to the investigation on the control of mechanical systems with friction and nonholonomic constraints.

The snowboarder's model is mechanical rod system with a board and a link AB, which represents a leg (Fig. 1).

A simplified model of snowboarder's dynamics corresponds to the system of two rigid bodies with a hinge. The system is described by five coordinates: φ_0 — angle determining the direction of the board relative to the axis OX , φ_1 — angle counting from the OX -axis counterclockwise to the projection of the l_1 link onto the XOY plane, ψ_1 — angle counting from the projection l_1 counterclockwise to the link itself and x_A, y_A — coordinates of the board's fastening to the leg. The mechanism in the plane of motion is affected by the component of the gravitational acceleration $g_1 = g \sin \alpha$, directed along the OX -axis. Chaplygin's approach is applied to construct a system of differential motion equations of the nonholonomic system. Fastening can be modelled by a system of two cylindrical hinges in the point A and by two control torques defining the orientation of the leg. M_1 provides maintaining the leg pose in the vertical plane and M_2 defines a rotation of

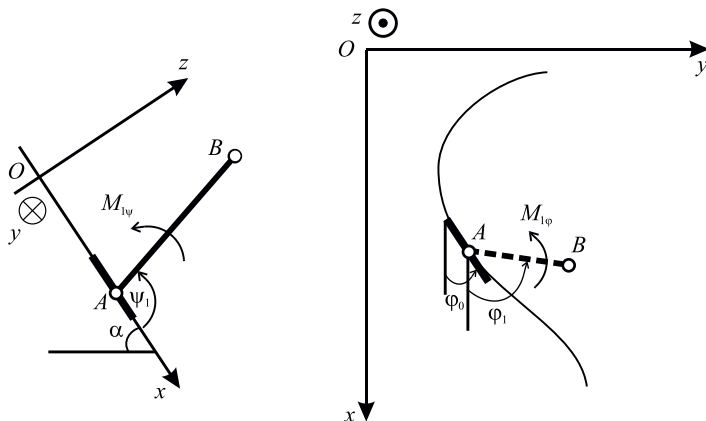


Fig. 1. Multilink snowboarder's model

the leg with respect to the board in the plane of motion XOY . The problem is to determine the expressions of the control torques so the motion of the model remains stable on its given trajectory. This can be accomplished by introducing extra holonomic constraints setting the model's motion mode. Reaction forces of these constraints are determined through the method of Lagrange multipliers. However, numerical integration of the motion equations with the Lagrange multipliers can not always provide a stable numerical solution in relation to the constraint equations. So, introducing extra variables estimating deviations from the constraints and constructing using them an expanded system of motion equations is required to solve the problem of constraint stabilization.

This work was supported by RFBR grant (No. 19-08-00261A).

References

- [1] Butenin N. V., Fufaev N. A. Introduction to analytical dynamics: sec. ed. Moscow.: Nauka, 1991. 250 p.
- [2] Neymark Yu. I., Fufaev N. A. Dynamics of nonholonomic systems. Moscow.: Nauka. 1991. 250 p.
- [3] Borisov A. V., Mamaev I. S., Kilin A. A. Some problems of nonholonomic mechanics. Moscow-Izhevsk: Institute of computer research, 2005. 289 p.
- [4] Kalyonova V. I., Karapetyan A. V., Morozov V. M., Salmina M. A. Nonholonomic mechanical systems and motion stabilization // Fundamental and applied mathematics, 2005, Vol. 11, Issue 7. P. 117–158.

- [5] Chernousko F.L., Ananievskiy I.M., Reshmin S.A. Methods of control of nonlinear mechanical systems. Moscow: Fizmatlit, 2006, 328 p.
- [6] Chernousko F.L., Bolotnik N.N. Locomotion of multi-link systems on plane: dynamics, control, optimization. Moscow.: Publisher IPMekh RAS (Preprint 1128), 2016, 154 p.
- [7] Mukharlyamov R.G. Modeling of control processes, stability and stabilization of systems with program constraints // Bulletin of the RAS. Journal of Computer and Systems Sciences International, 2015, Issue 1, p. 15–28.
- [8] Mukharlyamov R.G. Dynamics control of systems with holonomic constraints // Analytical mechanics, stability and control.: Proceedings of XI International Chetaev conference. Vol. 3. Section 3. Control. Ch. P. Kazan: KNRTU KAI, 2017, P. 140–146.
- [9] Kaspirovich I.E., Mukharlyamov R.G. Application of constraint stabilization to nonholonomic mechanics // LII Russian conference on problems of dynamics, particle physics, plasma physics and optoelectronics: proceedings. Moscow, RUDN. P. 112–116.

Limit cycles and resonances in asymmetric laser dimers: new oscillatory phenomena in photonic arrays

Anastasios Bountis¹, Yannis Kominis², Joniald Shena^{1,3}, Vassilios Kovanis⁴

¹ Department of Mathematics, School of Science and Technology, Nazarbayev University, Nur-Sultan, Republic of Kazakhstan

² School of Applied Mathematical and Physical Science, National Technical University of Athens, Athens, Greece ³ National University of Science and Technology MISiS, Leninsky prosp. 4, Moscow, 119049, Russia ⁴ Department of Electrical and Computer Engineering, Virginia Tech, Arlington VA

Coupled semiconductor lasers are systems possessing complex dynamics that are interesting for numerous applications in photonics. In this paper, we first review earlier results on the existence and stability of asymmetric phase-locked states of a *single dimer* consisting of two coupled semiconductor lasers with carrier density dynamics. We show that stable phase-locked states of arbitrary asymmetry exist whose field amplitude ratio and phase difference can be dynamically controlled by appropriate current injection. We emphasize the importance of Exceptional (fixed) Points, with large stability domains and Hopf bifurcations, beyond which small-signal modulations lead to sharp resonances and anti-resonances at very high frequencies. We obtain limit cycles with frequencies ranging from a few to a hundred GHz characterized by asymmetry and controllable via differential pumping and optical frequency detuning. Finally, we describe our recent findings in optically coupled arrays of driven dimers, each of which can perform limit cycle oscillations, and study some fascinating phenomena that may prove useful for applications in beam forming and beam shaping. Coupling in an appropriate way large numbers of dimers, we find that they can exhibit oscillatory patterns involving *high amplitude oscillations* coexisting with *very low amplitude motions* close to the unstable fixed points. Both behaviors are shown to be spatially robust, when we calculate the discrete Laplacian of their amplitudes for long times.

References

- [1] Kominis Y., Kovanis V. and Bountis A. Controllable Asymmetric Phase-Locked States in Coupled Semiconductor Lasers // Physical Review A, 96, 043836 (2017).
- [2] Kominis Y., Kovanis V. and Bountis A. Spectral Signatures of Exceptional Points and Bifurcations in the Fundamental Active Photonic Dimer // Physical Review A 96, 053837 (2017).

- [3] Kominis Y., Choquette K.D., Bountis A. and Kovanis V. Exceptional Points in Two Dissimilar Coupled Diode Lasers // *Appl. Phys. Lett.* 113, 081103 (2018).
- [4] Kominis Y., Choquette K.D., Kovanis V. and Bountis A. Antiresonances and Ultrafast Resonances in Coupled Twin Photonic Oscillator // *IEEE Photonics* (January 2019).
- [5] Shena J., Kominis Y., Bountis A. and Kovanis V. Controlling localized patterns in coupled array of semiconductor lasers. Preprint (2019).
- [6] Kominis Y., Erneux Th., Bountis A., Kovanis V. Controllable Limit Cycles of a Widely Tunable Photonic Oscillator. Preprint (2019).

Controlling of DC motor robots via INS

Pavol Božek

*Slovak University of Technology,
Faculty of Materials Science and Technology Trnava, Slovakia*

The paper describes the system of activities and the importance of INS with the possibility of implementation into robot control. The paper also introduces the implementation of DC motor control, which is used to position the rotary arm. Motor control includes current control, angular velocity, and rotation of the motor shaft attached to the arm with respect to the desired course of angular variation of the arm rotation. The DC motor control structure is executed in MATLAB / Simulink. The arm movement is examined using a mathematical model and a virtual dynamic model created in MSC.ADAMS.

Accuracy of inertial sensors plays a key role in autonomous navigation. Current inertial sensor errors are approximately $0.01^\circ/\text{hr}$ for gyroscopes and $100 \mu\text{g}$ for accelerometers. These errors are integrated over time and cause a positioning error, which is expressed by measurement uncertainty per hour, but is minimal.

The following is an example of how to move the robot arm in one axis. Also the possibility to extend the result of the simulation of the arm movement solved by the mathematical model in the virtual environment and the MATLAB/Simulink program.

References

- [1] Heimann, B., W. Gerth, and K. Popp, “Mechatronik – Komponenten – Methoden – Beispiele”, HANSER, 2007.
- [2] Weber, W., “Industrieroboter”, HANSER, 2009.
- [3] Barbour, N., J. Elwell, and R. Setterlund, “Inertial instruments: Where to now”, www.media.mit.edu/resenv/classes/.../Inertialnotes/DraperOverview.pdf, [cit. 2011-07-15].
- [4] Nikitin, Y.R., and I.V. Abramov, “Models of information processes of mechatronic systems diagnosis”, *University Review*. 2011. V. 5. No. 1. P. 12–16.
- [5] Šípoš, Ľ., Publikácia, “Inertial navigation”, Zvolen, 2011.
- [6] Nikitin, Y.R., “Diagnostic models of mechatronic modules and analysis techniques”, *Proceeding of 2-d International Conference Advances in Mechatronics*, December 2007, Brno, Czech Republic.

- [7] Soták, M., “Integration navigation systems”, Košice, 2006.
- [8] Božek P., J. Šuriansky, 2011. Riadenie robota na báze inerciálneho systému. Ostrava: TU v Ostrave, Mechanical Series 1/2011. [cit: 2017-04-20]. KEGA 3-7285-09, no. 1833
- [9] Diaz E.M. et al., 2015. Evaluation of AHRS Algorithms for Inertial Personal Localization in Industrial Environments. Seville [cit: 2017-04-20].
- [10] Jizhou Lai, Pin LV, Jianye Liu and Bin Jiang, 2012. Noncommutativity Error Analysis of Strapdown Inertial Navigation System under the Vibration in UAVs. International Journal of Advanced Robotic Systems, 2012, Vol. 9, 136:2012.
- [11] LYNXMOTION, 2016. Robotic Arms AL5B. [online] [cit: 2017-04-20]. Dostupné na internete: <<http://www.lynxmotion.com/c-126-al5b.aspx>>.
- [12] Madgwick, S., 2013. Oscillatory-Motion-Tracking-With-x-IMU. [online] [cit: 2017-04-27]. Dostupné na internete: <https://github.com/xioTechnologies/Oscillatory-MotionTracking-With-x-IMU>.
- [13] Mihalík, J., I. Gladišová, 2013. Číslíková filtrácia signálov (Návody na cvičenia). LČSOV FEI TU Košice, 2013.
- [14] NOVATEL, 2014. IMU Errors and Their Effects. . [online] [cit: 2017-04-15]. Dostupné na internete: <http://www.novatel.com/assets/Documents/Bulletins/APN064.pdf>.
- [15] POLOLU CORPORATION, 2016. Pololu Maestro Servo Controller User’s Guide. [online] [cit: 2017-04-20]. Dostupné na internete: <<https://www.pololu.com/docs/0J40>>.
- [16] Quadri, S.A., o. Sidek, 2014. Error and Noise Analysis in an IMU using Kalman Filter. [online] Collaborative Microelectronic Design Excellence Centre (CEDEC), Universiti Sains Malaysia, Engineering Campus, Nibong Tebal 2014. [cit: 2017-03-12]. Dostupné na internete: http://www.sersc.org/journals/IJHIT/vol7_no3_2014/6.pdf.
- [17] Qassem, M. A., I. Abuhadrous, H. Elaydi, 2009. Modeling and Simulation of 5 DOF Educational Robot Arm. The 2nd IEEE International Conference on Advanced Computer Control, Shenyang. [online] [cit: 2017-04-20]. Dostupné na internete: <http://ieeexplore.ieee.org/document/5487136/>. ISBN 978-1-4244-5848-6
- [18] Qazizada M. E., E. Pivarčiová, 2016. Mobile Robot Controlling Possibilities of Inertial Navigation System. Procedia Engineering, Volume 149, 2016, Pages 404–413, doi: 10.1016/j.proeng.2016.06.685
- [19] Soták M., 2008. Application of wavelet analysis to inertial measurements. Scientific papers: Science & Military 2/2008. [cit: 2017-04-20]. SPP-852-08-RO02_RU21-240
- [20] Tianmiao Wang, CHaoLei Wang, Jianhong Liang, Yang CHen, Yicheng Zhang, 2013. Vision-Aided Inertial Navigation for Small Unmanned Aerial Vehicles

- in GPS-Denied Environments. *International Journal of Advanced Robotic Systems*, 2013, Vol. 10, 276:2013.
- [21] Turygin Y., Božek P., Nikitin Y. R., Sosnovich E. V., Abramov, A. I., 2016. Enhancing the reliability of mobile robots control process via reverse validation. *International Journal of Advanced Robotic Systems*, 13. p. 1–8.
 - [22] X-IO TECHNOLOGIES, 2013. x-IMU User Manual 5.2. [online][PDF] Great Britain 2013. [cit: 2017-04-20]. Dostupné na internete: <http://x-io.co.uk/downloads/x-IMU-UserManual-v5.2.pdf>.
 - [23] Jekeli, C. (2001) *Inertial Navigation Systems with Geodetic Applications*. Cited 365 times. Walter de Gruyter GmbH & Co, Berlin.
 - [24] Groves, P.D. (2008) *Principles of GNSS, Inertial, and Multisensor Integrated Navigation Systems*. Cited 1021 times. Artech house remote sensing Library, London.
 - [25] Bar-Itzhack, I.Y., Berman, N. Control theoretic approach to inertial navigation systems (1988) *Journal of Guidance, Control, and Dynamics*, 11 (3), pp. 237–245. Cited 211 times. doi: 10.2514/3.20299.
 - [26] Silva F. O., Hemerly E. M., Leite Filho W. C. On the error state selection for stationary sins alignment and calibration kalman filters—Part II: Observability/estimability analysis.

The orbital stability analysis of planar rotations of a satellite in a circular orbit at the boundaries of a domain of stability in linear approximation

Evgeniya A. Chekina¹, Boris S. Bardin^{1,2}

¹ *Moscow Aviation Institute (National Research University), Moscow, Russia*

² *Mechanical Engineering Research Institute
of the Russian Academy of Sciences (IMASH RAN), Moscow, Russia*

We consider the motion of a satellite about its center of mass in a circular orbit in the Central Newtonian gravitational field. It is assumed that the satellite is a rigid body and has the mass geometry of a plate, i.e. its main central moments of inertia satisfy the ratio $J_x + J_y = J_z$. The equations of motion of the satellite can be written in canonical form. They admit a particular solution describing the planar pendulum-like motion of the satellite, in which its plane is perpendicular to the plane of the orbit [1]. Such motions are unstable with respect to perturbations of coordinates and velocities, however, the problem of their orbital stability is that of interest.

The type of motion depends on the constant of the energy integral and is either an oscillation or a rotation.

Orbital stability of planar oscillations was studied in [2–5]. In [6], a rigorous analysis of the orbital stability of the planar periodic rotations of the satellite is carried out. The values of the parameters corresponding to the regions of orbital stability in the first approximation were found, for the values of the parameters lying within these areas, conclusions were obtained about the stability for most initial conditions and formal stability. Nonlinear stability analysis has not been performed at the boundaries of the stability regions previously.

In this paper we provide a stability analysis at the boundaries of the region corresponding to that of the stability in the first approximation for the reverse rotations (see Fig. 1).

The Hamiltonian of perturbed motion has two parameters — an inertial parameter $\mu = J_x/J_y$ and the average angular velocity of the unperturbed motion Ω .

The conclusions about the stability of the reverse rotations of a satellite can be obtained on the basis of the analysis of the coefficients of the normal form of the Hamiltonian, which can be calculated using the algorithms developed in [4, 7, 8]. These algorithms are based on the method proposed in [9].

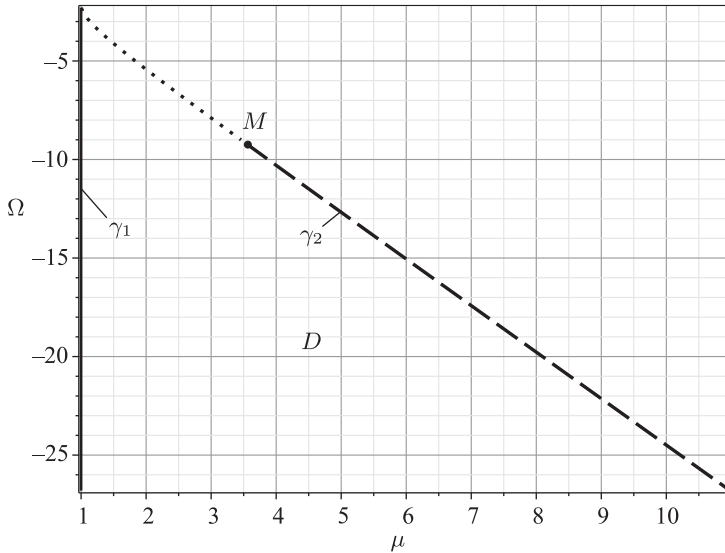


Fig. 1. The region of orbital stability in the linear approximation for reverse rotations of the satellite

Calculations performed in accordance with the above algorithms have shown that at the boundary γ_1 corresponding to the first order resonance instability occurs. On the curve γ_2 that implements the resonance of the second order (combinational resonance), in a part of the curve marked with a dotted line, there is formal orbital stability, in the area marked by the dashed-dotted line is the instability.

Acknowledgments

This work was supported by the grant of the Russian Scientific Foundation (project No. 19-11-00116) at the Moscow Aviation Institute (National Research University).

References

- [1] Beletsky. V. V., *The motion of the satellite relative to the center of mass in a gravitational field*. M: Moscow State University, 1975, 308 p.
- [2] Bardin B. S., Checkin A. M. *Orbital Stability of Planar Oscillations of a Satellite in a Circular Orbit*// *Cosmic Research*, 2008, vol. 46, no. 3, pp. 273–282

- [3] Bardin B.S., Chekina E.A. *On the Stability of Planar Oscillations of a Satellite-Plate in the Case of Essential Type Resonance*// Nelin. Dinam., 2017, vol. 13, no. 4, pp. 465–476
- [4] Bardin B.S., Chekina E.A. *On Orbital Stability of Planar Oscillations of a Satellite in a Circular Orbit on the Boundary of the Parametric Resonance*// AIP Conf. Proc., 2018, vol. 1959, no. 1, 040003.
- [5] Bardin B.S., Chekina E.A. *On the Constructive Algorithm for Stability Analysis of an Equilibrium Point of a Periodic Hamiltonian System with Two Degrees of Freedom in the Case of Combinational Resonance* // Regular and Chaotic Dynamics, 2019, vol. 24, no. 2, pp. 127–144.
- [6] Bardin B.S., Checkin A.M. *On Orbital Stability of Planar Rotations for a Plate Satellite Moving in a Circular Orbit*// Vestn. MAI, 2007, vol. 14, no. 2, pp. 23–36.
- [7] Bardin B.S., Chekina E. A., *On the Constructive Algorithm for Stability Analysis of an Equilibrium Point of a Periodic Hamiltonian System with Two Degrees of Freedom in the Second-Order Resonance Case*// Regul. Chaotic Dyn., 2017, vol. 22, no. 7, pp. 808–823.
- [8] Bardin B.S., Chekina E. A., *On the Constructive Algorithm for Stability Investigation of an Equilibrium Position of a Periodic Hamiltonian System with Two Degrees of Freedom in the First Order Resonance Case*// J. Appl. Math. Mech., 2018, vol. 82, no. 4, pp. 20–32.
- [9] Markeyev A.P. *A Constructive Algorithm for the Normalization of a Periodic Hamiltonian*// J. Appl. Math. Mech., 2005, vol. 69, no. 3, pp. 323–337.

Кавитационное обтекание нескольких пластинок

Елена Г. Ефимова¹, Александр Я. Корнилов¹

¹ ЧГУ имени И. Н. Ульянова, Чебоксары, Россия

Применение римановых поверхностей в исследовании кавитационного обтекания распространено достаточно широко. Максимально полно исследована задача обтекания двух пластин, поскольку в ней удается найти и аналитическое, и числовое решение. Если же пластин более двух, то получить аналитическое решение не так просто.

Рассмотрим обтекание N пластинок, расположенных на одной прямой и составляющих с ней малые углы наклона. Будем считать поток жидкости плоским и установившимся, а саму жидкость — идеальной несжимаемой. Вектор скорости на бесконечности направлен по прямой и задается конечной величиной. Пусть только одна пластина обтекается с кавитацией (будем считать таковой последнюю). Тогда необходимо задать либо число кавитации, либо точку замыкания каверны, а оставшийся параметр найти в ходе решения задачи. Уравнения пластин и число кавитации удовлетворяют условиям линеаризации.

Рассмотрим комплексную плоскость, в которой на действительной оси расположим разрезы — проекции пластин и каверны. Требуется найти возмущенную комплексно сопряженную скорость $W(z) = U - iV$ в виде аналитической функции, у которой $W(\infty) = 0$ и задается мнимая часть на всех берегах разрезов, кроме части последнего разреза. Эту часть предстоит найти, учитывая, что на ней задается действительная часть функции.

Решение получается явно после сведения задачи к краевой задаче Римана на римановой поверхности. В нем неизвестны действительные постоянные и либо граница каверны, либо число кавитации. В некоторых определенных случаях система содержит уравнения, линейные относительно всех неизвестных параметров.

Experimental studies of the movement of a mobile wheeled robot along optimal trajectories

Kirill S. Efremov¹, Andrey A. Ardentov², Yury L. Karavaev^{1,3}

¹ *Kalashnikov Izhevsk State Technical University, Izhevsk, Russia*

² *Ailamazyan Program Systems Institute of RAS, Pereslavl-Zalessky, Yaroslavl Region, Russia*

³ *Center for Technologies in Robotics and Mechatronics Components, Innopolis University, Russia*

The paper considers the use of Euler elastic as an algorithm for optimal control of a mobile nonholonomic robot. The task of determining the optimal trajectory is difficult to calculate and not unambiguous, depending on the criteria chosen as the best. The existing methods of planning trajectories are based on the use of sinusoids and splines [1–4]. Existing methods cannot provide the optimal trajectory for the n-trailer robot movement with the condition of fixed orientation at the start and end points. Euler elastics [1,6] allow to obtain optimal trajectories for single and n-trailer mobile robots from the point of view of control, taking into account speed and orientation at the start and end points. Locally elastics minimize the square of curvature:

$$\int u_E^2(s) ds \rightarrow \min. \quad (1)$$

For robots, this corresponds to uniform motion along elastica with local minimization of maneuvers. Curvature for inflectional elastic is expressed by the following equation:

$$u_E(s) = \frac{8kK}{\sigma} \operatorname{cn}\left(4K\left(p_E + \frac{s}{\sigma}\right); k\right), \quad (2)$$

where k — is a parameter determining the shape of an elastica, σ — is a parameter determining the length of a period, p_E — is a parameter defining the starting point of an elastica, K — is a complete elliptic integral of the 1st kind, $\operatorname{cn}()$ — is an Jacobi elliptic function.

Curvature for noninflectional elastic is expressed by the following equation:

$$u_E(s) = \pm \frac{4K}{\sigma} \operatorname{dn}\left(2K\left(p_E + \frac{s}{\sigma}\right); k\right), \quad (3)$$

where $\operatorname{dn}()$ — is the Jacobi elliptic function.

The algorithm of obtaining elastic for a certain point is given in [7]. The paper presents the results of modeling geometric errors with maximum deviations of dimensions. The exact geometric parameters of the robot were calculated by the method of least squares according to the results of experiments with deviations of the prototype of a mobile robot from the ideal trajectory. In addition, various acceleration and deceleration, providing movement along the elastic, are considered. Full-scale experiments for the new defined geometrical parameters and the nonlinear variant of acceleration was conducted for the motion of the mobile robot along the inflection and non-inflection elastics, and the motion along the trajectories planning the motion from the start point with a fixed orientation to the end point at given angles. The experiments qualitatively confirmed the observance of the forms of the given trajectories. Also obtained quantitative indicators of deviations.

Combined theoretical and full-scale experiments results are shown in Figure 1.

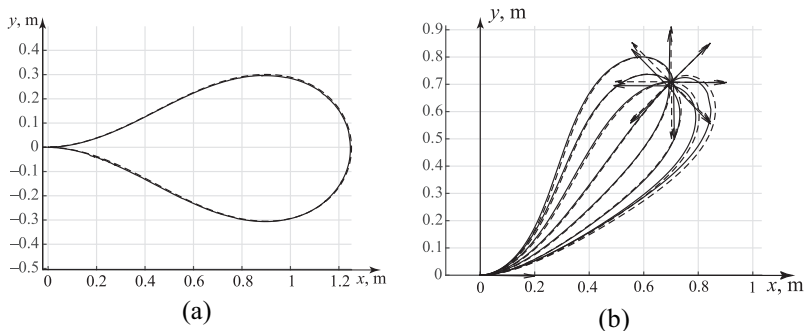


Fig. 1. Ideal and experimentally obtained trajectories. The dotted line shows the ideal trajectory, a solid line – experimental: a) trajectories of movement along the inflectional elastic in the form of a loop; b) trajectories of movement along the elastic with a start from one point with a fixed orientation and a stop to another with a change in the orientation angle $\theta_1 = (\pi n/4)$, $n = 1, \dots, 8$

The work of Yu. Karavaev, K. Efremov was supported by the grant of RFBR 18-38-00454, the work of A. Ardentov was supported by the Russian Science Foundation under grant 17-11-01387 and performed at the Ailamazyan Program Systems Institute of Russian Academy of Science

References

- [1] Murray R. M., Sastry S. S. *Nonholonomic motion planning: Steering using sinusoids*. IEEE transactions on Automatic Control, 1993, vol. 38, no. 5, pp. 700–716.
- [2] Laumond J.-P. *Nonholonomic motion planning for mobile robots*. Tutorial notes, 1998.
- [3] Lau B., Sprunk C., Burgard W. *Kinodynamic motion planning for mobile robots using splines*. IEEE/RSJ International Conference on Intelligent Robots and Systems, 2009, pp. 2427–2433). IEEE.
- [4] Ghilardelli F., Lini G., Piazzini A. *Path Generation Using η^4 -Splines for a Truck and Trailer Vehicle*. IEEE Transactions on Automation Science and Engineering, 2014 vol. 11, no. 1, pp. 187–203, doi: 10.1109/TASE.2013.2266962
- [5] Euler L. *De curvis elasticis*. Methodis Inveniendi, Addit. I, Lozanne, 1744.
- [6] Sachkov Yu. L. *Maxwell strata in Euler's elastic problem*. Journal of Dynamical and Control Systems, 2008, vol. 14, issue 2, pp. 169–234.
- [7] Ardentov A. A., Sachkov Y. L. *Solution to Euler's elastic problem*. Automation and Remote Control, 2009, vol. 70, no. 4, pp. 633–643.

High-speed transport system “Ekranoflot-Chuvashia”

Gennadiy A. Fedoreyev¹, Alexander S. Znatkov¹

¹ *Soyuzmordtrans Ltd., Vladivostok, Russia*

The project aims to:

- Creation of the first stage of the high-speed river transport system (SRTS) “Ekranoflot-Chuvashia” with two local high-speed river lines (SRTL) based on innovative water transport — ekranoplanes, with the prospect of entering the regional lines in the lower Volga;
- Regular commercial transportation of passengers, mail and baggage in the Volga trunk water area on transport lines between Cheboksary, Kazan and Nizhny Novgorod, as well as river cruises.

The paper proposes options for constructing SRTS and provides an analysis of technical and economic assessments of the efficiency of high-speed river passenger lines using modern Russian ekranoplanes.

Supported by the Russian Scientific and Technical Society of Shipbuilders of them ac A. N. Krylov.

References

- [1] Lyubimov V.I., Vasilyev E.V. The current state and prospects for the use of WIG in the basins of the rivers of Siberia and the Far East. scientific tr. “Modern trends in the development of transport in Siberia”. — Novosibirsk: NSAWT, 1999.
- [2] Fedoreyev G. A., Znatkov A. S., Schaub P. A. Ekranoplanes and high-speed transport systems for Primorye and the development of the Arctic regions of Yakutia // *Shipbuilding*. 2017. No. 2. P. 12–16.

WIG – transformer for effective logistics in far east and arctic

Gennadiy A. Fedoreyev¹, Alexander Yu. Zhurenko¹, Konstantin V. Gribov²,
Dmitry V. Nazarov³, Sergey M. Krivel⁴, Egor A. Galushko⁴

¹ *Soyuzmortrans Ltd., Vladivostok, Russia*

² *Far Eastern Federal University, Vladivostok, Russia*

³ *Samara State Aerospace University named after ac. S. P. Koroleva, Samara, Russia*

⁴ *Irkutsk State University, Irkutsk, Russia*

The aim of the project is to create a lightweight 2-seater high-speed, amphibious, WIG-boat – transformer for year-round individual and professional use on the rivers, reservoirs and coastal waters in the absence of transport infrastructure. The developed vehicle will combine several principles of movement adapted to different operating conditions: on the ice, snow, water, over water through its constructive transformation into a snowmobile, airboat and ekranoplane to ensure a competitive advantage in the consumer market for individual water transport.

Product purpose:

- Experimental studies of the dynamics of the on-screen maneuvering, the seaworthiness of the start / landing modes of the WIG on the seawaves;
- Working out technical solutions concept convertible modular collapsible design and industrial production technologies;
- Solving tasks: training in piloting, coastal and marine tourism, monitoring of emergency situations, oceanographic, hydrographic, meteorological research, fish-searching and fishing operations, including in automatic unmanned mode.

The scientific background of the project is based on:

- studies of aero-hydrodynamic characteristics of the model of the RT-6 ground effect vehicle at KSTU. A.N. Tupolev;
- results of aerotube tests of the ET-2 model in the wind tunnel of the Samara State Aerospace University them ac. S. P. Korolev and the model – an analogue of MT1 in the Krylov State Research Center them ac. A. N. Krylov;

- research and optimization of the dynamics and aerodynamics of mathematical 3D models of ET-2, held at Irkutsk State University.

At this stage, work is performed on optimizing the aero-hydrodynamic circuits of the transformer using air-tube testing and mathematical 3D modeling. The preliminary values of aerodynamic quality are obtained and the flight characteristics of the developed WIG are formed.

Supported by the Russian Scientific and Technical Society of Shipbuilders of them. ac A.N. Krylov.

References

- [1] Fedoreyev G. A., Znatkov A. S., Kizilov D. I., Schaub P. A., Moskovkina S. V. Ekranoplans today // Morskoy Vestnik, 2015, No. 4. P. 26–28.
- [2] Konstantin V. Gribov, Gennady A. Fedoreev. The concept of selection of aerodynamic schemes of ekranoplanes for transport corridors of the Arctic. The paper on TEAM-2018. The 32nd Asian-Pacific Technical Exchange and Advisory Meeting on Marine Structures. Wuhan, China, 2018. P. 9–23.

On some sufficient conditions for hyperbolicity and topological mixing

Sergey D. Glyzin¹, Andrey Yu. Kolesov¹, Nikolay K. Rozov²

¹ P. G. Demidov Yaroslavl State University, Yaroslavl, Russia

² M. V. Lomonosov Moscow State University, Moscow, Russia

Consider the open set $\mathcal{U} \subset \mathbb{R}^m$, where $m \geq 2$, and the map $f : \mathcal{U} \rightarrow \mathbb{R}^m$ from C^1 , that is a diffeomorphism from \mathcal{U} to $f(\mathcal{U}) \subset \mathbb{R}^m$.

Suppose there exists an open bounded set $\mathcal{V} \subset \mathcal{U}$, such that the closure $\overline{f(\mathcal{V})}$ is in \mathcal{V} and $\overline{\mathcal{V}} \subset \mathcal{U}$. Then the diffeomorphism f permits in \mathcal{V} the attractor

$$A = \bigcap_{n \geq 0} f^n(\mathcal{V}). \quad (1)$$

In the report certain sufficient conditions are proposed under which the attractor (1) is hyperbolic and topologically mixing.

Let us formulate the definitions we need. Fix arbitrarily the norm $\|\cdot\|_{\mathbb{R}^m}$ in the space \mathbb{R}^m . Next, for each point $x \in A$ let us set the operators

$$D(f^n(x)) = Df(x_{n-1}) \circ Df(x_{n-2}) \circ \dots \circ Df(x_0),$$

$$D(f^{-n}(x)) = [Df(x_{-n})]^{-1} \circ [Df(x_{-(n-1)})]^{-1} \circ \dots \circ [Df(x_{-1})]^{-1}, \quad n \in \mathbb{N},$$

where $Df(x) -$ is a Frechet derivative for the map f , $x_j = f^j(x)$, $j \in \mathbb{Z}$.

Definition 1 (see [1, 2]). Let us say that the attractor (1) is *hyperbolic*, if, firstly, for every $x \in A$ the space \mathbb{R}^m permits direct sum decomposition $E_x^u \oplus E_x^s$ of linear subspaces E_x^u , E_x^s and $Df(x)E_x^u = E_{f(x)}^u$, $Df(x)E_x^s = E_{f(x)}^s$; secondly, there exist constants $\mu_1, \mu_2 \in (0, 1)$, $c_1, c_2 > 0$, such that

$$\|D(f^{-n}(x))\xi\|_{\mathbb{R}^m} \leq c_1 \mu_1^n \|\xi\|_{\mathbb{R}^m} \quad \forall x \in A, \quad \forall \xi \in E_x^u, \quad \forall n \in \mathbb{N},$$

$$\|D(f^n(x))\xi\|_{\mathbb{R}^m} \leq c_2 \mu_2^n \|\xi\|_{\mathbb{R}^m} \quad \forall x \in A, \quad \forall \xi \in E_x^s, \quad \forall n \in \mathbb{N}.$$

Definition 2. We call $f|_A$ a *topological mixing*, if for every two nonempty sets $U, V \subset A$, that are open in the topology of the space (A, ρ) with metric $\rho(x_1, x_2) = \|x_1 - x_2\|_{\mathbb{R}^m} \quad \forall x_1, x_2 \in \mathbb{R}^m$, there exists a natural $n_0 = n_0(U, V)$, such that $f^n(U) \cap V \neq \emptyset$ for all $n \geq n_0$.

Now let us describe constraints providing the attractor (1) hyperbolicity.

Condition 1. For $\forall x \in \overline{\mathcal{V}}$ the spectrum $\sigma(x)$ of the operator $Df(x)$ decomposes into two nonempty subsets $\sigma_1(x) \subset \{\lambda \in \mathbb{C} : |\lambda| > 1\}$, $\sigma_2(x) \subset \{\lambda \in \mathbb{C} : |\lambda| < 1\}$.

The condition above leads to the decomposition $\mathbb{R}^m = E_1(x) \oplus E_2(x) \forall x \in \overline{\mathcal{V}}$, where the sum of subspaces $E_1(x), E_2(x)$ is direct, $Df(x)E_j(x) = E_j(x)$, $j = 1, 2$ and the spectrums of $Df(x)|_{E_j(x)}$, $j = 1, 2$ coincide with $\sigma_1(x)$ and $\sigma_2(x)$ respectively. Next, the mentioned decomposition allows to introduce projectors $P(x), Q(x)$, which act on arbitrary vector $\xi \in \mathbb{R}^m$ by the rules: $\forall \xi = \xi_1(x) + \xi_2(x)$, where $\xi_1(x) \in E_1(x)$, $\xi_2(x) \in E_2(x)$, we have $P(x)\xi = \xi_1(x)$, $Q(x)\xi = \xi_2(x)$. From Condition 1 and representation of these projectors via contour integrals we have continuity of $P(x), Q(x)$ on $x \in \overline{\mathcal{V}}$.

To formulate the next constraint we need the following operators:

$$\Lambda_{j,1}(x) = P(f(x))Df(x) : E_j(x) \rightarrow E_1(f(x)), \quad j = 1, 2,$$

$$\Lambda_{j,2}(x) = Q(f(x))Df(x) : E_j(x) \rightarrow E_2(f(x)), \quad j = 1, 2.$$

Assuming the invertibility of the operator $\Lambda_{1,1}(x)$ for $\forall x \in \overline{\mathcal{V}}$ and letting the norms in the spaces $E_1(x), E_2(x)$ to be adopted from \mathbb{R}^m , let us introduce the values

$$\begin{aligned} \alpha_1 &= \max_{x \in \overline{\mathcal{V}}} \|\Lambda_{1,1}^{-1}(x)\|_{E_1(f(x)) \rightarrow E_1(x)}, & \alpha_2 &= \max_{x \in \overline{\mathcal{V}}} \|\Lambda_{2,2}(x)\|_{E_2(x) \rightarrow E_2(f(x))}, \\ \beta_1 &= \max_{x \in \overline{\mathcal{V}}} \|\Lambda_{1,2}(x)\|_{E_1(x) \rightarrow E_2(f(x))}, & \beta_2 &= \max_{x \in \overline{\mathcal{V}}} \|\Lambda_{2,1}(x)\|_{E_2(x) \rightarrow E_1(f(x))}. \end{aligned}$$

Condition 2. Following inequalities hold

$$\alpha_1 < 1, \quad \alpha_2 < 1, \quad \beta_1\beta_2 < (1 - \alpha_1)(1 - \alpha_2)/\alpha_1. \quad (2)$$

Theorem 1. *Under Conditions 1, 2 the attractor (1) of the diffeomorphism f is hyperbolic.*

Theorem 2. *If in addition to Conditions 1, 2 the set $\overline{\mathcal{V}}$ is connected and at least one of the following requirements hold:*

- a) for $\forall x_1, x_2 \in A$ we have $W^u(x_1) \cap W^s(x_2) \neq \emptyset$,
- b) for $\forall x \in A$ the set $W^u(x)$ is dense in A , where as usual

$$\begin{aligned} W^s(x) &= \{y \in \overline{\mathcal{V}} : \rho(f^n(x), f^n(y)) \rightarrow 0, \quad n \rightarrow +\infty\}, \\ W^u(x) &= \{y \in A : \rho(f^{-n}(x), f^{-n}(y)) \rightarrow 0, \quad n \rightarrow +\infty\}, \end{aligned}$$

and ρ is a metric from Definition 2. Then $f|_A$ is a topological mixing.

Ideas of proofs of Theorems 1, 2 is the same as in papers [3], [4]. Namely, under Conditions 1, 2 the subspaces E_x^u, E_x^s from Definition 1 can be found in parametric form $E_x^u = \{\xi = u_1 + u_2 \in \mathbb{R}^m : u_1 = u, u_2 = a(x)u, u \in E_1(x)\}$ and $E_x^s = \{\xi = u_1 + u_2 \in \mathbb{R}^m : u_2 = u, u_1 =$

$b(x)u, u \in E_2(x)\}$, where the linear operators $a(x) : E_1(x) \rightarrow E_2(x)$, $b(x) : E_2(x) \rightarrow E_1(x)$ are continuous on $x \in A$ in the uniform operator topology.

Next, from invariance conditions of $Df(x)E_x^\sigma = E_{f(x)}^\sigma$, $\sigma = u, s$ for $a(x), b(x)$ we get certain nonlinear operator equations to which the contracting maps principle is applied (the validity of this principle in appropriate functional spaces is guaranteed by inequalities (2)). As for the Theorem 2, if its conditions are satisfied then the spectral decomposition of nonwandering set $NW(f|_A)$ is trivial, that is, it contains from one connected basis set A . It is known [2] that in this case $f|_A$ is a topological mixing.

References

- [1] Anosov D. V. *Geodesic flows on closed Riemannian manifolds with negative curvature* // Proc. Steklov Inst. Math., 1967, vol. 90, pp. 3–210.
- [2] Katok A. B. and Hasselblatt B. *Introduction to the Modern Theory of Dynamical Systems*, Cambridge: Cambridge Univ., 1995.
- [3] Glyzin S. D., Kolesov A. Yu., and Rozov N. Kh. *Hyperbolic annulus principle* // Differ. Equations, 2017, vol. 53, no. 3, pp. 281–301.
- [4] Glyzin S. D., Kolesov A. Yu. and Rozov N. Kh. *On a version of the hyperbolic annulus principle* // Differ. Equations, 2018, vol. 54, no. 8, pp. 1000–1025.

Connections and Time Reperametrizations in Nonholonomic Mechanics

Borislav Gajić¹, Božidar Jovanović¹

¹ *Mathematical Institute SANU, Belgrade, Serbia*

We consider nonholonomic system (M, L, D) on configuration space M given with Lagrangian L and nonintegrable distribution D defined by linear nonholonomic constraints. The equations of motion are obtained from the Lagrange-d'Alembert principle. In classical works of Synge [14], Vranceanu [18], Shouten [13], Wagner [15, 16] the problem of motion of nonholonomic systems from the geometric point of view is considered. The equations can be rewritten in terms of suitable vector bundle connection ∇^P over configuration space M :

$$\nabla_{\dot{q}}^P \dot{q} = -\text{grad}_D V.$$

In the case when the potential V vanishes, the solutions becomes the geodesic lines of ∇^P . We recall on the extensions of the vector-bundle connection to the linear connection on TM considered in [3, 17] and [12], as well as on so called partial connection (see [7]).

We compare various approaches in geometrical formulation of nonolonomic systems by using affine connections, including the Chaplygin reduction performed by Bakša [1]. Although mentioned objects are very well studied, some natural relationships between them are pointed out. In addition, we consider the Newton type equations on a Riemannian manifold (M, g) and look for a conformal metric $g^* = f^2 g$ such that solutions of the Newton equations, after a time reparametrization, become the geodesic lines of g .

This is a generalization of the Chaplygin multiplier method for Hamiltonization of G -Chaplygin systems [4, 5]. Also, we obtain variants of the Maupertuis principle in nonholonomic mechanics as they are given in [1, 11].

Acknowledgments

The research was supported by the Serbian Ministry of Science Project 174020, Geometry and Topology of Manifolds, Classical Mechanics and Integrable Dynamical Systems.

References

- [1] Bakša A., *On geometrisation of some nonholonomic systems*, Mat. Vesnik, 1975, vol. 27, 233–240 (in Serbian). English translation: 2017 Theoretical and Applied Mechanics 44, pp. 133–140.
- [2] Barrett D. I., Biggs R., Remsing C. C., *Invariant Nonholonomic Riemannian Structures on Three-Dimensional Lie Groups*, J. Geom. Mech., 2016, vol. 8, pp. 139–167.
- [3] Bloch A. M., Crouch P. E., *Newton's law and integrability of nonholonomic systems*, SIAM J. Control Optim., 1998, vol. 36, pp. 2020–2039.
- [4] Bolsinov A. V., Borisov A. V., Mamaev I. S., *Geometrisation of Chaplygin's reducing multiplier theorem*, Nonlinearity, 2015, vol. 28, pp. 2307–2318.
- [5] Cantrijn F., Cortes J., de Leon M., Martin de Diego D., *On the geometry of generalized Chaplygin system*, Math. Proc. Cambridge Philos. Soc., 2002, vol. 132, no. 2, pp. 323–351; arXiv: math.DS/0008141.
- [6] Chaplygin S. A., *On the theory of the motion of nonholonomic systems. Theorem on the reducing multiplier*, Mat. Sbornik, 1911, vol. 28, no. 2, pp. 303–314 (Russian).
- [7] Dragović V., Gajić B., *The Wagner Curvature Tensor in Nonholonomic Mechanics*, 2003, Regular and Chaotic Dynamics, vol. 8, pp. 105–123, arXiv:math-ph/0304018.
- [8] Fernandes O. E., Bloch A. M., 2011 *The Weitzenbock connection and time reparametrization in nonholonomic mechanics*, J. Math. Phys., 2011, vol. 52, 012901, 18 pages.
- [9] Gorbatenko E. M. *Differential geometry of Nonholonomic Systems (by V.V.Wagner)*, Geom. sb. Tomsk. u-ta, 1985, pp. 31–43.
- [10] Gajić B., Jovanović B., *Nonholonomic connections, time reparametrizations, and integrability of the rolling ball over a sphere*, Nonlinearity, 2019, vo. 32, no. 5, arXiv:1805.10610.
- [11] Koiller J., *Reduction of some classical non-holonomic systems with symmetry*, Arch.Rational Mech., 1992, vol. 118, pp. 113–148.
- [12] Lewis A. D., *Affine connctions and distributions with aplication to nonholonomic mechanics*, Rep. Math. Phys, 1998, vol. 42, pp. 135–164.
- [13] Shouten J. A. *On nonholonomic connections*, Koninklijke akademie van wetenschappen te Amsterdam, Proceeding of sciences, 1928, vol. 31, No. 3, pp. 291–298.
- [14] Synge J. Z. *Geodesics in nonholonomic geometry*, Math. Ann., 1928, vol. 99, pp. 738–751.

- [15] Wagner V. V. *Differential geometry of nonholonomic manifolds*, Tr. sem. po vekt. tenz. anal. II-III, 1935, pp. 269–315. (French)
- [16] Wagner V. V. *Geometrical interpretation of motion of nonholonomic dynamical systems*, Tr. sem. po vekt. tenz. anal. V, 1941, pp. 301–327. (Russian)
- [17] Vershik A. M., Faddeev L. D. *Differential geometry and Lagrangian mechanics with constraints*, Sov. Phys. Dokl., 1972, vol. 17 (1), pp. 34–36. (Russian)
- [18] Vranceanu G. *Parallelisme et courlure dans une variete non holonome*, Atti del congress Inter. del Mat. di Bologna, 1928.

The problem of general multi-dimensional rigid bodies rolling on the plane

Luis C. García-Naranjo

IIMAS-UNAM, Mexico City, Mexico

We consider the rolling and rolling without spinning of multi-dimensional rigid bodies of the plane. We identify cases of measure preservation, existence of first integrals and Hamiltonization that extend known results in 3D.

MEMS Sensor of Force

Rene Hartansky¹, Jaroslav Hricko², Martin Mierka¹, Michal Dzuris¹

¹ Institute of Electrical Engineering, Faculty of Electrical Engineering and Information Technology, Slovak University of Technology, Bratislava, Slovakia

² Institute of Informatics, Slovak Academy of Sciences, Banska Bystrica, Slovakia

The paper is focused to design of the compact compliant mechanical body (MM) that will be used as a transducer of the one-axis force to the distance of two plates. The conversion principle of the distance to the frequency of the electrical signal is carefully described in the article too.

Optimized sensor's elastic body is shown in Fig. 1a and Fig. 1b shows its transfer function as dependence between an acting load and distance of the sensor's plates. The analytical methods have been utilized for calculation of the MM basic parameters. The optimization of dimensions and mechanical body parameters by FEM analysis in Comsol Multiphysics were executed as a consequence of different results from analytical and numerical calculations (3–10% for one flexure element [4]). As come out from calculations results two groups of physical samples were produced [1, 2]. The first MM was produced from the PTFE by the water cutting technology; second MM is printed by a 3D printer from Polylactic acid.

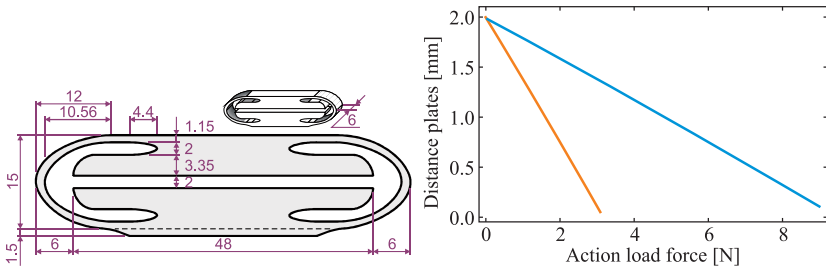


Fig. 1. a) Dimensions of designed elastic body, b) Dependences of acting force and displacement plates of the elastic body (Polylactic acid, Teflon)

In both cases, the dependence between the distance of plates and acting load (force) is inversely proportional. In the next step, it is necessary to convert the distance of MM plates to the easily measurable electrical quantities. Such are for instance time and frequency. Both quantities are most accurately measurable SI units. In the MM should be integrated electrical

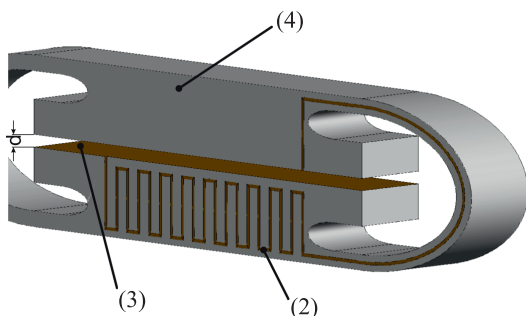


Fig. 2. MEMS, 4 – MM, 3 – capacitor, 2 – inductor

part – parallel resonance circuit (PRO). The capacitor of the PRO will be constituted by the MM's plates.

The PRO's resonance frequency were sensed wireless by our developed method based on the change of the high-frequency emitter dispersion parameters [3]. The article will compare theoretical values and measured values of resonance frequencies depending on the acting force.

Acknowledgment

This work was supported by the Slovak Research and Development Agency under the contract No.: APVV-14-0076 — “MEMS structures based on load cell” and by the national scientific grant agency VEGA under project No.: 2/0155/19 — “Processing sensory data via Artificial Intelligence methods”.

References

- [1] Hricko J. Design and shape optimization of novel load cell, in *Advances in intelligent systems and computing // Advances in robot design and intelligent control*, Wroclaw: Springer, 2016, 2017, vol. 540, pp. 80–87.
- [2] Andok R., Harňanský R., Hricko J., Halgoš J. Concept of a MEMS load cell sensor of mechanical quantities based on the EM field principle // *AIP Conference Proceedings: Applied Physics of Condensed Matter (APCOM 2018)*, 2018, vol. 1996, no. 020002.
- [3] Marsalka, L. Electromagnetic field properties influence by the changes of dielectric material constant // *Przeglad elektrotechniczny*, R92, NR 2/2016.
- [4] Linß, S., Schorr, P., Zentner, L.: General design equations for the rotational stiffness, maximal angular deflection and rotational precision of various notch flexure hinges // *Mech. Sci.* 8 (2017), 29–49.

Dynamics of toroidal bodies in a fluid

Yehor S. Hladkov¹, Evgeny V. Vetchanin²

¹ Udmurt State University, Izhevsk, Russia

² Kalashnikov Izhevsk State Technical University, Izhevsk, Russia

This paper is concerned with studying the motion of heavy homogeneous toroidal bodies of circular cross section in a fluid. To describe the motion we introduce two coordinate systems: a fixed one, $Oxyz$, and the moving one, $O_1e_1e_2e_3$, (see Fig. 1).

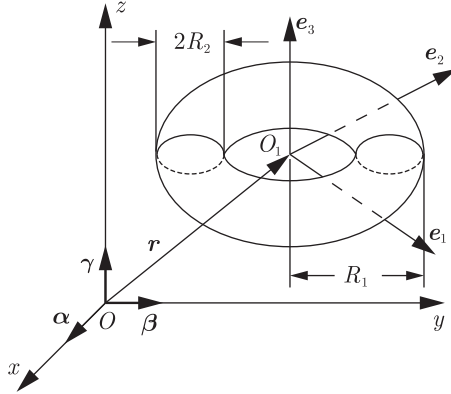


Fig. 1.

The motion is governed by the following equations:

$$\begin{aligned}
 \mathbf{C}\dot{\mathbf{v}} &= (\mathbf{C}\mathbf{v} + \mathbf{a}) \times \boldsymbol{\omega} - \mu\boldsymbol{\gamma} - \mathbf{F}, \\
 \mathbf{I}\dot{\boldsymbol{\omega}} &= (\mathbf{I}\boldsymbol{\omega} + \mathbf{b}) \times \boldsymbol{\omega} + (\mathbf{C}\mathbf{v} + \mathbf{a}) \times \mathbf{v} - \mathbf{G}, \\
 \dot{\mathbf{r}} &= \mathbf{Q}^T \mathbf{v}, \quad \dot{\boldsymbol{\alpha}} = \boldsymbol{\alpha} \times \boldsymbol{\omega}, \quad \dot{\boldsymbol{\beta}} = \boldsymbol{\beta} \times \boldsymbol{\omega}, \quad \dot{\boldsymbol{\gamma}} = \boldsymbol{\gamma} \times \boldsymbol{\omega}, \\
 \mathbf{Q} &= \begin{pmatrix} \alpha_1 & \beta_1 & \gamma_1 \\ \alpha_2 & \beta_2 & \gamma_2 \\ \alpha_3 & \beta_3 & \gamma_3 \end{pmatrix}, \quad F_i = f_i v_i |v_i|, \quad G_i = g_i \omega_i |\omega_i|
 \end{aligned} \tag{1}$$

where \mathbf{v} is the linear velocity of the body, $\boldsymbol{\omega}$ is the angular velocity of the body, \mathbf{F} , \mathbf{G} are resistance force and torque, \mathbf{C} is the matrix taking into account the mass of the body and the added masses, \mathbf{I} is a matrix taking into account the tensor of inertia of the body and the tensor of added moments of

inertia, \mathbf{a} and \mathbf{b} are the constant vector taking into account circular motion of a fluid through a hole of the body [1], \mathbf{r} is the radius-vector of the center of mass of the body, α, β, γ are the unit vectors directed along axes of the fixed coordinate system, and f_i, g_i are the drag coefficients.

We perform the Motion Capture experiment with natural model of torus (see Fig. 2b). To determining the drag coefficients f_i, g_i and vectors \mathbf{a}, \mathbf{b} we minimise deviation between calculated trajectory and experimental one using real coded genetic algorithm. The calculated and experimental trajectories are shown in Fig. 2a.

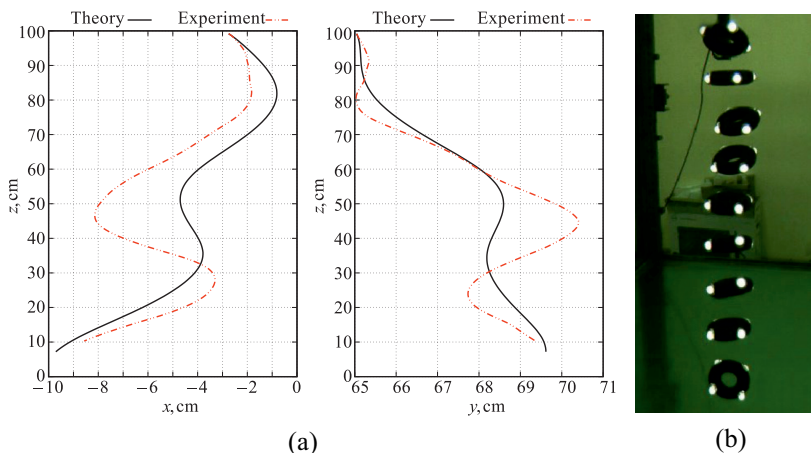


Fig. 2. a) projections of trajectory of the body on the coordinate planes of the system $Oxyz$, b) Motion Capture experiment

More detailed description of results presented in [2].

This work was supported by the RFBR under grant 18-29-10050-mk.

References

- [1] Lamb H. Hydrodynamics. New York: Dover; 1945, p. 728.
- [2] Vetchanin E. V., Gladkov E. S. Identification of parameters of the model of toroidal body motion using experimental data, Russian Journal of Nonlinear Dynamics, 2018, vol. 14, no. 1, pp. 99–121.

Verifying the Performance Characteristics of the (micro) Robotic Devices

Jaroslav Hricko¹, Stefan Havlik¹, Rene Hartansky²

¹ *Institute of Informatics, Slovak Academy of Sciences, Banská Bystrica, Slovakia*

² *Institute of Electrical Engineering (FEEIT),
Slovak University of Technology in Bratislava, Slovakia*

The miniaturization of the mechatronic devices lead to the utilization of the novel approaches to the devices design. In the case of micro-mechatronic devices, it is clear that classic constructions based on the assembly from discrete parts cannot satisfy desired requirements. The single solutions are compact structures using micro-system technology or other precise production methods. Such structures can be used as compliant mechanisms in micro-positioning devices, actuators for optoelectronics, micro-surgery, etc. A large group of MEMS devices represents micro-actuators and sensors (e.g. force/torque, pressure, speed, acceleration, flow rate. . .) [1].

In solving such mechanical structures specific approaches to design, kinematic, force and flexural analysis are used. Nevertheless, there is still a need to improve the quality of the mathematical description of micro-electro-mechanical systems (MEMS) based on the comparison of results from ordinary (linear) models and measured values, where the error on one elastic element is in the range of 2–16% [2].

In general, the performance characteristics of compliant mechanisms are relatively linear, but this follows from small motions of the devices. On the other side, the nonlinear behavior of compliant structures can be indicated, when the high precision positioning with high payload is required. The common precise positioning device usually used a stepper motor with the positional encoder the no-backlash high ratio reduction gear and the ball screw, but the study [3] shows that the positioning errors from the ball screw are present. Consequently that the motion reduction compliant mechanism can be utilized as a device those potential positional errors can minimize. The solution to such a device leads to a complex optimization problem. The movement of such devices is usually in the range of 10% of maximum device dimensions, on the other side, for minimizing positioning error to e.g. 10% (from the positioning error 30 μm to 3 μm) it is required considerable input displacement what have a direct impact to the dimensions of the whole device. Other mentioned problem could be the device's robustness and its dynamical properties. For instance, the thickness of the flexure hinges, if is

this thickness bigger the mechanisms is stiffer, but the arisen stress is higher, on the other side very thin hinges can lead to the unwanted oscillations, because mathematical expression of the compliant mechanism is mass-spring (damping) system.

In the design procedure are two main variables that should be calculated, the displacement as a dependence of acting load (or rather dependence between input and output movement) and maximum arisen stress as a dependence of maximum expected displacement and acting load. The calculations should be in the validity of Hooke's law and the area of elastic deformation. The dependence between displacement and acting load is expressed as

$$\mathbf{u} = \mathbf{C}\mathbf{F} \rightarrow \mathbf{F} = \mathbf{K}\mathbf{u}, \quad (1)$$

where \mathbf{u} is deflection vector (6×1), \mathbf{C} is compliance matrix (6×6) what is inverse matrix of stiffness \mathbf{K} , $K = |bfC^{-1}|$.

The maximum arisen stress in flexure hinge can be expressed as [4]

$$\sigma_{\max} = \frac{1}{wt} \left\{ K_{ta} K_{xFx} u_x + \frac{6K_{tb}}{t} [(l_F K_{yFy} + K_{\theta z Mz}) u_y + (l_F K_{yMz} + K_{\theta z Mz} \theta_z)] \right\}, \quad (2)$$

where K_{ta} and K_{tb} are theoretical stress concentration factors, where K_{ta} is connected with axial load, and K_{tb} is connected with bending. Parameters w and t are joint width and thickness (respectively), l_F is distance between joint and actuation place of force F_y , K_{ij} are elements of stiffness matrix (i — displacement/rotation in direction, j — acting load) and u_x , u_y , θ_z are displacements and rotation in particular direction (also components of the vector \mathbf{u}). Theoretical stress concentration factors are given on the base of experimental measurements or by approximate theoretical calculation.

In this work, the results from the design and analysis of motion reduction device are compared with measurements on the test bed. There are evaluated displacements of a device in two states when the mechanism works without load, and with a load. It turns out that in the case of a mechanism under load; its behavior is non-linear, which must be avoided by a suitable control system. Acknowledgment

This work was supported by the Slovak Research and Development Agency under the contract No.: APVV-14-0076 – “MEMS structures based on load cell”, contract No.: APVV-18-0117 and by the national scientific grant agency VEGA under project No.: 2/0155/19 – “Processing sensory data via Artificial Intelligence methods”.

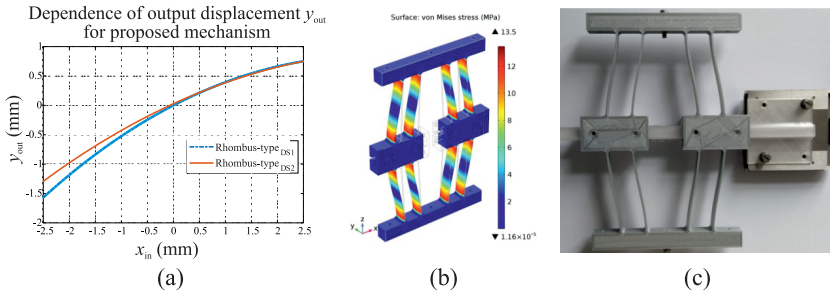


Fig. 1. a) Dependence of output displacement for proposed motion reduction device, b) Distribution of stress (von Mises) in proposed mechanism, c) 3D printed physical model of the proposed device

References

- [1] Howell L. L., Magleby S. P., Olsen B. M. Handbook of Compliant Mechanisms, John Wiley & Sons Ltd., 2013.
- [2] Linß S., Schorr P., Zentner L. General design equations for the rotational stiffness, maximal angular deflection and rotational precision of various notch flexure hinges, Mech. Sci., 8, 29-49, 2017
- [3] Zhang Y., Pan S., Deng J. Methods for Measuring and Compensating Ball Screw Error on Multi-mode Industrial CT Scanning Platform. 2016 5th International Conference on Measurement, Instrumentation and Automation (ICMIA 2016). Atlantis Press, 2016.
- [4] Lobontiu N. Compliant Mechanisms: Design of Flexure Hinges, CRC Press, 2003.

The residual method for solving ill-posed system of algebraic inequalities and linear programming problems with approximate data

Alexander Yu. Ivanitskiy¹, Fedor P. Vasilyev², Vladimir V. Ejov³

¹ *Chuvash State University, Cheboksary, Russia*

² *Moscow State University, Moscow, 119899, Russia*

³ *Flinders University of South Australia, Badfort Park, SA 5042*

We consider the following problem [1]:

$$\|u\|_1 = \sum_{j=1}^n |u_j| = \sum_{j=1}^n u_j \rightarrow \inf, \quad u \in \bar{U} = \{u \in \mathbf{R}^n : u \geq 0, \bar{D}u \leq \bar{h}\} \neq \emptyset. \quad (1)$$

Suppose that, instead of the exact data $\bar{D} = \{\bar{d}_{ij}\} \in \mathbf{R}^{m \times n}$, $\bar{h} = [\bar{h}_1, \bar{h}_2, \dots, \bar{h}_m]^T \in \mathbf{R}^m$, we know their approximations $\tilde{D} = \{\tilde{d}_{ij}\} \in \mathbf{R}^{m \times n}$, $\tilde{h} = [\tilde{h}_1, \tilde{h}_2, \dots, \tilde{h}_m]^T \in \mathbf{R}^m$ such that

$$\left| \tilde{d}_{ij} - \bar{d}_{ij} \right| \leq \delta_{ij}, \quad \left| \tilde{h}_i - \bar{h}_i \right| \leq \delta_i, \quad i = \overline{1, m}, \quad j = \overline{1, n}, \quad (2)$$

δ_{ij} , δ_i are the given pointwise levels of the input-data errors. Instead of individual system $\tilde{D}u \leq \tilde{h}$ we consider the aggregate systems

$$Du \leq h, \quad D \in \mathbf{D}, \quad H \in \mathbf{H}, \quad (3)$$

where [2]

$$\mathbf{D} = \{D = \{d_{ij}\} \in \mathbf{R}^{m \times n} : \left| \tilde{d}_{ij} - d_{ij} \right| \leq \delta_{ij}, i = \overline{1, m}, j = \overline{1, n}\},$$

$$\mathbf{H} = \{h = [h_1, h_2, \dots, h_m]^T \in \mathbf{R}^m : \left| \tilde{h}_i - h_i \right| \leq \delta_i, i = \overline{1, m}\}.$$

Consider the problem

$$\|u\|_1 = \sum_{j=1}^n |u_j| = \sum_{j=1}^n u_j \rightarrow \inf, \quad (4)$$

$$u \in U_1 = \{u \in \mathbf{R}^n : u \geq 0, Du \leq h, \exists D \in \mathbf{D}, \exists h \in \mathbf{H}\},$$

where U_1 is set of the admissible solutions of systems (3).

Theorem 1. *The problem (4) equals to the next problem*

$$\|u\|_1 = \sum_{j=1}^n |u_j| = \sum_{j=1}^n u_j \rightarrow \inf, \quad (5)$$

$$u \in U_2 = \{u \in \mathbf{R}^n : u \geq 0, \tilde{D}u - \tilde{h} \leq \Delta u + \delta\},$$

where $\Delta = \{\Delta_{ij}\} \in \mathbf{R}^{m \times n}$, $\delta = [\delta_1, \delta_2, \dots, \delta_m]^T \in \mathbf{R}^m$.

When we realize the residual method numerically, we do not have to obtain the exact solutions of (5). It is sufficient to find

$$u_\varepsilon \in U_2, \quad \|u_q\|_1 \leq \inf_{u \in U_2} \|u\|_1 + \varepsilon, \quad \varepsilon \geq 0. \quad (6)$$

Theorem 2. *Suppose $\bar{U} \neq \emptyset$, then*

$$\begin{aligned} \rho(u_\varepsilon, U_*) &= \inf_{u \in U_*} \|u_\varepsilon - u\|_2 = \\ &= \inf_{u \in U_*} \left(\sum_{j=1}^n |u_{\varepsilon j} - u_{*j}|^2 \right)^{1/2} = O(\|\Delta\|_\infty + \|\delta\|_\infty + \varepsilon) \end{aligned} \quad (7)$$

where u_ε satisfies the inequality (6) and $U_* = \{u \in \bar{U} : \|u\|_1 = \inf_{u \in \bar{U}} \|u\|_1\} \neq \emptyset$ is set of solution of problem (1).

The estimate (7) shows that pointwise method (6) allows one to obtain the approximate solutions of (1) with the same accuracy as the error in the definition of \bar{D} and \tilde{h} .

The problem of finding of the normal solutions of the linear programming problems can be reduced to the problem (1).

References

- [1] Vasilyev F.P., Ivanitskiy A.Yu. In-depth Analysis of Linear Programming. Kluwer Academic Publishers. Boston, London, Dodrecht, 2001.
- [2] Tikhonov A. N. On the approximate systems of linear algebraic equations // Zh. Vychisl. Mat. Mat. Fiz., 1980, vol. 20, no. 6, pp. 1373–1383.

Two integrable models of rolling balls over a sphere

Božidar Jovanović¹, Borislav Gajić¹

¹*Mathematical Institute SANU, Kneza Mihaila 36, 11000 Belgrade, Serbia*

In this talk we consider the nonholonomic problem of rolling without slipping and twisting of a n -dimensional ball over a fixed $(n-1)$ -dimensional sphere. This is a $SO(n)$ -Chaplygin system with an invariant measure that reduces to the tangent bundle TS^{n-1} . We describe two classes of inertia operators, such that corresponding systems are integrable. In the first class we use the Chaplygin reducing multiplier method, while in the second class we obtain integrability directly — without Hamiltonization.

References

- [1] Bolsinov A. V., Borisov A. V., Mamaev I. S. *Rolling of a ball without spinning on a plane: the absence of an invariant measure in a system with a complete set of integrals* // Regular and Chaotic Dynamics, 2012 vol. 17, pp. 571–579.
- [2] Ehlers K., Koiller J. *Rubber rolling over a sphere* // Regular and Chaotic Dynamics, 2007 vol. 12, pp. 127–152, arXiv:math/0612036.
- [3] Fasso F., Garcia-Naranjo L. C., Montaldi J. *Integrability and dynamics of the n -dimensional symmetric Veselova top* // Journal of Nonlinear Science, 2018, <https://doi.org/10.1007/s00332-018-9515-5>, arXiv:1804.09090
- [4] Gajić B., Jovanović B., *Nonholonomic connections, time reparametrizations, and integrability of the rolling ball over a sphere* // to appear in Nonlinearity, arXiv:1805.10610.
- [5] Jovanović B., *Invariant measures of modified LR and L+R systems* // Regular and Chaotic Dynamics, 2015, vol. 20, pp. 542–552, arXiv:1508.04913 [math-ph]
- [6] Jovanović B., *Rolling balls over spheres in R^n* // Nonlinearity, 2018, vol. 31, pp. 4006–4031, arXiv:1804.03697 [math-ph].

On resonances in Hamiltonian systems with three degrees of freedom

Alexander A. Karabanov¹, Albert D. Morozov²

¹ *Sir Peter Mansfield Imaging Centre, School of Physics and Astronomy, University of Nottingham*

² *Lobachevsky State University of Nizhni Novgorod, Russia*

We address the dynamics of near-integrable Hamiltonian systems with three degrees of freedom in extended vicinities of unperturbed resonance-invariant Liouville tori. Depending on the number of independent resonance conditions satisfied by the unperturbed torus, the resonances are subdivided into single and double. Normal forms and resonance averages of the isoenergetically reduced system are produced for both cases. It is shown that the average dynamics in the zone of a single resonance is 3-dimensional, fully integrable and reduced to a family of pendulum-like motions under a conservative force on the circle. A degeneracy with respect to one of slow variables is revealed and linked to the potential diffusive instability of the initial system. The average dynamics in the zone of a double resonance is 4-dimensional, reduced to motions under a conservative force on the two-torus and generically non-integrable. The methods of differential topology are applied to analysis of equilibrium states and phase foliations of the average system. The results are illustrated by a simple model combining the non-degeneracy and non-integrability of the reduced system.

This work has been partially supported by the Russian Foundation for Basic Research under grants no. 18-01-00306 and by the Ministry of Education and Science of the Russian Federation (project no. 1.3287.2017/PCh).

The dynamics of a spherical robot of the combined type by periodic control actions

Yury L. Karavaev^{1,2}, Alexander A. Kilin³

¹ *Kalaschnikov Izhevsk State Technical University, Izhevsk, Russia*

² *Center for Technologies in Robotics and Mechatronics Components, Innopolis University*

³ *Udmurt State University, Izhevsk, Russia*

In recent studies of nonholonomic systems the problems of moving a Chaplygin sleigh and Chaplygin top with small periodic control actions are considered. The results confirm the possibility of constant acceleration (speedup) of the wheeled vehicle due to the periodic change in the mass distribution [1,2], as well as acceleration of the Chaplygin top with the help of an internal rotor [3].

This paper presents the results of the study of the dynamics of a real spherical combined-type robot in case of controlling using small periodic oscillations. The spherical robot sets in motion by controlled moving the position of center of mass and generating variable gyrostatic momentum [4–6].

We demonstrate how to use small periodic controls for stabilization of spherical robot during motion. The results of numerical simulation are obtained for various initial conditions and control parameters that ensure a change in the position of the center of mass and a variation of gyrostatic momentum.

The problem of the motion of a spherical robot of the combined type on a surface that performs flat periodic oscillations is also considered. The results of numerical simulation are obtained for different initial conditions, control actions and parameters of oscillations. Possible modes of motion of spherical robot on oscillating plane are discussed.

The work funded by the Russian Science Foundation under grant 18-71-00096.

References

- [1] Bizyaev I. A., Borisov A. V., Kuznetsov S. P., Chaplygin sleigh with periodically oscillating internal mass. *EPL*, 2017, vol. 119, no. 6, 60008, 7 pp.
- [2] Bizyaev I. A., Borisov A. V., Mamaev I. S., The Chaplygin Sleigh with Parametric Excitation: Chaotic Dynamics and Nonholonomic Acceleration. *Regular and Chaotic Dynamics*, 2017, vol. 22, no. 8, pp. 955–975.

- [3] Borisov A. V., Kilin A. A., Pivovarova E. N., Speedup of the Chaplygin Top by Means of Rotors, *Doklady Physics*, 2019, vol. 64, no. 3, pp. 120–124.
- [4] Kilin, A. A., Pivovarova, E. N., and Ivanova, T. B., Spherical Robot of Combined Type: Dynamics and Control, *Regular and Chaotic Dynamic*, 2015, vol. 20, no. 6, pp. 716–728.
- [5] Kilin A. A., Karavaev Y. L., Experimental research of dynamic of spherical robot of combined type, *Russian Journal of Nonlinear Dynamics*, 2015, vol. 11, no. 4, pp. 721–734.
- [6] Borisov A. V., Kilin A. A., Karavaev Y. L., Klekovkin A. V., Stabilization of the motion of a spherical robot using feedbacks, *Applied Mathematical Modelling*, 2019, vol. 69, pp. 583–592.

Experimental evaluation of mobile wheeled robot control using artificial neural network

Yury L. Karavaev¹, Kirill S. Efremov¹, Ivan S. Zvonarev¹

¹ *Izhevsk State Technical University, Izhevsk, Russia*

Control systems of mobile robot are often developed using fuzzy regulators or neural networks [1–5]. The use of artificial intelligence methods is justified especially for complex systems, which include mobile wheeled robots. In the framework of this work, the task of planning the trajectory of movement for a mobile wheeled robot using artificial neural networks is considered. The formation of the trajectory from the initial position to the final one is based on the solution of the problem of control optimization using Euler’s elasticas. Two types of elasticas inflection and non-inflection are calculated by the following formulas [6]:

$$\text{a) inflection: } u_E(s) = \frac{8kK}{\sigma} \text{cn}\left(4K\left(p_E + \frac{s}{\sigma}\right); k\right);$$

$$\text{b) non-inflection: } u_E(s) = \pm \frac{4K}{\sigma} \text{dn}\left(2K\left(p_E + \frac{s}{\sigma}\right); k\right),$$

where k is the parameter that determines the forms of elasticity; σ is the length of the full period of elasticity; p_E is the starting point of elasticity, K is the elliptic integral of the first kind, $\text{cn}()$ and $\text{dn}()$ are the elliptic Jacobi functions. Based on a mathematical model we prepared a training dataset of basic trajectories in the form of Euler’s elasticas relate various possible positions of a mobile robot taking into account different orientations.

The proposed control system consists of two artificial neural networks (ANN) (Fig. 1). ANN1 processes data from different sensors and forms a circle describing the obstacle (the coordinates of the center and radius) and the time of the possible motion. ANN2 calculates the coefficients needed to calculate the elastic. The basic ANN is a multilayer perceptron trained by backpropagation algorithm. To implement the ANN, the Python language with the TensorFlow machine-learning library was used.

The geometric features of the controlled mobile robot were taken into account when forming the training samples. To check the performance of this control system (CS), several experiments were implemented to form a trajectory: with an obstacle on the trained data, without an obstacle on the trained data and for a non-standard situation (for which the ANN was not trained).

The paper presents the results of testing the proposed neural network controller in practice.

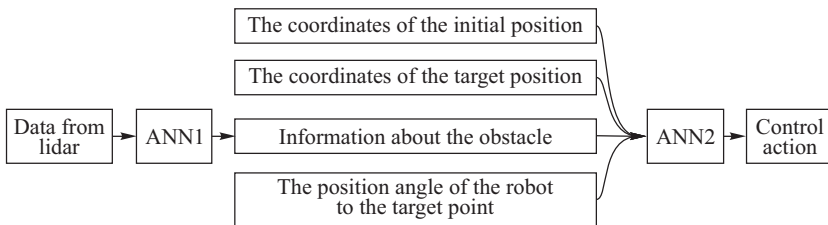


Fig. 1. Structure of neural network controller

References

- [1] Kasyanik V.V., Dunets A.P., Dunets I.P., Joke V.N. Application of neural network approach for odometer error estimation // Neuroinformatics. 2012. 14 all-Russian scientific and technical conference. Section 7.
- [2] Muratov S.T., Lakhman K.V., Burtsev M.S. Neuroevolutionary synthesis of the controller in the problem of sequence generation // Neuroinformatics. 2014, no. 2. P. 117–127.
- [3] Zimmerman T.A. Neural Network Based Obstacle Avoidance Using Simulated Sensor Data. ASEE 2014 Zone I Conference, April 3–5, 2014. University of Bridgeport, Bridgeport, CT, USA.
- [4] Tanaka K., Yoshioka K. Fuzzy trajectory control and GA-based obstacle avoidance of a truck with five trailers // In: Proceedings of IEEE International Conference on Systems, Man and Cybernetics, Intelligent Systems for the 21st Century, 1992. Vol. 5. P. 4378–4382.
- [5] Kong S.-G., Kosko B. Adaptive fuzzy systems for backing up a truck-and-trailer // Proc. IEEE Trans. Neural. Netw., 1992. Vol. 3, no. 2. P. 211–223.
- [6] Sachkov Yu.L. Maxwell strata in Euler’s elastic problem, Journal of Dynamical and Control Systems, 2008, Vol. 14, Issue 2. P. 169–234.

Numerical research of flow of profiles system near screen

Tatiana V. Kartuzova¹, Alevtina G. Kulagina¹, Lyudmila V. Seliverstova¹

¹ *Chuvash State University, Cheboksary, Russia*

The work offers a method to calculate the flow of profiles system based on an integrated ratio of current function for infinite area [1]. At the same time the numerical method — a method of boundary elements (MBE) with constant elements is used. Influence of the screen is simulated by means of the profiles located specularly relative to the screen.

This work considers the direct boundary-value problem, which has the system of profiles (the main wing, the slat, the flap, etc.) and their mutual arrangement against motionless screen. The paper studies the problem of continuous flow of a profile system near the screen by a stream of ideal incompressible liquid [2]. The contours of profiles are supposed to be closed and smooth. The flow of a single profile, profile with the slat, with the slat and the flap near the screen are investigated in detail. Thereby the flow of a system of two, four and six profiles is calculated.

The dependence of lifting capacity of a profile at approach to the screen on its thickness is investigated; influence of an angle of rotation of the flap on lifting capacity coefficient and also influence of the screen on various aerodynamic features of the system of profiles.

References

- [1] Terentyev A. G., Kartuzova T. V. Numerical research of a profile flow near screen // News of AS of Chuvash Republic. 1996. No. 6. P. 94–104.
- [2] Kartuzova T. V. Numerical research of wing profile with slat and flap // Works of the VI All-Russian scientific conference “Hydrodynamics of High Speeds”. — Cheboksary: Chuvash State University publishing house, 1996. — P. 90–96.

Non-rough cycles in a model of two delayed oscillators

Alexandra A. Kashchenko

P. G. Demidov Yaroslavl State University, Yaroslavl, Russia

Consider system of two delay differential equations

$$\begin{aligned}\dot{u}_0 + u_0 &= \lambda F(u_0(t - T)) + \gamma_1 \lambda^{-\alpha} (u_1 - u_0), \\ \dot{u}_1 + u_1 &= \lambda F(u_1(t - T)) + \gamma_1 \lambda^{-\alpha} (u_0 - u_1).\end{aligned}\tag{1}$$

Here u_0 and u_1 are scalar functions, delay time T , coefficient λ , and coupling parameter γ_1 are positive, parameter α belongs to interval $(1/2, 1)$, $F(u)$ is some nonlinear function. We assume that function $F(u)$ is bounded, piecewise smooth and compactly supported, i.e., there exists a positive p such that

$$F(u) = \begin{cases} f(u), & |u| \leq p, \\ 0, & |u| > p, \end{cases}\tag{2}$$

where function $f(u)$ satisfies conditions

$$\begin{aligned}uf(u) &> 0 \text{ for all } 0 < |u| < p, \quad f(-p) = f(0) = f(p), \\ f'(p) &\neq 0, \quad f'(-p) \neq 0.\end{aligned}\tag{3}$$

System (1) with this type of nonlinearity simulates two coupled oscillators with delayed feedback. Such oscillators can be applied to manufacture D-class amplifiers and sonars, and to control ultrasonic welding [1].

We assume that parameter λ is sufficiently large

$$\lambda \gg 1.\tag{4}$$

Using asymptotic methods, we investigate [2] existence of relaxation periodic solutions of system (1) under conditions (2), (3), (4). For this purpose we construct a special set in the phase space of initial system. Then we build asymptotics of all solutions of the given system with initial conditions from this set. Using this asymptotics, we construct a special finite-dimensional mapping. Dynamics of this mapping describes the dynamics of the initial problem in general: non-rough cycles of this mapping correspond to non-rough inhomogeneous relaxation periodic asymptotic (by the discrepancy) solutions of initial infinite-dimensional system. It is proved that all solutions of constructed mapping are non-rough cycles of period two. As a result, we obtain that the initial system has a two-parameter family of non-rough inhomogeneous relaxation periodic asymptotic (by the discrepancy) solutions with amplitude $O(\lambda)$ and period $T_0(\lambda) = (1 + o(1)) \ln \lambda$ as $\lambda \rightarrow +\infty$.

References

- [1] Kiliyas T. et al. *Electronic chaos generators-design and applications*// International journal of electronics, 1995, vol. 79, no. 6, pp. 737–753.
- [2] Kashchenko A. A. *A Family of Non-Rough Cycles in a System of Two Coupled Delayed Generators*// Automatic Control and Computer Sciences, 2017, vol. 51, no. 7, pp. 753–756.

Asymptotic of spatially inhomogeneous solutions of the system with a space deviation

Iliia S. Kashchenko

P. G. Demidov Yaroslavl State University, Yaroslavl, Russia

Consider parabolic equation with deviation of spatial variable

$$\frac{\partial u}{\partial t} + u = \varepsilon \frac{\partial^2 u}{\partial x^2} + K \sin u(t, x - h) \quad (1)$$

and periodic boundary conditions

$$u(t, x + 2\pi) \equiv u(t, x). \quad (2)$$

Here $0 < \varepsilon \ll 1$, $K \in R$. Value h describes the deviation of the spatial variable (rotation of the field at an angle of h). Let h be close to rationally proportional to 2π number, i.e. for some coprime m_1 and m_2

$$h = 2\pi \frac{m_1}{m_2} + \mu,$$

where μ is another small parameter: $0 < \mu \ll 1$.

Let u_0 be uniform equilibrium of (1), (2): $u_0 = K \sin u_0$. The problem is to investigate the behavior of solutions (1), (2) for $t \geq 0$ in some sufficiently small (but fixed) neighborhood of u_0 .

Denote $p = K \cos u_0$. If $|p| < 1$ then the behavior of solutions with initial conditions from some neighborhood of u_0 is trivial: all of them tends to u_0 . If $|p| > 1$ then almost all solutions from some neighborhood of u_0 leave it. The dynamics is nonlocal. Other two cases are critical.

The most interesting case occurs when the parameter p is close to -1 . So for some small ν we have $p = -1 - \nu$.

Thus, the problem contains three small parameters at once: ε , μ and ν . Their ratio is very important and has a significant impact on the results and the course of research.

In the critical case under consideration, the real parts of the infinite set of roots of the characteristic equation tend to zero as $\varepsilon, \mu, \nu \rightarrow 0$. Thus, we can say that the realizable critical case has infinite dimension.

The main result of the work is that the original problem in the case under study is reduced to a so-called. the quasinormal form – a family of nonlinear equations independent of small parameters whose solutions give the

main parts of the asymptotic approximation of the solutions of the original problem that is uniform over all $t \geq 0$ [1,2].

The author were supported by the Russian Foundation for Basic Research (project no. 18-01-00672).

References

- [1] Kashchenko S. A. *Asymptotics of spatially inhomogeneous structures in coherent nonlinear-optical systems* // U.S.S.R. Comput. Math. Math. Phys., 1991, vol. 31, No. 3, pp. 97–102.
- [2] Kashchenko I. S., Kashchenko S. A. *Rapidly oscillating spatially inhomogeneous structures in coherent nonlinear optical systems* // Doklady Mathematics, 2010, vol. 82, No. 3, pp. 850–853.

Generalization of the Joukowski-Chaplygin solution of the plane hydrodynamic problem in eccentric ring

Anastasia O. Kazakova

Chuvash State University, Cheboksary, Russia

In 1906 N. E. Joukowski and S. A. Chaplygin have considered a friction of a lubricating layer between the spike and the bearing from a mathematical point of view [1]. By its hydrodynamic essence, this is the problem of research of a viscous fluid between two eccentrically arranged circular cylinders, one of which (the spike, inner cylinder) rotates with a constant angular velocity and the second one (the bearing, outer cylinder) is motionless. In this work we will consider the rotation of both inner and outer cylinders. Such a statement has many important applications in other fields too. Mathematical model of the problem is described by boundary value problem for biharmonic equation in eccentric ring. For solving it we will use bipolar coordinates in the same way as N. E. Joukowski and S. A. Chaplygin. The Reynolds number is assumed to be small and the equations of motion are solved in the linear Stokes approximation.

Fig. 1 shows the cross section of the domain between two circular cylinders. The radii of the outer and inner circles are ρ_1 and ρ_0 , respectively, and the distance between their centers is Δx .

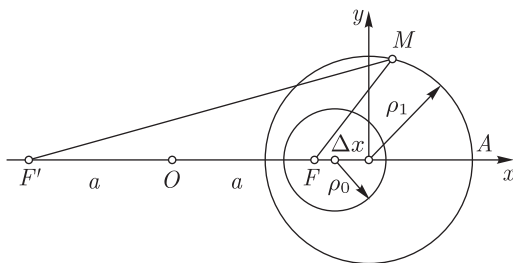


Fig. 1. Bipolar coordinates $\xi_M = \angle MFA - \angle MF'A$, $\eta_M = \ln(F'M/FM)$ and lines $\eta = \text{const}$

In order for the center of the outer circle to lie at the origin of the Cartesian coordinate system, we will use the bipolar coordinates which are somewhat different from those used in [1]. The relation between the considered

bipolar coordinates and the Cartesian coordinates expresses by formulas:

$$\eta = \frac{1}{2} \ln \frac{(x-c+a)^2 + y^2}{(x-c-a)^2 + y^2}, \quad \xi = \operatorname{arctg} \frac{x-c+a}{y} - \operatorname{arctg} \frac{x-c-a}{y}, \quad (1)$$

where $2a$ is the distance between the poles F and F' and $c = -a \operatorname{cth} \eta_1$.

The problem reduces to determination of the biharmonic stream function Ψ inside the domain between two circles: the outer circle $\eta = \eta_1$ of radius ρ_1 and the inner circle $\eta = \eta_0$ of radius ρ_0 , the distance between their centers is equal to Δx . From (1) the equalities follow:

$$a = \frac{\sqrt{(\Delta x^2 - \rho_1^2 - \rho_0^2)^2 - 4\rho_1^2\rho_0^2}}{2\Delta x}, \quad (2)$$

$$\eta_1 = \ln \frac{\sqrt{a^2 + \rho_1^2} + a}{\rho_1}, \quad \eta_0 = \ln \frac{\sqrt{a^2 + \rho_0^2} + a}{\rho_0}.$$

In [1] it was shown that the function Ψ can be represented as the linear combination of biharmonic functions. Using simple algebraic transformations we bring it to the following form:

$$\Psi = N(\eta) + M(\eta) / (\operatorname{ch} \eta - \cos \xi), \quad N(\eta) = A\eta - F \operatorname{ch} 2\eta - G \operatorname{sh} 2\eta$$

$$M(\eta) = B \operatorname{sh} \eta + C \operatorname{ch} \eta + E\eta \operatorname{sh} \eta + F \operatorname{ch} \eta \operatorname{ch} 2\eta + G \operatorname{ch} \eta \operatorname{sh} 2\eta. \quad (3)$$

The boundary conditions of the problem: the inner and the outer cylinders rotate with angular velocities ω_0 and ω_1 , respectively; then on their surfaces the velocities are equal to $U_0 = \omega_0\rho_0$ and $U_1 = \omega_1\rho_1$. The stream function Ψ is constant on both surfaces. Hence there follow the conditions for the functions $M(\eta)$ and $N(\eta)$ which enter into (3):

$$M(\eta_k) = 0, \quad \left. \frac{dN}{d\eta} \right|_{\eta=\eta_k} = 0, \quad \left. \frac{dM}{d\eta} \right|_{\eta=\eta_k} = -U_k a, \quad k = \overline{0, 1}. \quad (4)$$

From the conditions (4) we can determine coefficients of the function Ψ . Thus, we obtain the solution of the generalized Joukowski–Chaplygin problem for the stream function $\Psi(\xi, \eta)$.

The report also provides a detailed analysis of the structure of viscous fluid flow. The flow structure is determined by the presence of stagnation points at which the flow velocity vanishes. They can be located on the x axis. For example, in Fig. 2, in which we have reproduced the streamlines for $\rho_1 = 1$, $\rho_0 = 0.3$, $\Delta x = 0.35$, $\omega_0 = 1$, $\omega_1 = -4$, there are two stagnation points K_0 and K_1 . A vortex is formed in the neighborhood of these points.

The reported study was funded by RFBR according to the research project No. 18-31-00220.

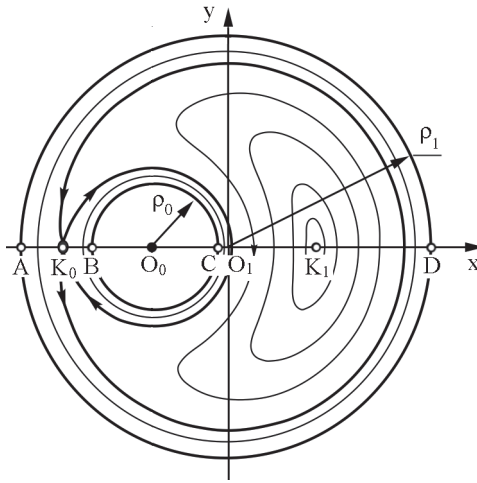


Fig. 2. Diagram of fluid flow between two cylinders rotating in opposite directions

References

- [1] Joukowski N. E., Chaplygin S. A. Friction of a Lubricating Layer between the End Journal and the Bearing // Tr. Otdeleniya Fiz. Nauk O-va Lyubitelei Estestvoznaniya, 1906, vol. 13, no. 1, pp. 24–33. (In Russian).

Numerical solution of the boundary value problems for the Poisson's equation in the plane domain

Anastasia O. Kazakova¹, Evgenia A. Mikishanina¹

¹ *Chuvash State University, Cheboksary, Russia*

The generalization of the numerical boundary element method [1] for the Poisson's equation with a known right-hand side in a plane domain D

$$\Delta u(x, y) = f(x, y), \quad (x, y) \in D \quad (1)$$

is given. Two boundary value problems with the following boundary conditions are considered:

1) Dirichlet condition:

$$u|_{\partial D} = g_0(s), \quad s \in \partial D, \quad (2)$$

2) Neumann condition:

$$\left. \frac{\partial u}{\partial n} \right|_{\partial D} = g_1(s), \quad s \in \partial D, \quad (3)$$

where $\frac{\partial}{\partial n}$ is the normal derivative, $g_0(s)$, $g_1(s)$ are given real functions, Δ is the Laplace operator.

If the function $f(x, y)$ is a polyharmonic function of some order $n - 1$ it follows from equation (1) that u is the polyharmonic function of n order and satisfies the equation

$$\Delta^n u = 0. \quad (4)$$

In particular, the piecewise polynomial approximation of the function f in the domain D can be applied. As $n - 1$ missing boundary conditions for equation (4), it is easy to obtain the following equations [2]:

$$\Delta u = f(x, y), \quad \Delta^2 u = \Delta f(x, y), \quad \dots, \quad \Delta^{n-1} u = \Delta^{n-2} f(x, y). \quad (5)$$

The polyharmonic equation (4) reduces to a system of linear integral equations [3]:

$$\varepsilon u_j + \sum_{p=0}^{n-j-1} \oint_{\partial D} u_{j+p} H_p ds - \sum_{p=0}^{n-j-1} \oint_{\partial D} q_{j+p} G_p ds = 0, \quad (6)$$

$$(j = \overline{0, n-1}), \quad \varepsilon = 0.5$$

where

$$u_j = \Delta^j u, \quad q_j = \frac{\partial u_j}{\partial n},$$

$$G_p = \frac{1}{2\pi} \frac{r^{2p}}{4^p (p!)^2} \left(\ln \frac{1}{r} + \sum_{m=1}^p \frac{1}{m} \right), \quad H_p = \frac{\partial G_p}{\partial n}. \quad (7)$$

To construct a numerical solution using the linear boundary element method, the boundary of the domain D is replaced by a polygon C with N sides (elements), the boundary conditions are satisfied at the middle (control) points of the elements. So the system (6) is written as a system of nN linear algebraic equations with respect to $2nN$ discrete values of functions $u_j(Z_k)$ and their normal derivatives $q_j(Z_k) = \mathbf{n}_k \cdot \Delta u_j(Z_k)$ at control points Z_k . To solve this system, it is necessary to set nN values of these functions, they are determined by the boundary conditions (2) and (5), or (3) and (5) depending on the type of the boundary value problem. By solving the system, the value of the function $u(z)$ at an arbitrary interior point of the domain D can be determined from the equality (6) when $\varepsilon = 1$.

The effectiveness of the method is confirmed by comparison of numerical results and analytical solutions on test examples, one of which is presented below.

Example 1. To compare the numerical solution with the analytical function, we consider a polyharmonic function $u(x, y) = x^3(x^2 - 5y^2)$, which is a solution to the equation

$$\Delta u = 10x^3 - 30xy^2. \quad (8)$$

We solve equation (8) numerically in a circular ring with inner and outer radii $a = 4$, $b = 5$, if the Dirichlet condition is given.

Using the method described above the equation (8) is reduced to the biharmonic equation and then we obtain a system of linear equations relatively unknown values of functions q_0, q_1 . On Fig. 1 the results of the analytical and numerical ($N = 50$) solutions on the contour

$$x = 4.5 \cos s, \quad y = 4.5 \sin s, \quad s \in [0, 2\pi),$$

are presented.

The reported study was funded by RFBR according to the research project No. 18-31-00220.

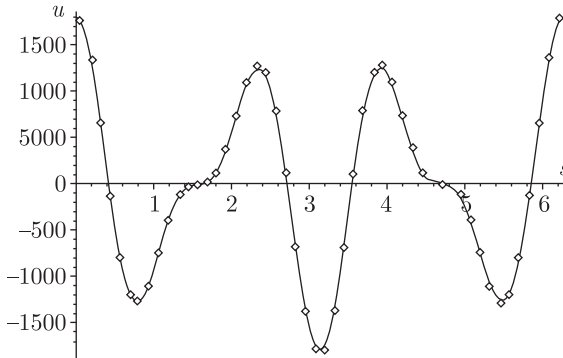


Fig. 1. Analytical (solid line) and numerical (points) solutions of the Dirichlet problem for equation (8)

References

- [1] Kazakova A. O., Terent'ev A. G. Numerical solution of boundary value problems for a polyharmonic equation // *Zh. Vychisl. Mat. i Mat. Fiz.*, 2012, vol. 52, no. 11, pp. 2050–2059. (in Russian)
- [2] Kazakova A. O. The numerical modeling of the arbitrary shape thin plate's bending // *Nauchno-tekhnicheskii vestnik Povolzh'ya*, 2013, no. 6, pp. 301–304. (in Russian)
- [3] Kazakova A. O. The boundary integral representation of polyharmonic function // *Scientific forum: technical and physical-mathematical Sciences. Proc. Int. Conf.*, 2018, pp. 76–77. (in Russian)

Nonlinear stability analysis of relative equilibria of a solid carrying a movable point mass in the central gravitational field

Olga V. Kholostova

Moscow Aviation Institute (National Research University), Moscow, Russia

We consider the motion of a solid body of mass M in the central Newtonian gravitational field. Let the body contain a point of mass m moving along one of the principal central axes of inertia of the body (Oy) according to a given law $s = s(t)$. The orbit of the center of mass of the system "body-point" is assumed to be elliptic with an arbitrary eccentricity e ($0 < e < 1$).

Earlier [1], for an arbitrary law of motion of a point mass in the body, differential equations of motion of this system (of the Euler - Poisson equation type) were obtained. For the mentioned straight-line law, the existence of planar motions of a body was shown, for which its principal axis of inertia Oz is perpendicular to the orbit plane. These motions are described by the equations

$$\begin{aligned} \frac{d}{dt}[(J_z + \mu s^2)(\dot{\varphi} + \dot{\nu})] + \frac{3k}{R_C^3}(J_x - J_y + \mu s^2) \sin \varphi \cos \varphi &= 0, \\ \dot{\nu} &= \frac{n}{(1 - e^2)^{3/2}}(1 + e \cos \nu)^2, \\ \frac{k}{R_C^3} &= \frac{n^2}{(1 - e^2)^3}(1 + e \cos \nu)^3, \quad \mu = \frac{mM}{m + M}. \end{aligned}$$

Here J_x, J_y, J_z are the principal central moments of inertia of the body, ν is the true anomaly, n the average motion of the center of mass of the system in orbit.

If the relation $s = s(\nu)$ when passing to ν instead of t is given by

$$J_z + \mu y^2(\nu) = [J_z + \mu y^2(0)] \left(\frac{1 + e}{1 + e \cos \nu} \right)^2, \quad (1)$$

then in the system "body-point", there are relative equilibria $\varphi = 0$ and $\varphi = \pi/2$,

Equation (1) with regard to expression (2) can be rewritten in the form of Hamiltonian canonical equations with the Hamiltonian function

$$\begin{aligned} H &= \frac{1}{2} p_\varphi^2 + \frac{1}{2} \left(\frac{(s - 3)(1 + e \cos \nu)}{(1 + e)^2} + \frac{3}{1 + e \cos \nu} \right) \sin^2 \varphi, \\ s &= 3 \frac{J_x - J_y + \mu y^2(0)}{J_z + \mu y^2(0)} \quad (-3 \leq s \leq 3), \end{aligned} \quad (2)$$

in which a new independent variable ν is introduced.

A linear stability analysis of the particular solutions $\varphi = \varphi_0$, $p_\varphi = 0$ and $\varphi_0 = 0$ or $\pi/2$ of the system with Hamiltonian (2) was carried out in [1].

In this paper, we perform a nonlinear stability analysis of these relative equilibria in the linearly stable regions and on the boundary curves of parametric resonance regions. For this purpose, using the algorithm developed in [2], the area-preserving mapping generated by the motions of the considered Hamiltonian system has been normalized over a time interval equal to the period 2π . Then, using this function, the form of the normalized Hamiltonian in terms up to the fourth degree inclusive with respect to perturbations has been restored, and the known conditions for stability and instability of nonlinear time-periodic one-degree-of-freedom Hamiltonian systems have been examined.

A non-resonant case, fourth order resonance cases, and first and second order resonance cases (corresponding to the boundaries of parametric resonance regions) were distinguished. It is revealed that in non-resonant cases the conditions of the Arnold - Moser theorem are always satisfied (and there are no degeneracy cases), therefore the relative equilibria considered are stable. On the fourth-order resonance curves, the stability of these solutions always holds. At the boundaries there is an alternation of stable and unstable curves.

The report was supported by RFBR (project no. 17-01-00123).

References

- [1] Markeev A.P. *Dynamics of a Satellite Carrying a Point Mass Moving about It* // Mech. Solids. 2015, vol. 50, no. 6, pp. 603-614.
- [2] Markeyev A.P. *A method for analytically representing area-preserving mappings* // J. Appl. Math. Mech. 2014, vol. 78, no. 5, pp. 435-444.

Topological Analysis and Absolute Dynamics of the Nonholonomic Rolling of a Rubber Wheel with Sharp Edges

Alexander A. Kilin¹, Elena N. Pivovarova²

¹ *Moscow Institute of Physics and Technology, Dolgoprudny, Russia*

² *Udmurt State University, Izhevsk, Russia*

We consider the dynamics of a body formed by truncating a ball by two parallel planes at an equal distance from its geometric center (Fig. 1), and call it a wheel. The sections formed by the intersection of the ball with the planes are two flat segments on it (with sharp edges).

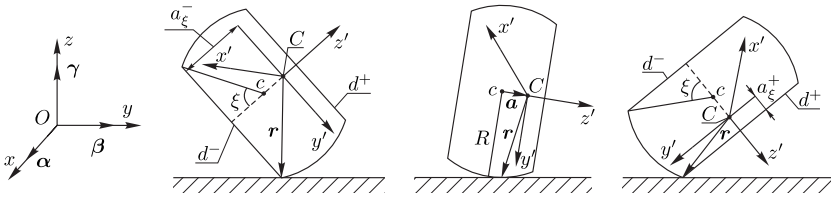


Fig. 1. A schematic model of a moving wheel in cases where the point of contact with the supporting plane lies on the edge of disk d^- , on the spherical part, and on the edge of disk d^+ (from left to right).

We assume that the center of mass of the wheel is (in the general case) displaced along its symmetry axis. To describe the dynamics of the wheel, we use two models of motion: the ball's model featuring a rolling wheel with its spherical part in contact with the supporting plane, and the model of a rolling disk with its sharp edge in contact with the supporting plane. We also assume that the wheel rolls without slipping on the horizontal plane at the point of contact and without rotation of the body about the vertical.

The equations of motion of the system have the form [1,2]

$$\begin{aligned} \tilde{\mathbf{I}}\dot{\boldsymbol{\omega}} &= \tilde{\mathbf{I}}\boldsymbol{\omega} \times \boldsymbol{\omega} - m\mathbf{r} \times (\boldsymbol{\omega} \times \dot{\mathbf{r}}) - mg(\boldsymbol{\gamma} \times \mathbf{r}) + \lambda_0\boldsymbol{\gamma}, \\ \dot{\boldsymbol{\gamma}} &= \boldsymbol{\gamma} \times \boldsymbol{\omega}, \end{aligned} \quad (1)$$

where $\boldsymbol{\gamma}$ is the unit vector of the vertical, $\boldsymbol{\omega}$ is the angular velocity vector of the wheel, m is the mass of the wheel, $\tilde{\mathbf{I}} = \mathbf{I} + m(\mathbf{r}, \mathbf{r}) \cdot \mathbf{E} - m\mathbf{r} \cdot \mathbf{r}^T$ is the tensor of inertia of the body relative to the contact point, $\mathbf{I} = \text{diag}(I_1, I_1, I_3)$ is the main tensor of inertia of the wheel, \mathbf{E} is the unit

matrix, and g is the free-fall acceleration. The multiplier λ_0 corresponds to the no-spin constraint and the radius vector of the contact point \mathbf{r} depends on the model of motion.

The aim of the work is to carry out a topological analysis of the partial solutions of the system (in particular, to construct a bifurcation diagram) and to analyze the dynamics of the wheel in a fixed reference frame depending on the system parameters.

In this work we show that the parameter space (a_0, ξ) can be divided into three regions, each of which has its own number of bifurcations of fixed points (degenerate solutions) of the system and hence its own type of bifurcation diagram on the plane (k, h) of first integrals:

- I. the region of existence of three degenerate solutions — two in the disk models and one on the boundary of change of the models of the ball and the disk d^+ ;
- II. the region of existence of one degenerate solution in the model of the disk d^- ;
- III. the region of existence of two degenerate solutions in the disk models ($a_0 = 0$).

All three types of bifurcation diagram are shown in Fig. 2.

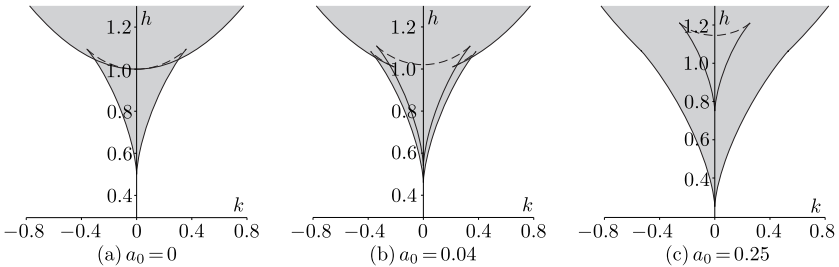


Fig. 2. Types of bifurcation diagrams plotted for constant values of the angle $\xi = \pi/3$ for different values of the displacement of the center of mass. The region of possible motions of the system is colored grey

We investigate the trajectories of the contact point on the surface of the wheel and make a classification of its motion depending on the presence or absence of transitions between the situations where the contact point lies on the spherical part of the wheel and on its edge. We also analyze the trajectories of the contact point on the plane and obtain conditions for their boundedness.

In particular, we show that for almost all permanent rotations the trajectory of motion of the wheel in a fixed reference frame is a circle. Exceptions are the cases of a balanced ball or a balanced thin disk, for which, with $\theta_0 = \pi/2$ (where θ_0 is the angle of inclination of the wheel's symmetry axis related to the vertical), the trajectory of motion is a straight line.

For the other rotations, we introduce the notion of rotation number ν as a ratio of rotation frequencies ω_ψ and ω_θ and formulate the following

Proposition. *Depending on the value of the rotation number, two types of trajectories of the contact point are possible for the resonant trajectories:*

- $\nu \in \mathbb{Z}$: in this case, an unbounded drift of the trajectory of the contact point to infinity takes place.
- $\nu \in \mathbb{Q} \setminus \mathbb{Z}$: in this case, the trajectories of motion are closed periodic curves.

Some examples of the trajectories of the wheel on a plane xy are shown in Fig. 3.

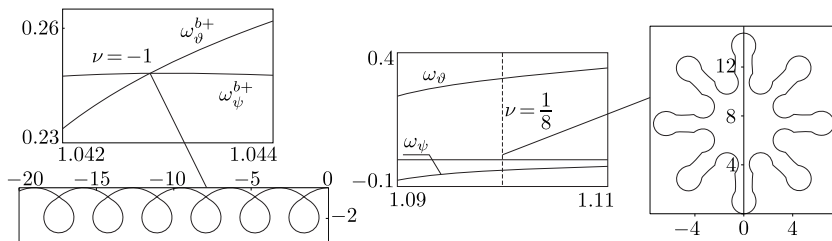


Fig. 3. Trajectories of motion of the wheel on the plane xy which correspond to different resonances for the case $a_0 = 0.04, k = 0.3$

This work is supported by the RFBR grants nos. 18-08-00999-a, 18-38-00344 mol_a and is carried out at MIPT under project 5-100 for state support for leading universities of the Russian Federation.

References

- [1] Kilin A. A., Pivovarova E. N., *Integrable Nonsmooth Nonholonomic Dynamics of a Rubber Wheel with Sharp Edges* // Regul. Chaotic Dyn., 2018, vol. 23, nos. 7–8, pp. 887–907.
- [2] Kilin A. A., Pivovarova E. N., *Qualitative Analysis of the Nonholonomic Rolling of a Rubber Wheel with Sharp Edges* // Regul. Chaotic Dyn., 2019, vol. 24, no. 2, pp. 212–233.

Appearance of working memory mechanism in self-organizing liquid state machine

Mikhail V. Kiselev

Chuvash State University, Cheboksary, Russia

Nowadays, usage of artificial neural networks in almost all spheres of everyday life is one of the most noticeable features of modern IT technologies. Neural network theory and applications have now several growth points. The most actively developed research directions are spiking neural networks (SNN) [1], convolutional and deep learning networks. Since SNNs themselves are complex non-linear dynamic systems, their specific application area is processing of dynamic signals such as video streams, sensory data in robotics or signals from technological sensors.

The most common form of SNN architecture used for solution of this kind of problems is the so called liquid state machine (LSM) [2], a computational model consisting of the two parts, chaotic SNN (a “liquid”) and read-out mechanism interpreting activity of the SNN. SNN included in LSM is chaotic in the sense that it has no predefined structure such as layers. Instead, its connectivity is random — presence of synaptic connection between two given neurons, weight of this connection and its delay are random variables obeying certain statistical distributions. Input data streams to be processed by LSM should be represented in the form of spike sequences (spike is a short pulse of the constant amplitude and negligible duration used for communication between neurons in SNN). The network responds to the external stimulation by activity of its neurons which may also depend on recent history of the input signal. The read-out mechanism uses measure of activity of the neurons as predictors for solution of various supervised learning problems. For this purpose, it can utilize any appropriate data mining method - logistic regression, support vector machine, anything else.

The crucial feature of SNN as a part of LSM is memory. In order to recognize a spatio-temporal pattern taking a significant interval on the time axis, SNN should store in memory the context of its beginning until its end is presented. It is why the question which SNN parameters provide it with long and stable memory is so important.

In the original version of LSM which is used now by the majority of researchers, neurons are not plastic — the synaptic plasticity is switched off. However, there are many reasons to believe that generalization of LSM where neurons are made plastic could gain significant advantages. In case

of appropriately selected synaptic plasticity rule, network self-organization could eliminate its circuits performing senseless or trivial operations and facilitate growth of neural ensembles producing informative predictors. This consideration has led us to concept of self-organizing LSM (SOLSM) — LSM with plastic neurons.

However, formation of the memory mechanism in evolving chaotic SNN is very poorly explored process. Some of the earlier works of the author were devoted to this subject [3, 4] (but for the structured SNNs). At present, the majority of working memory models in SNN is based on short-term plasticity sometimes combined with the concept of attractors, meta-stable states of the network preserving information in time [5], or effect of polychronization of neuronal groups [6]. However these approaches either cannot be used for chaotic networks or require too complicated two-component synaptic plasticity model (while traditional LSM does not use synaptic plasticity at all). It determined the goal of our project — finding chaotic SNN configuration making possible formation of working memory mechanism on the basis of conventional long-term synaptic plasticity.

In this research we explored chaotic SNN consisting of leaky integrate-and-fire neurons with plastic synapses. A homeostatic generalization of classic STDP plasticity model was used [7] (to avoid instability of SNN dynamics due to positive feedback inherent to STDP). Network memory ability was measured on simple simulated Poissonian external signals. LSM task was to determine set of input neurons emitting spikes with increased frequency but with significant time lag after returning their frequency to the base line (when another set of input neurons becomes more active).

Several SNN connectivity configurations have been tested. For example:

- “Neural gas”. Homogenous network with equal probability of synaptic connection, weight distribution and synaptic delay distribution for every pair of neurons.
- “Bottleneck”. Similar to “neural gas” but with only small part of neurons connected with input neurons.
- “Sphere”. Connections are chaotic but obey the “small world” distribution law — the neurons correspond to points of sphere and the connection probability for close neurons is much higher than for distant ones.

It was found that memory mechanism with satisfactory characteristics is formed in the third case only. The optimum connectivity parameters for this case were determined using genetic algorithm. Estimation of classification

efficiency of the best found SNN configuration shows its potential usability in real world problems.

References

- [1] Gerstner W., Kistler W. Spiking Neuron Models. Single Neurons, Populations, Plasticity. Cambridge University Press. 2002.
- [2] Maass W., Liquid state machines: motivation, theory, and applications, in Computability in context: computation and logic in the realworld. World Scientific, 2011, pp. 275–296.
- [3] Kiselev M. Self-Organization Process in Large Spiking Neural Networks Leading to Formation of Working Memory Mechanism // Proceedings of IWANN 2013 in LNCS 7902, I. Rojas, G. Joya, and J. Cabestany (Eds.), Part I, pp. 510–517.
- [4] Kiselev M. Self-organized Short-Term Memory Mechanism in Spiking Neural Network // Proceedings of ICANN 2011 Part I, Ljubljana, pp. 120–129.
- [5] Seeholzer A., Deger M., Gerstner W. Stability of working memory in continuous attractor networks under the control of short-term plasticity. // PLoS Comput Biol 15(4), 2019: e1006928. <https://doi.org/10.1371/journal.pcbi.1006928>
- [6] Szatmari B., Izhikevich E. Spike-Timing Theory of Working Memory // PLoS Computational Biology, 6(8):e1000879. 2010.
- [7] Kiselev M. Homogenous Chaotic Network Serving as a Rate/Population Code to Temporal Code Converter // Computational Intelligence and Neuroscience, vol 2014, Article ID 476580, 8 pages, 2014. doi:10.1155/2014/476580

A dynamic study of screwless fish-like robot with internal rotor

Anton V. Klekovkin^{1,3}, Evgeny V. Vetchanin², Ivan S. Mamaev^{1,3}

¹ *Kalashnikov Izhevsk State Technical University, Izhevsk, Russia*

² *Udmurt State University, Izhevsk, Russia*

³ *Center for Technologies in Robotics and Mechatronics Components, Innopolis University, Innopolis, Russia*

Many floating robotic vehicles move by rotating of propeller screws. Also mechanisms which copy organisms moving are popular. There are methods of moving in water by jet reaction drive, moving by transforming of body shape, moving by action of internal mechanisms. Using moving by action of internal mechanisms all driving elements are in body and don't associate with fluid. As a result construction of these robots are simple because contact movable elements with water is missing. First theoretical researches were presented at the beginning 2000 years [1,2].

There are some papers which describe different self-propulsion bodies in a fluid [3–10]. Experimental work with fish-like robots using internal mechanisms for moving describe in [11,12].

The paper describes control problem of the screwless overwater fish-like mobile robot, driven by an internal rotating rotor. The robot has a rigid case which doesn't be transform while moving.

Mathematical model of robot movement was developed. The equations describing the dynamic of moving of screwless fish-like robot taking into account circulation and viscous friction forces were written. Circulation is calculated according to the Kutta-Chaplygin condition. Coefficients of fluid resistance depend on moving mode and they were determined from experiments.

The robot is a hollow object with dimensions of 340×134 mm. The height of the robot is 80 mm (see Fig. 1). The rotor with the motor is fixed inside the body. The motor is a gear-motor Pololu with encoder. Also inside the robot the battery and control board with STM32F303K8 microcontroller are placed. To control the motor, a DC motor driver VNH3SP30 is used.

To confirm theoretical moving model five series of experimental researches with different control actions were carried out in circular pool. The rotor changed rotational direction at regular intervals. The interval were different for each series of experimental researches, but rotational velocity and acceleration were maximal and limit oneself to possibilities of the motor. Results of experimental researches were compared with modelling results.

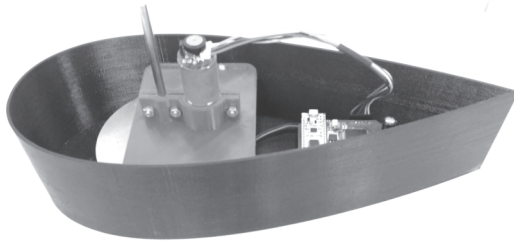


Fig. 1. Screwless fish-like robot with internal rotor

This work is supported by the RFBR under grant 18-08-00995-a.

References

- [1] Kozlov V.V. Ramodanov, S.M. *The Motion of a Variable Body in an Ideal Fluid*// J. Appl. Math.Mech., 2001, vol. 65, no. 4, pp. 579–587.
- [2] Kozlov, V.V., Ramodanov, S.M. *On the Motion of a Body with a Rigid Hull and Changing Geometry of Masses in an Ideal Fluid*// Dokl. Phys., 2002, vol. 47, no. 2, pp. 132–135.
- [3] Tallapragada P., Kelly S.D., Bhattacharya T., Fairchild M. J. *Self-propulsion of a spherical body shedding coaxial vortex rings in an ideal fluid: Hamiltonian modeling and simulation*// 2012 American Control Conference (ACC), IEEE, 2012, pp. 1755–1760.
- [4] Vetchanin E. V., Kilin A. A., Mamaev I. S. *Control of the Motion of a Helical Body in a Fluid Using Rotors*// Regular and Chaotic Dynamics, 2016, vol. 21, no. 7–8, pp. 874–884.
- [5] Borisov A. V., Mamaev I. S., Vetchanin E. V., *Self-propulsion of a Smooth Body in a Viscous Fluid Under Periodic Oscillations of a Rotor and Circulation*// Regular and Chaotic Dynamics, 2018, vol. 23, no. 7–8, pp. 850–874.
- [6] Mamaev I. S., Vetchanin E. V. *The Self-propulsion of a Foil with a Sharp Edge in a Viscous Fluid Under the Action of a Periodically Oscillating Rotor*// Regular and Chaotic Dynamics, 2018, vol. 23, no. 7–8, pp. 875–886.
- [7] Volkova L. Yu., Jatsun S.F. *Control of the Three-Mass Robot Moving in the Liquid Environment*// Rus. J. Nonlin. Dyn., 2011, vol. 7, no. 4, pp. 845–857 (Russian).
- [8] Chernous'ko F.L., Bolotnik N. N. *Mobile Robots Controlled by the Motion of Internal Bodies*// Tr.Inst.Mat.iMekh.UrORAN, 2010, vol. 16, no. 5, pp. 213–222 (Russian).

- [9] Vethanin E. V., Karavaev Yu. L., Kalinkin A. A., Klekovkin A. V., Pivovarova E. N. *Model of screwless underwater robot*// Vestn. Udmurtsk. Univ. Mat. Mekh. Komp. Nauki, 2015, vol. 25, no. 4, pp. 544–553.
- [10] Karavaev Y. L., Kilin A. A., Klekovkin A. V. *Experimental investigations of the controlled motion of a screwless underwater robot*// Regular and Chaotic Dynamics, 2016, vol. 21, no. 7–8, pp. 918–926.
- [11] Tallapragada P. *A swimming robot with an internal rotor as a nonholonomic system*// 2015 American Control Conference (ACC), IEEE, 2015, pp. 657–662.
- [12] Pollard B., Tallapragada P. *An aquatic robot propelled by an internal rotor*// IEEE/ASME Transactions on Mechatronics, 2017, vol. 22, no. 2, pp. 931–939.

Chaplygin parabolic pendulum problem: Liouville equivalence invariants

Ivan F. Kobtsev

Moscow State University, Moscow, Russia

The parabolic pendulum problem was formulated by S. A. Chaplygin. In [1] possible motions of this mechanical system were studied and first integrals were found.

The formulation of the problem: massive particle moves on the surface P given by equation $\frac{y^2}{a+b} + \frac{z^2}{b} = 2x + b$, $a, b > 0$. The force $m\vec{g} = (-mg, 0, 0)$ is applied to the particle; friction equals zero. The main goal is to describe phase topology of this mechanical system. This is Hamiltonian system with two degrees of freedom, it has two first integrals: total energy H and additional integral F . The system is defined on symplectic manifold $M^4 = T^*P$ with canonical symplectic structure, dimension of M^4 equals 4.

In [2] the theory of Hamiltonian systems two degrees of freedom is constructed. According to this theory we will describe the phase topology in terms of Fomenko–Zieschang invariants. Namely, it is a way to describe topology of isoenergetic manifold $Q_h^3 = \{x \in M^4 : H = h\}$. Classical way of topological analysis in this case is rather complicated due to the explicit evaluating bifurcation diagram by differentiation. Nevertheless there exists coordinate system (v, w) , in which the equations of motion take the next form:

$$\dot{v} = \pm \frac{4}{w-v} \sqrt{R(v)}, \quad \dot{w} = \pm \frac{4}{w-v} \sqrt{R(w)},$$

where

$$R(z) = 2 \frac{(a-z)z}{(z+b)} (\alpha z^2 - \beta z + f), \quad \alpha = \frac{m^2 g}{8}, \quad \beta = \frac{m^2 g}{8}(a+b) + \frac{mh}{4},$$

$H = h$, $F = f$ are fixed values of first integrals; (v, w) are parabolic coordinates such that

$$x = \frac{v+w-b-a}{2}, \quad y^2 = \frac{(a+b)(a-v)(w-a)}{a}, \quad z^2 = \frac{b}{a}vw$$

This representation makes possible to obtain integral manifolds and their bifurcations in algebraical way. The new method of topological analysis is described in [3].

One remarkable fact is that the type of integral manifolds depends on g . So, if $g > 0$, integral manifolds are compact and homeomorphic to the union of 2-dimensional tori. If $g < 0$, integral manifolds are homeomorphic to the union of 2-dimensional cylinders $\mathbb{R}^1 \times S^1$. Their bifurcations are non-compact too (atoms with non-compact foliations are denoted by bar in fig. 1; all notations are the same as in [2]).

Full list of Fomenko–Zieschang invariants obtained in this problem is given in fig. 1 (in case $g > 0$) and fig. 2 (in case $g < 0$).

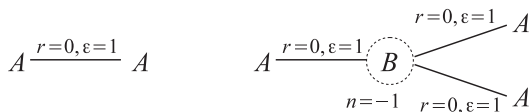


Fig. 1. Isoenergetic invariants in Chaplygin problem, $g > 0$

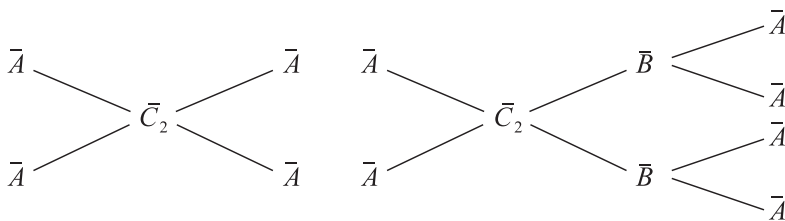


Fig. 2. Isoenergetic invariants in Chaplygin problem, $g < 0$

References

- [1] Chaplygin S.A. *On the paraboloidal pendulum.* // Complete works. Vol.1 Leningrad, 1953. pp. 194–200.
- [2] Bolsinov A.V., Fomenko A.T. *Integrable hamiltonian systems: geometry, topology, classification* Izhevsk: Publishing house "Udmurt University", 1999.
- [3] Kharlamov M.Ā. *Topological analysis and boolean functions: I. Methods and applications to classical systems* // Nonlinear dynamics, 2010, vol.6, no.4, pp. 769–805.

The flow around a thin profile with perforated contour lines

Alexander Ja. Kornilov¹, Alevtina G. Kulagina¹, Ildus Ju. Jusupov¹,
Dmitry V. Bobin¹

¹ *Chuvash State University, Cheboksary, Russia*

The study of the flow around permeable plates and profiles is of great theoretical and practical interest. The most important contribution to this branch of mechanics was made by A.I. Nekrasov [2] (“Obtekanie profilja Zhukovskogo pri nalichii na nem istochnika i stoka” [The flow around Zhukovski profile with a source and a sink], 1947), G.P. Tumashev and M.G. Nuzhin (“Obratnye kraevye zadachi i ih prilozhenija” [Inverse boundary value problems and their applications], 1955), Yu.F. Orlov (“O glisirovanii plastiny v prisutstvii svjazannogo vihrja po poverhnosti ideal’noj zhidkosti konechnoj glubiny” [On the gliding of a plate in the presence of a coupled vortex over the surface of an ideal fluid of finite depth], 1967), A.V. Galanin (“O vlijanii osobennostej na pod'emnuju silu profilja v ogranichenom potoke zhidkosti” [On the influence of features on the lifting force of the profile in a limited fluid flow], 1974).

In [1], the simulation results of the flow around a plate with special characteristics on contours are presented, the thickness of the profile being neglected. The paper presents the results of solving the problem of flowing around a thin profile with perforations on the contours. The perforations are modeled using a “sink-and source” hydrodynamic method. The formulas were obtained and a numerical experiment was carried out to calculate the main force vector of the flow pressure on the profile, as well as the profile moment relative to the leading edge.

The results:

1. Permeable holes in any of their locations on the profile and in any set of them reduce the lifting force.

2. The maximum positive effect for the moment of pressure forces can be achieved when one hole is located on the back side of the profile (closer to the rear edge) and perforate half of the lower edge of the profile closer to the axis of rotation.

References

- [1] Kornilov A. Ja. Obtekanie plastiny s osobennostjami na konturah /A.Ja. Kornilov, E.V. Vasil’eva. Matematicheskie metody i ih prilozhenija: sb. nauch. trudov [The

flow around a plate with special characteristics on contours. In: *Mathematical methods and their applications: collection of Academic works*, Cheboksary, Chuvash State University Publ., 2016. P. 96–99.

- [2] Nekrasov A. I. Obtekanie profilja Zhukovskogo pri nalichii na profile istochnika i stoka /A.I. Nekrasov. *PMM* [The flow around Zhukovski profile with a source and a sink. In: *J. Appl. Math. Mech.*], 1947. V. 11. No. 1. P. 41–54.

About realization of Jordan-Kronecker invariants of Lie algebras

Ivan K. Kozlov

*Faculty of Mathematics and Mechanics,
M. V. Lomonosov Moscow State University, Moscow, Russia*

Two Poisson brackets \mathcal{A} and \mathcal{B} on a finite-dimensional manifold M are called *compatible* if their sum $\mathcal{A} + \mathcal{B}$ is also a Poisson bracket. Since each Poisson bracket is given by a Poisson bivector, two Poisson brackets on M define a pair of skew-symmetric forms in each cotangent space T_p^*M . The canonical form for a pair of skew-symmetric bilinear forms is given by the well-known Jordan-Kronecker theorem (see e.g. [1]).

Jordan-Kronecker theorem. *For any two skew-symmetric bilinear forms A, B on a finite-dimensional vector space V over an algebraically closed field \mathbb{K} there exists a basis of V such that the matrices of A and B are block-diagonal:*

$$A = \begin{pmatrix} A_1 & & \\ & \ddots & \\ & & A_n \end{pmatrix}, \quad B = \begin{pmatrix} B_1 & & \\ & \ddots & \\ & & B_n \end{pmatrix}$$

where each pair of corresponding blocks A_i and B_i is one of the following:

- the Jordan block with eigenvalue $\lambda \in \mathbb{K} \cup \{\infty\}$:

$$A_i = \begin{pmatrix} 0 & J_{\lambda,k} \\ -J_{\lambda,k}^T & 0 \end{pmatrix}, \quad B_i = \begin{pmatrix} 0 & E_k \\ -E_k & 0 \end{pmatrix}.$$

Here $J_{\lambda,k}$ and E_k are the $k \times k$ Jordan block and identity matrix respectively. Here the jordan ∞ -block for A and B is the Jordan 0-block for B and A .

- the Kronecker block:

$$A_i = \left(\begin{array}{ccc|ccc} & & & 1 & 0 & \\ & 0 & & & \ddots & \ddots \\ & & & & & 1 & 0 \\ \hline -1 & & & & & & \\ 0 & \ddots & & & & & 0 \\ & \ddots & -1 & & & & \\ & & & 0 & & & \end{array} \right),$$

$$B_i = \left(\begin{array}{ccc|ccc} & & & 0 & 1 & \\ & & & & \ddots & \ddots \\ & 0 & & & & 0 & 1 \\ \hline 0 & & & & & & \\ -1 & \ddots & & & & & \\ & \ddots & & 0 & & & \\ & & & -1 & & & \end{array} \right)$$

Here each Kronecker block is a $(2k_i + 1) \times (2k_i + 1)$ block, where $k_i \geq 0$.

Jordan-Kronecker invariants of a pair of compatible Poisson brackets are:

- 1) the number of distinct eigenvalues λ_i of the Jordan blocks,
- 2) the number and sizes of the Jordan blocks for each eigenvalue λ_i ,
- 3) the number and sizes of the Kronecker blocks.

We are interested in the Jordan-Kronecker invariants for *the argument shift pencil* on Lie coalgebras. For any finite-dimensional Lie algebra \mathfrak{g} there exist natural compatible Poisson brackets on the dual space \mathfrak{g}^* :

- the linear (*Lie-Poisson bracket*) bracket defined by the formula

$$\{f, g\}(x) := \langle x, [df|_x, dg|_x] \rangle,$$

- and the so-called “*bracket with a frozen argument*”

$$\{f, g\}_a(x) := \langle a, [df|_x, dg|_x] \rangle,$$

for any fixed $a \in \mathfrak{g}^*$.

Jordan-Kronecker invariants of a Lie algebra \mathfrak{g} are the JK invariants of $\{, \}$ and $\{, \}_a$, for a generic pair $(x, a) \in \mathfrak{g}^* \times \mathfrak{g}^*$.

In the talk we would partially answer the following question from [2] (see also [3]):

Question: *What JK invariants can be realised by a suitable Lie algebra?*
In particular, we would

- 1) answer that question completely in the Jordan and Kronecker cases,

- 2) describe some differential-geometric obstructions for realization of JK invariants in the general case.

The obstructions arise from the canonical form of compatible non-degenerate Poisson bracket described in [4].

Acknowledgments. This work was supported by the program “Leading Scientific Schools” (grant no. NSh-6399.2018.1, Agreement No. 075-02-2018-867)

References

- [1] Thompson R.C. , *Pencils of complex and real symmetric and skew matrices* // Linear Algebra and its Applications, 1991, vol. 147, pp. 323–371.
- [2] Bolsinov A. V., Izosimov A. M., Konyaev A. Y., Oshemkov A. A.: *Algebra and topology of integrable systems: research problems* // Trudy seminara po vektornomu itenzornomu analizu, 2012, vol. 28., pp. 119–191.
- [3] Bolsinov A. V., Zhang P., *Jordan–Kronecker invariants of finite-dimensional Lie algebras*, [arXiv:1211.0579v1](https://arxiv.org/abs/1211.0579v1)
- [4] Turiel F. J. *Classification locale simultanée de deux formes symplectiques compatibles* // Manuscripta Math., 1994, vol. 82, no.1, pp. 349–362.

Mechanical systems with hyperbolic chaotic attractors based on Froude pendulums

Sergey P. Kuznetsov^{1,2}, Vyacheslav P. Kruglov¹, Yulia V. Sedova¹

¹ *Saratov Branch Kotelnikov Institute of Radioengineering and Electronics of RAS, Saratov, Russia*

² *Udmurt State University, Izhevsk, Russia*

We introduce two mechanical models with uniformly hyperbolic Smale–Williams attractor based on Froude pendulums. Froude pendulum is a well-known example of mechanical self-oscillator [1].

The first model with Smale–Williams attractor consists of two Froude pendulums placed on a common shaft rotating at a constant angular velocity [2]. Pendulums undergo alternate braking by periodic application of frictional forces. The pendulums are weakly connected with each other by viscous friction. The dynamical equations of the system are:

$$\begin{aligned} \ddot{x} - [a - d(t) - bx^2]\dot{x} + \sin x &= \mu + \varepsilon(\dot{y} - \dot{x}), \\ \ddot{y} - [a - d(t + T/2) - by^2]\dot{y} + \sin y &= \mu + \varepsilon(\dot{x} - \dot{y}), \end{aligned} \tag{1}$$

$$d(t) = \begin{cases} 0, & t < T_0, \\ D, & T_0 < t < T/2, \\ 0, & T/2 < t < T, \end{cases} \quad d(t + T) = d(t),$$

where x and y are the angular coordinates of two pendulums. Parameters are assigned as follows:

$$\begin{aligned} a = 0.36, \quad b = 0.16, \quad \mu = 0.087, \quad \varepsilon = 0.0003, \\ D = 0.8, \quad T = 250, \quad T_0 = T/4. \end{aligned} \tag{2}$$

The parameters are chosen in such way that the basic frequency of the developed self-oscillatory mode is half of the frequency of the small oscillations. Therefore, when the brake of the pendulum is switched off, it will begin to swing in a resonant manner due to the action of the second harmonic from the another pendulum. As a result, when the second pendulum approaches the sustained self-oscillatory state, its phase appears to be doubled in comparison with the initial phase of the first pendulum. This corresponds to the expanding circle map (Bernoulli map) for the phase. As a volume contraction takes place along the remaining directions in the state space of the system, this will correspond to occurrence of the Smale–Williams solenoid as an attractor of the Poincaré map.

The second model is a single Froude pendulum placed on a shaft rotating at a constant angular velocity with delayed feedback and braking by periodic application of frictional force. Delayed feedback can be implemented using spring with one end contacting pendulum with viscous friction and another free. The equation is:

$$\ddot{x} - [a - d(t) - bx^2]\dot{x} + \sin x = \mu + \varepsilon[\dot{x}(t - \tau) - \dot{x}],$$

$$d(t) = \begin{cases} 0, & t < T_0, \\ D, & T_0 < t < T/2, \\ 0, & T/2 < t < T. \end{cases} \quad d(t + T) = d(t). \quad (3)$$

Parameters are assigned the same as (2) with $\tau = T/2$. The explanation of emergence of Smale–Williams solenoid in system (3) is similar to (1), but phase doubling occurs due to second harmonics of the signal transmitted through delayed feedback. Smale–Williams solenoid appears embedded in the infinite-dimensional phase space of the Poincaré map.

Models (1) and (3) were analyzed numerically. Lyapunov exponents of attractors were evaluated with largest close to Lyapunov exponent of Bernoulli mapping. The hyperbolicity of the chaotic attractors was tested numerically with the help of criterion based on analysis of angles of intersection of stable and unstable invariant subspaces of small perturbation vectors. Absence of tangencies between these subspaces was verified.

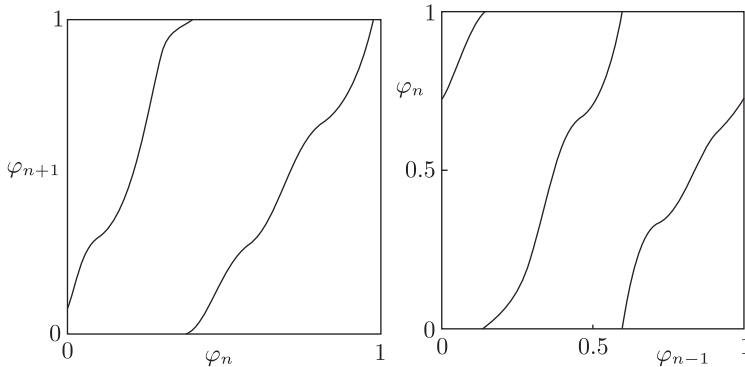


Fig. 1. Phase iteration diagrams of Poincaré maps of systems (1) (left) and (3) (right). Diagrams roughly correspond to Bernoulli map.

The development of the concept of the systems (1) and (3), the construction of a mathematical models and the verification of hyperbolicity were

carried out with the support of the grant of Russian Science Foundation No. 15-12-20035. Numerical calculations demonstrating a hyperbolic attractor of system (3) were carried out with the support of the grant of Russian Science Foundation No. 17-12-01008.

References

- [1] Rayleigh J. W. S., Lindsay R. B. *The Theory of Sound* // edition of 1945 // New York, 1877, pp. 243–305.
- [2] Kuznetsov S. P., Kruglov V. P. *Hyperbolic chaos in a system of two Froude pendulums with alternating periodic braking* // Communications in Nonlinear Science and Numerical Simulation, 2019, vol. 67, pp. 152–161.

Dynamics of phases and chaos in lattices of locally coupled conservative or dissipative oscillators

Vyacheslav P. Kruglov¹, Sergey P. Kuznetsov^{1,2}

¹ *Saratov Branch Kotelnikov Institute of Radioengineering and Electronics of RAS, Saratov, Russia*

² *Udmurt State University, Izhevsk, Russia*

We discuss three models of oscillator lattices with dynamics close to the model of phase lattice with nearest-neighbor coupling suggested by Topaj and Pikovsky [1]:

$$\dot{\psi}_k = \Delta_k + \varepsilon \sin \psi_{k+1} + \varepsilon \sin \psi_{k-1} - 2\varepsilon \sin \psi_k, \quad (1)$$

where ψ_k is a phase shift between nearest-neighboring oscillators, k runs from 1 to $N - 1$, Δ_k are frequency shifts, ε is coupling constant. Boundary conditions are $\psi_0 = \psi_N = 0$.

System (1) manifests a quasi-Hamiltonian dynamics for small couplings ε at linear frequency distribution ($\Delta_k = 1$ for all k). The average phase volume at small ε is conserved [1] due to reversibility – a symmetry of phase space under some special change of variables $\mathbf{R} : \{\psi_k\} \rightarrow \{\psi'_k\}$ called involution (\mathbf{R}^2 is identical transformation) together with time reversal transformation $\mathbf{T} : t \rightarrow -t$. For Topaj – Pikovsky model (1) the involution is $\psi_k \rightarrow \pi - \psi_{N-k}$.

Topaj – Pikovsky model (1) describes only dynamics of phases and does not account variations of amplitudes of oscillations. It is interesting to deepen the model by introducing amplitude-phase equations. We turn first to a conservative lattice [2, 3] of oscillators with Hamiltonian function

$$\begin{aligned} \mathcal{H}(\mathbf{I}, \Phi) = & \sum_k^N \omega_k I_k + \frac{1}{2} \beta \sum_k^N I_k^2 - \\ & - \varepsilon \sum_k^N \sqrt{I_{k+1} I_k} (I_{k+1} - I_k) \sin(\phi_{k+1} - \phi_k) - \\ & - \varepsilon \sum_k^N \sqrt{I_{k-1} I_k} (I_{k-1} - I_k) \sin(\phi_{k-1} - \phi_k). \end{aligned} \quad (2)$$

The Hamiltonian function (2) describes e.g. oscillations in tilted optical lattice [2, 3], $\sqrt{I_k}$ and ϕ_k are amplitudes and phases of spatial modes

$\sqrt{I_k} \exp(i\phi_k - ik\pi/2)$ of nonlinear Schrödinger equation with tilted potential [2, 3], nearest-neighbor coupling at linear distribution of frequencies ($\omega_{k+1} - \omega_k = 1$). The equations of motion for populations of wells (or intensities of oscillations) I_k and phases ϕ_k are:

$$\begin{aligned} \dot{I}_k &= -\frac{\partial \mathcal{H}}{\partial \phi_k} = -2\varepsilon \sqrt{I_{k+1} I_k} (I_{k+1} - I_k) \cos(\phi_{k+1} - \phi_k) - \\ &\quad - 2\varepsilon \sqrt{I_{k-1} I_k} (I_{k-1} - I_k) \cos(\phi_{k-1} - \phi_k), \\ \dot{\phi}_k &= \frac{\partial \mathcal{H}}{\partial I_k} = \omega_k + \beta I_k + \varepsilon \left(3\sqrt{I_{k+1} I_k} - \sqrt{I_{k+1}^3 / I_k} \right) \sin(\phi_{k+1} - \phi_k) + \\ &\quad + \varepsilon \left(3\sqrt{I_{k-1} I_k} - \sqrt{I_{k-1}^3 / I_k} \right) \sin(\phi_{k-1} - \phi_k). \end{aligned} \quad (3)$$

There are two known constants of motion for equations (3): Hamiltonian function $\mathcal{H}(\mathbf{I}, \mathbf{\Phi})$ (2) and total population of the lattice $\sum_k^N I_k = N/2$. The dynamics is equivariant in respect to arbitrary phase shift because equations (3) depend on phase differences $\psi_k = \phi_{k+1} - \phi_k$.

The dynamics of equations (3) is reversible, with involution $\mathbf{R} : I_k \rightarrow I_{N-k}, \phi_{k+1} - \phi_k \rightarrow \pi - (\phi_{N-k-1} - \phi_{N-k})$. If we set populations of every potential well equal to each other ($I_k \equiv 1/2$) they remain constant, and equations of motions become equivalent to the Topaj – Pikovsky model (1) on an invariant torus. This invariant torus is unstable [2] to perturbations of populations I_k .

We also introduce two dissipative models close to Topaj – Pikovsky system. The first one is an array of locally coupled rotators with inertia:

$$m\ddot{\psi}_k + \dot{\psi}_k = \Delta_k + \varepsilon \sin \psi_{k+1} + \varepsilon \sin \psi_{k-1} - 2\varepsilon \sin \psi_k, \quad (4)$$

where m is mass of rotators. Equations (4) are not reversible because of presence of the second derivatives, but if $m = 0$ they reduce exactly to the Topaj – Pikovsky model. If masses are small, equations (4) demonstrate transient dynamics very close to Topaj – Pikovsky model. Asymptotically all of the trajectories condense on a small number of attractors.

Phase equations (1) can be derived also for a chain of locally coupled van der Pol equations under some special assumptions. We consider truncated coupled van der Pol oscillator equations for small perturbations of constant amplitudes:

$$\begin{aligned} \dot{\rho}_k &= -\lambda \rho_k + \varepsilon \cos \psi_{k+1} - \varepsilon \cos \psi_{k-1}, \\ \dot{\psi}_k &= \Delta_k + \varepsilon (1 + \rho_{k+1}) \sin \psi_{k+1} + \varepsilon (1 - \rho_{k-1}) \sin \psi_{k-1} - 2\varepsilon \sin \psi_k. \end{aligned} \quad (5)$$

The observed destruction of quasi-conservative dynamics in (5) looks similar to that in way with the situation describing the incorporation of dissipation in nonholonomic mechanical systems [4].

The work was supported by the grant of Russian Science Foundation No. 15-12-20035.

References

- [1] Topaj D., Pikovsky A. *Reversibility vs. synchronization in oscillator lattices* // *Physica D: Nonlinear Phenomena*, 2002, vol. 170, no. 2, pp. 118–130.
- [2] Witthaut D., Timme M. *Kuramoto dynamics in Hamiltonian systems* // *Physical Review E*, 2014, vol. 90, no. 3, pp. 032917.
- [3] Thommen Q., Garreau J.C., Zehnlé V. *Classical chaos with Bose-Einstein condensates in tilted optical lattices* // *Physical review letters*, 2003, vol. 91, no. 21, pp. 210405.
- [4] Bizyaev I. A., Borisov A. V., Kuznetsov S. P. *The Chaplygin sleigh with friction moving due to periodic oscillations of an internal mass* // *Nonlinear Dynamics*, 2018, vol. 95, no. 1, pp. 699–714.

Modelling and dynamics of rigid body systems with 3D frictional and impact contacts

Grzegorz Kudra¹, Jan Awrejcewicz¹

¹ *Lodz University of Technology, Lodz, Poland*

The work concerns problems of modelling and investigations of dynamics of different mechanical systems composed of one or more rigid bodies with spatial frictional and impact contacts. There are developed and tested special simplified models of contact allowing for fast and reliable numerical simulations and bifurcation dynamics analysis of specific dynamical systems taking into account influence shape and size of the contact. The bodies are assumed to be quasi-rigid, i.e. in their global motion they are treated as rigid with constant shape but assumed to be locally deformable in the sense that shape and size of the contact area is variable. Among the examples of mechanical systems, where assumption of point contact and one-dimensional friction model does not allow to obtain reliable simulations, one can mention billiard ball, dynamics of the balls in a bearing, wobblestone or polishing machine.

Discretization of space in the vicinity of the contact area and application of specific numerical methods allows for exact simulation results but also requires relatively high computational costs. Instead we propose special reduced models based on assumption of fully developed sliding and classical Coulomb friction law valid at each element of the contact [1]. The integral expressions are replaced by special approximations being generalizations and extensions of Padé approximations and models exhibited in the earlier works [2]. Related friction models for finite contact zone with translational and rotational relative motion of the contacting bodies are presented and investigated experimentally in the work [3].

The developed approximate models of friction forces are then connected with compliant models of impact based on generalized Hertz theory. The proposed models are tested during simulations of the following examples of mechanical systems: a) rattleback also known as wobblestone or Celtic stone (see the work [1]); b) full ellipsoid of revolution rolling and sliding over the plane and horizontal surface; c) billiard ball; d) double spatial pendulum with links connected by the use of Cardan-Hooke joints, equipped with rigid obstacle. In addition, bifurcation dynamics of the Celtic stone placed on oscillation table is analysed.

References

- [1] Kudra G., Awrejcewicz J. Application and experimental validation of new computational models of friction forces and rolling resistance // *Acta Mechanica*, 2015, vol. 226, no. 9, pp. 2831–2848.
- [2] Kireenkov A. A., Coupled model of sliding and spinning friction // *Doklady Physics*, 2011, vol. 56, no. 12, pp. 626–631.
- [3] Borisov A. V., Erdakova N. N., Ivanova T. B., Mamaev I. S. The dynamics of a body with an axisymmetric base sliding on a rough plane // *Regular and Chaotic Dynamics*, 2014, vol. 19, no. 6, pp. 607–634.

Traveling wave solutions of some mathematical models for description of propagation pulses in optical fibers

Nikolay A. Kudryashov

*National Research Nuclear University (MEPHI),
Russian Federation, Moscow, Kashirskoe shosse, 31*

At the present one of the important theoretical and technological tasks is the solution of the problem for description of propagation pulses in an optical fiber. We know a sufficiently large number of mathematical models to describe the behavior of optical solitons in a fiber, but there is still no complete solution to the problem, because first of all this task is connected with the need to create new types of optical fiber. As a rule, a nonlinear Schrödinger equation with different types of nonlinearity is used to theoretically describe the propagation of pulses in an optical fiber. Let us mention here the Kaup-Newell equation, the nonlinear Schrödinger equation with quadratic-cubic and with anti-cubic nonlinearity, the Radhakrishnan-Kundu-Laksmanan equation, the Triki-Biswas equation, the Chen-Lee-Liu equation, the Gerdjikov-Ivanov equation, the Kundu-Mukherjee-Naskar equation and the Biswas-Arched equation. As a rule the Cauchy problem for this equation is not solved by the inverse scattering transform and we study these equations using the traveling wave reduction. We show that there are two first integrals for the system of equations corresponding to real and imaginary parts of these equations. These first integrals are used to obtain the nonlinear first-order differential equation. The general solution of the first-order ordinary differential equation is found via the Weierstrass and Jacobi elliptic functions [1-5]. Periodic and solitary waves of these equations in the form of the traveling reuction are presented and illustrated.

References

- [1] Kudryashov N. A., *First integrals and solutions of the traveling wave reduction for the Triki-Biswas equation*// *Optik*, 2019, vol. 185, pp. 275–281.
- [2] Kudryashov N. A. *First integrals and general solution of the traveling wave reduction for Schrödinger equation with anti-cubic nonlinearity*// *Optik*, (2019), vol.185, pp.665-671
- [3] Kudryashov N. A., *General solution of traveling wave reduction for the Kundu-Mukherjee-Naskar model*// *Optik*, 2019, vol. 186, pp. 22–27.
- [4] Kudryashov N. A., *General solution of the traveling wave reduction for the perturbed Chen-Lee-Liu equation*// *Optik*, 2019, vol. 186, pp. 339–349.

On the stability of discrete vortex structures in two-layer rotating fluid and in homogeneous fluid

Leonid G. Kurakin^{1,2}, Irina V. Ostrovskaya¹

¹ *Southern Federal University, Rostov-on-Don, Russia*

² *Southern Mathematical Institute, Vladikavkaz Scientific Center of RAS,
Vladikavkaz, Russia*

A two-layer quasigeostrophic model is considered. The stability analysis of the stationary rotation of a system of N identical point vortices lying uniformly on a circle of radius R in one of layers is presented. The vortices have identical intensity and length scale is $\gamma^{-1} > 0$. The problem has three parameters: N , γR and β , where β is the ratio of the fluid layers thicknesses. The stability of the stationary rotation is interpreted as orbital stability. The instability of the stationary rotation is instability of system reduced equilibrium. The quadratic part of the Hamiltonian and eigenvalues of the linearization matrix are studied.

The parameters space $(N, \gamma R, \beta)$ is divided on three parts: **A** is the domain of stability in an exact nonlinear setting, **B** is the linear stability domain, where the stability problem requires the nonlinear analysis, and **C** is the instability domain. The case **A** takes place for $N = 2, 3, 4$ for all possible values of parameters γR and β . In the case of $N = 5$ we have two domains: **A** and **B**. In the case $N = 6$ part **B** is curve, which divides the space of parameters $(\gamma R, \beta)$ into the domains: **A** and **C**. In the case of $N = 7$ there are all three domains: **A**, **B**, and **C**. The instability domain **C** takes place always if $N = 2n \geq 8$. In the case of $N = 2\ell + 1 \geq 9$ there are two domains: **B** and **C**. The results of research are presented in two versions: for parameter β and parameter α , where α is the difference between layers thicknesses.

The stability problem for $N + 1$ vortices is considered for a two-layer quasigeostrophic model and model of homogeneous fluid. In the case of two-layer fluid the quadratic part of the Hamiltonian and eigenvalues of the linearization matrix are studied for the vortex structure consisting of a central vortex of arbitrary intensity Γ and two/three identical peripheral vortices ($N = 2, 3$). The identical vortices, each having a unit intensity, are uniformly distributed over a circle of radius R in a single layer. The central vortex lies either in the same or in another layer. Some new results on stability of $N + 1$ vortices are obtained for Kirchhoff's model.

The stability of the Thomson vortex N -gon is also studied in the case of the model of the Bessel vortices for any $N \geq 2$.

A number of statements about the stability is obtained for the systems of interacting particles with the general Hamiltonian depending only on distances between the particles.

The main results are published in the papers [1–4].

The work was supported by the Ministry of Education and Science of the Russian Federation, Southern Federal University (Projects No. 1.5169.2017/8.9).

References

- [1] Kurakin L. G., Ostrovskaya I. V., Sokolovskiy M. A. *Stability of discrete vortex multipoles in homogeneous and two-layer rotating fluid*// Doklady Physics, 2015, vol. 60, no 5, pp. 217–223.
- [2] Kurakin L. G., Ostrovskaya I. V., Sokolovskiy M. A. *On the stability of discrete tripole, quadrupole, Thomson' vortex triangle and square in a two-layer/homogeneous rotating fluid*// Regul. Chaotic Dyn., 2016, vol. 21, no 3, pp. 291–334.
- [3] Kurakin L. G., Ostrovskaya I. V. *On stability of the Thomson's vortex N-gon in the geostrophic model of the point Bessel vortices*// Regul. Chaotic Dyn., 2017, vol. 22, no. 7, pp. 865–879.
- [4] Kurakin L. G., Lysenko I. A., Ostrovskaya I. V., Sokolovskiy M. A. *On Stability of the Thomson's Vortex N-gon in the Geostrophic Model of the Point Vortices in Two-layer Fluid*// Journal of Nonlinear Science, 2018. URL: <https://doi.org/10.1007/s00332-018-9526-2>

On stability of orbit and invariant set of Thomson's vortex polygon in two-fluid plasma

Leonid G. Kurakin^{1,2}, Irina A. Lysenko¹

¹ *Southern Federal University, Rostov-on-Don, Russia*

² *Southern Mathematical Institute of the Vladikavkaz Scientific Center of the Russian Academy of Sciences, Vladikavkaz, Russia*

The motion of the system of N point vortices with identical intensity Γ in the Alfvén model of two-fluid plasma is described by the equations with Hamiltonian [1]

$$\mathcal{H} = -\frac{\Gamma}{4\pi} \sum_{1 \leq j < k \leq N} W(|z_j - z_k|), \quad W(\xi) = \ln \xi + cK_0(\xi).$$

Here, $z_k = q_k + ip_k$, (q_k, p_k) are Cartesian coordinates of the k -th vortex, K_0 is a modified Bessel function, parameter $c > 0$.

The stability of the stationary rotation of N identical vortices disposed uniformly on a circle with radius R is studied for $N = 2, \dots, 5$. The analytical analysis of eigenvalues of the linearization matrix and the quadratic part of Hamiltonian is given. Two different definitions of the stability are used. Instability is interpreted as instability of equilibrium of the system reduced.

The conclusions of the orbital stability were partly published in [2], where the results of the papers [1, 3, 4] are used. In this case the parameter space (N, R, c) of the problem is divided into three parts: the domain of stability in an exact nonlinear problem setting, the linear stability domain, where the additional nonlinear analysis is needed, and the domain of exponential instability.

Also, the stability of three-dimensional invariant set founded by the orbits of continuous family of stationary rotations is studied. The stability theory of invariant multiplicities for the systems with a few integrals [5] is applied. As a result, for $N = 2, \dots, 5$ the new statements about the stability in the domains, where the nonlinear analysis at research of orbital stability is needed, are received.

The work was carried out within the framework of the basic part of the state task of the Ministry of education and science of Russian Federation (1.5169.2017/8.9).

References

- [1] Bergmans J., Kuvshinov B.N., Lakhin V.P., Schep T.J. *Spectral stability of Alfvén filament configurations*// Physics of plasmas, 2000, vol. 7, no. 6, pp. 2388–2403.
- [2] Lysenko I.A. *On stability of a vortex triangle, square and pentagon in the two-fluid plasma*// Izvestiya Vuzov. Severo-Kavkazskii Region. Natural Science, 2019, no. 1, pp. 17–23.
- [3] Kurakin L.G., Lysenko I.A., Ostrovskaya I.V., Sokolovskiy M.A. *On Stability of the Thomson's Vortex N-gon in the Geostrophic Model of the Point Vortices in Two-layer Fluid*// Journal of Nonlinear Science, 2018. URL: <https://doi.org/10.1007/s00332-018-9526-2>
- [4] Kurakin L.G., Yudovich V.I. *The stability of stationary rotation of a regular vortex polygon*// Chaos, 2002, vol. 12, no. 3, pp. 574–595.
- [5] Karapetyan A.V. *Invariant Sets of Mechanical Systems: Lyapunov's Methods in Stability and Control*// Math. Comput. Modelling, 2002, vol. 36, no. 6, pp. 643–661.

Semi-invariant form of equilibrium stability criteria for systems with one or two cosymmetries

Leonid G. Kurakin^{1,2}, Aik V. Kurdoglyan¹

¹ Southern Federal University, Rostov-on-Don, Russia

² Southern Mathematical Institute – Branch of the Vladikavkaz Scientific Center, Russian Academy of Sciences, Vladikavkaz, Russia

The systems of differential equations with one/two cosymmetries are considered [1]. The ordinary object for such systems is one-dimensional (two-dimensional) continuous family of equilibria. The stability spectrum changes along this family, but it necessarily contains zero. We consider the nondegeneracy condition, thus the boundary equilibria separate the family on linearly stable and instable areas. Stability of the boundary equilibria depends on nonlinear terms of the system.

The stability problem for the systems with one or two cosymmetries is studied in [2, 3]. The general problem to apply the stability criteria is to compute coefficients of the model system. It is especially difficult if the system has a large dimension while a number of critical variables may be small. The coefficients calculation method is proposed in [4].

In this work the expressions for the known stability criteria are proposed in a convenient form to calculate. The explicit formulas of the coefficients of the model system are given in semi-invariant form. They are expressed using the root vectors of the linear matrix and its conjugate matrix.

The work was supported by the Ministry of Education and Science of the Russian Federation, Southern Federal University (Projects No. 1.5169.2017/8.9).

References

- [1] Yudovich V.I. *Cosymmetry, degeneration of solutions of operator equations, and onset of a filtration convection* // Math. notes, 1991. Vol. 49, No. 5, pp. 142–148.
- [2] Kurakin L.G. *Critical cases of stability. Converse implicit function theorem for dynamical systems with cosymmetry* // Math. notes, 1998. Vol. 63, No. 4, pp. 572–578.
- [3] Kurakin L.G., Kurdoglyan A.V. *Critical stability cases of equilibria for two-cosymmetric differential equations* // Izvestiya Vuzov. Severo-Kavkazskii Region. Natural Science, 2018. No. 1, pp. 26–32.
- [4] Kurakin L.G., Yudovich V.I. *Semi-invariant form of equilibrium stability criteria in critical cases* // Applied Mathematics and Mechanics, 1986. Vol. 50, No. 5, pp. 543–546.

Application of boundary element techniques to the solution of tasks of hydrodynamics

Valentina V. Kuritsyina¹, Tatiana V. Mitrofanova¹, Tatiana N. Smirnova¹

¹ *Chuvash State University, Cheboksary, Russia*

The method of discretization of the boundary element techniques (BET) is used, in which the boundary of the region is replaced by a polyline (the links are called elements), at the links of which the sought function is approximated by a special shape. Constant elements [1] were chosen as working tools. BET is based on the transformation of the differential equation in partial derivatives into an integral equation, the numerical solution of which determines the boundary values. Generalized Green's relations, obtained in [2] to the real and imaginary parts of the function $W(z) = U(z) + iV(z)$ (which is an analytical function in the domain D_z ; C_z — is the boundary of domain D_z), take the form:

$$\begin{aligned}\varepsilon(z)U(z) + \int_{C_z} U(t)G_n(z, t)ds(t) &= \int_{C_z} U_n(t)G(z, t)ds(t) + \operatorname{Re} F(z), \\ \varepsilon(z)V(z) + \int_{C_z} V(t)G_n(z, t)ds(t) &= \int_{C_z} V_n(t)G(z, t)ds(t) + \operatorname{Im} F(z), \\ F(z) &= \sum_{k=0}^m B_k z^k + \sum_{k=1}^n \frac{A_k}{(z-a)^k} + \frac{D}{2(z-c)},\end{aligned}$$

where the function $F(z)$ takes into account all the features of the function $W(z)$ — the poles inside the domain, at the boundary and at an infinitely remote point.

References

- [1] Brebbia C.A. Boundary element techniques / C.A. Brebbia, J.C.F. Telles, L.C. Wrobel. — M.: Mir, 1987. — 524 p.
- [2] Terentiev A.G. Numerical study of the hydrodynamics / A.G. Terentiev // Izvestiya NANI CHR. 1994. Issue 1. No. 2. P. 61–84.

Mathematical modeling of plasma dynamics for processes in capillary discharges

Victor V. Kuzenov^{1,2}, Sergei V. Ryzhkov¹

¹ *Bauman Moscow State Technical University, Moscow, Russia*

² *Dukhov All-Russian Research Institute of Automatics, Moscow, Russia*

The statement of the problem is presented and numerical modeling of plasma-gas-dynamic processes in the capillary discharge plume and other applications is performed as the development of Ref. [1–14]. In the developed model, plasma dynamic processes in a capillary discharge are determined by the intensity, duration of plasma formation processes in the capillary discharge channel, and thermodynamic parameters in the surrounding gaseous medium. A vector equation is formulated that describes the vorticity $\vec{\Omega}$ in a gas flow, which is affected by an external magnetic field. This equation (a generalization of Son's equation [15]) $\frac{\partial \vec{\Omega}}{\partial t} + (\vec{V} \cdot \nabla) \vec{\Omega} = \frac{1}{\rho^2} \nabla \rho \times \left(\nabla P - \frac{1}{c} [\vec{j} \times \vec{H}] \right) + v \Delta \vec{\Omega}$, allows us to introduce the following condition for the emergence of a toroidal vortex in the presence of an external magnetic field:

$$t_{\text{vort}} \approx \frac{\Omega_{\text{char}} \rho_{\text{char}} \varepsilon^2}{\left| P_{\text{char}} \mp \frac{H_{\text{char}}^2}{8\pi} \right|}, < \min \left(t_{\text{conv}} \approx \frac{L_{\text{char}}}{V_{\text{char}}}, t_{\text{diff}} \approx \frac{r_0^2}{\nu} \right)$$

where ε , r_0 are the nucleus radius and the large radius of the self-induced toroidal vortex with circulation Γ . Comparison of the results of calculations in a single plume of a capillary discharge with known and available experimental data was made. Their satisfactory compliance is noted. Calculations of pulsed jets arising from adjacent channels of a high-current capillary discharge were carried out. The spatial distribution of temperature and pressure of pulsed jets of several capillary discharge channels is presented. Calculations of pulsed jets were performed taking into account the additional magnetic field. Magnetic pressure has the most noticeable effect on the heated axial part of a pulsed jet ($T > 20$ kK).

Free shear flows (jets, traces, mixing layers, shear layers) are often used in technical devices. One of the important features of shear flows is instability (one of the main causes of hydrodynamic instability is the shear of velocity (in this case the longitudinal flow, i.e. the presence of points of inflection in its profile), which leads to the formation of large-scale vortex

structures. That is, the motion of the pulsed jet is exponentially unstable in relation to any wave disturbance in the presence of tangential discontinuity. The growth rate depends on the wave number $k = 2\pi/\lambda$ (λ is the wavelength) and equal to $\gamma = kU$ (U is the velocity shift). We note that the elimination of the velocity discontinuity (which is observed for $t \geq 144 \mu\text{s}$) leads to the stabilization of the flow in relation to small-scale disturbances. This research is supported by the Russian Ministry of Science and Higher Education (Project No. 13.5240.2017/8,9) and Bauman Moscow State Technical University Target Program for 2018-2020.

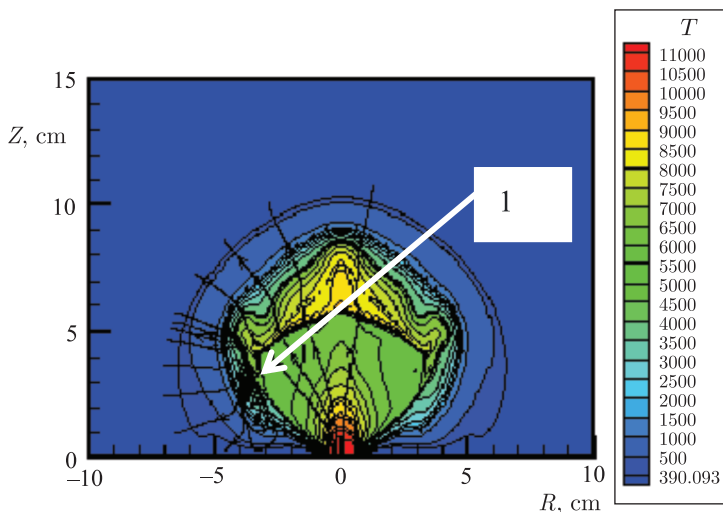


Fig. 1. Spatial temperature distribution in a pulsed jet at the time $t = 58.2 \mu\text{s}$: 1 — acceleration vortex area

References

- [1] Ogurtsova N. N., Podmoshenskii I. V., Shelemina V. M. Influence of the Evaporation Rate of the Wall Material on the Properties of a Capillary Discharge Plasma // High Temperature, 1974, v. 12, p. 5.
- [2] Pashchina A. S. et al. Specific features of the radial distributions of plasma parameters in the initial segment of a supersonic jet generated by a pulsed capillary discharge // Plasma Phys. Rep., 2017, 43, p. 796.
- [3] Varaksin A. Yu. Air Tornado-like Vortices: Mathematical Modeling // High Temperature, 2017, v. 55, p. 286.

- [4] Kuzenov V.V., Polozova T.N., Ryzhkov S.V. Numerical simulation of pulsed plasma thruster with a preionization helicon discharge // *Problems of Atomic Science and Technology*, 2015, 4(98), pp. 49.
- [5] Zarubin V.S., Kuvyrkin G.N., Savel'eva I.Y. Radiative-conductive heat transfer in a spherical cavity // *High Temperature*, 2015, vol. 53, pp. 234–239.
- [6] Varaksin A. Yu. Concentrated Air and Fire Vortices: Physical Modeling // *High Temperature*, 2016, 54, 409.
- [7] Loktionov E. Yu., Protasov Yu. Yu. Experimental Study of the Dynamics and Macrostructure of Laser-Induced High-Pressure Dust Gas-Plasma Flows // *High temperature*, 2011, vol. 49, pp. 36–44.
- [8] Ryzhkov S.V., Kuzenov V.V. Analysis of the ideal gas flow over body of basic geometrical shape // *International Journal of Heat and Mass Transfer*, 2019, vol. 132, pp. 587–592.
- [9] Kuzenov V.V., Ryzhkov S.V., Gavrilova A. Yu., Skorokhod E.P. Computer simulation of plasmadynamic processes in capillary discharges // *High Temperature Material Processes*, 2014, vol. 18, pp. 119–130.
- [10] Kuzenov V.V., Ryzhkov S.V. Numerical Modeling of Laser Target Compression in an External Magnetic Field // *Mathematical Models and Computer Simulations*, 2018, vol. 10, pp. 255–264.
- [11] Kuzenov V.V., Ryzhkov S.V. Approximate method for calculating convective heat flux on the surface of bodies of simple geometric shapes // *J. Physics: Conference Series*, 2017, vol. 815, 012024.
- [12] Ryzhkov S.V., Kuzenov V.V. New realization method for calculating convective heat transfer near the hypersonic aircraft surface // *Zeitschrift für Angewandte Mathematik und Physik*, 2019, vol. 70, p. 46.
- [13] Kuzenov V.V., Ryzhkov S.V. Radiation-hydrodynamic modeling of the contact boundary of the plasma target placed in an external magnetic field // *Applied Physics*, 2014, no. 3, pp. 26–30.
- [14] Kuzenov V.V., Ryzhkov S.V. Individual elements of the physical and mathematical model for a helicon discharge // *Applied Physics*, 2015, no. 2, pp. 37–44.
- [15] Son E.E., Tereshonok D.V. Control of supersonic gas flow by thermal vortices // *High temperature*, 2010, vol. 48, pp. 3–8.

Complex dynamics in generalizations of the Chaplygin sleigh

Sergey P. Kuznetsov

Udmurt State University, Izhevsk, Russia

Chaplygin sleigh is one of the simplest paradigmatic systems for non-holonomic mechanics. The model can be thought of as a platform that can move on a surface in such a way that one of the points of the sleigh allows motion only in a fixed direction relative to the platform, which can be interpreted as a skate installed at this point, or a knife edge, along which the movement is allowed.

The report is devoted to review of some generalizations of the classical problem of the Chaplygin sleigh, where complex dynamics are possible, including chaos. Particularly, we will discuss the Chaplygin sleigh under the action of impulse kicks [1], the motion with periodic switching of the nonholonomic constraint location [2], the self-acceleration of the Chaplygin sleigh in the presence of an oscillating mass attached to them [3], the random walk of the Chaplygin sleigh on the plane due to presence of a strange attractor in equations describing the dynamics of the generalized momenta [4].

One of the interesting problems is the movement of the Chaplygin sleigh in a potential field that forms a two-dimensional potential well on a plane, assuming that the potential force is supplied at the mass center. In the case of sliding down the slope and then moving up by inertia, the sleigh tends to orient itself so that the knife edge is at the back. After the sleigh begins to slide in opposite direction, a turn occurs so that the knife edge appears to be back again. With a relatively small initial energy, the resulting motions turn out to be quasi-periodic, while with sufficiently large energies the chaotic motions become typical. The system is described by a set of equations

$$\begin{aligned}m\dot{u} &= maw^2 - U_X \cos \phi - U_Y \sin \phi, \\(J + ma^2)\dot{\omega} &= -mawu + U_X \sin \phi - U_Y \cos \phi, \\ \dot{\phi} &= \omega, \\ \dot{X} &= u \cos \phi - a\omega \sin \phi, \\ \dot{Y} &= u \sin \phi + a\omega \cos \phi,\end{aligned}$$

where u is velocity of the sleigh along the knife edge, ω is angular velocity, X and Y are the center mass coordinates in the laboratory frame, φ is the rotation angle of the sleigh, the function $U(X, Y)$ defines the form of

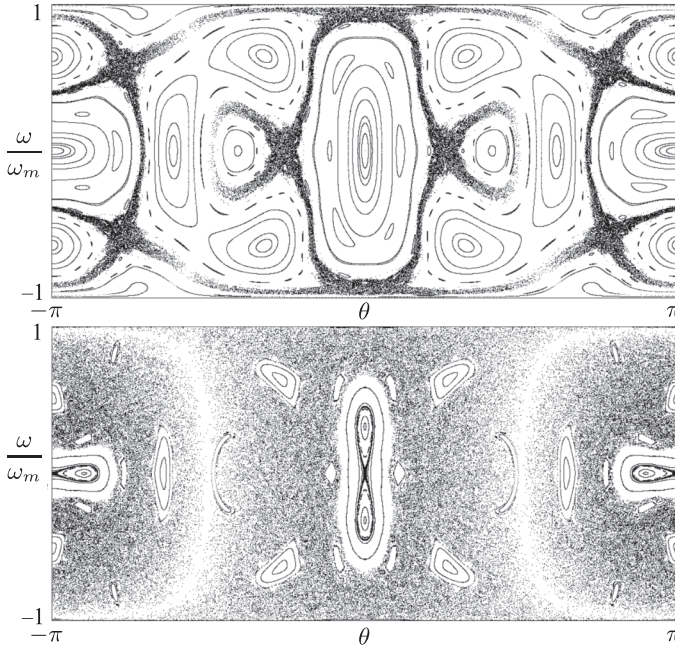


Fig. 1. Poincaré sections for the motion of Chaplygin sleigh at $W = 1.5$ (top) and $W = 2$ (bottom) defined by the condition $u = 0$. Normalizing factor for the angular velocity is $\omega_m = \sqrt{wW/(J + ma^2)}$

the potential well, m is mass of the sleigh, J is moment of inertia about the center of mass, a is distance between the knife edge and the center of mass. The center of mass is considered to be placed on the straight line that is continuation of the knife edge. The system has an integral of energy $W = \frac{1}{2}m(u^2 + a^2\omega^2) + \frac{1}{2}J\omega^2 + U(X, Y) = \text{const}$. Considering the dynamics of the system we can treat the energy W simply as an additional parameter of the system. If the potential well is symmetric with respect to rotations, then the problem is reduced to a set of four equations. Taking into account the energy integral, the Poincaré map turns out to be two-dimensional. Figure 1 shows the numerically obtained pictures of the phase space of the system in the Poincaré section determined by the condition $u = 0$, when the sleigh moves in a potential field $U = \frac{1}{2}(X^2 + Y^2)$ in the case of $m = 1$, $a = 1$, $J + ma^2 = 10$, for two values of the energy. Observe that with growth of the energy the islands of regular motions decrease in size while the chaotic sea occupies larger and larger area.

The work is supported by Russian Science Foundation, Grant No. 15-12-20035.

References

- [1] Borisov A.V., Kuznetsov S.P. Regular and Chaotic Motions of a Chaplygin Sleigh under Periodic Pulsed Torque Impacts // RCD, 2016, vol. 21, no. 7–8, pp. 792–803.
- [2] Kuznetsov S.P. Regular and chaotic motions of the Chaplygin sleigh with periodically switched location of nonholonomic constraint // EPL, 2017, vol. 118, no. 1, 10007.
- [3] Bizyaev I.A., Borisov A.V., Kuznetsov S.P. Chaplygin sleigh with periodically oscillating internal mass // EPL, 2017, vol. 119, no. 6, 60008.
- [4] Bizyaev I.A., Borisov A.V., Kuznetsov S.P. The Chaplygin sleigh with friction moving due to periodic oscillations of an internal mass // Nonlinear Dynamics, 2019, vol. 95, pp. 699–714.

Some lattice models with hyperbolic chaotic attractors

Sergey P. Kuznetsov

Udmurt State University, Izhevsk, Russia

Kotelnikov's Institute of Radio-Engineering and Electronics of RAS, Saratov, Russia

The Smale–Williams attractor belongs to the category of uniformly hyperbolic attractors, whose theory was developed in the 1960s – 1970s by efforts of Smale, Anosov, Sinai, and other mathematicians [1]. Hyperbolic attractors are characterized by roughness or structural stability. In the context of physical or technical objects this property implies insensitivity of the dynamic behavior to small variations in parameters, manufacturing imperfections, interferences, etc., which may be significant for possible applications.

This report presents examples of systems in the form of one-dimensional lattices, in which patterns of spatial scale distinct by an integer number of times alternate, so that the transformation of the spatial phase over a full cycle corresponds to an expanding circle map [2]. Due to the compression of the phase volume elements in the remaining directions of the multidimensional state space, the attractor has the form of a Smale–Williams solenoid [1, 2].

One example is a ring system of coupled pendulums, corresponding to a spatially discrete version of the sine-Gordon equation [3], with parametric excitation due to vertical oscillations of the suspension in the presence of dissipation. If we assume that the frequency of oscillations of the suspension periodically switches to provide alternate parametric excitation of standing waves, which fit one or three wavelengths around the chain, then it is possible to observe chaotic dynamics, corresponding to the Smale – Williams solenoid type attractor. The model is described by the following dimensionless equations

$$(1 + \varepsilon\delta_i)[\ddot{\theta}_i + (1 + a(t)) \sin \theta_i] = -\gamma\dot{\theta}_i + D(\theta_{i-1} - 2\theta_i + \theta_{i+1}), \quad (1)$$
$$i = 0, 1, \dots, N - 1,$$

with boundary conditions of periodicity $\theta_{i+N} = \theta_i$. Here θ_i is deflection angle of the i -th pendulum, γ is dissipation parameter, D is parameter of coupling between adjacent pendulums, $\varepsilon\delta_i$ is relative deviation of the mass of the i -th pendulum from the average value, the function $a(t)$ sets the

suspension oscillations alternately with frequencies ω_1 and ω_2 in the form

$$a(t) = \begin{cases} \kappa_2 \sin \omega_2 t, & 0 \leq t < \tau, \\ \kappa_1 \sin \omega_1 (t - \tau), & \tau \leq t < T, \end{cases} \quad (2)$$

$$a(t) = a(t + T), \quad \tau = 2\pi \frac{N_2}{\omega_2}, \quad T = 2\pi \left(\frac{N_2}{\omega_2} + \frac{N_1}{\omega_1} \right).$$

Figure 1a shows typical oscillation plots in the form of dependences of the angular accelerations of the pendulums on time according to the results of the numerical solution of the equations (3) for the sustained chaotic motion.

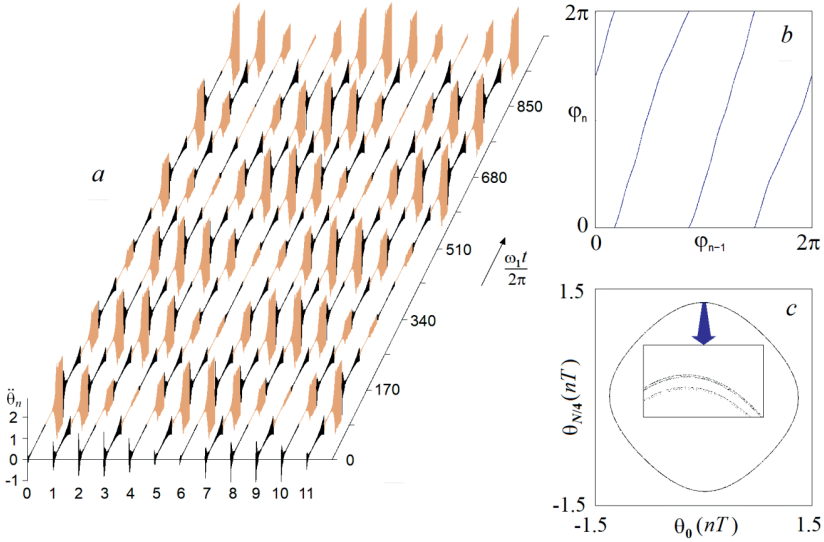


Fig. 1. (a) The oscillation plots for the chain of pendulums in the form of dependences of the angular accelerations on time, built for a sustained chaotic mode basing on results of numerical solution of the differential equations, where the stages of slow and fast oscillations of the suspension are marked with color and black. (b) Diagram of the spatial phase transformation on each one modulation period of pumping. (c) Portrait of the attractor of the Poincaré map in projection on the plane. The number of chain elements is $N = 12$, the coupling parameter is $D = 1.19$, the dissipation parameter is $\gamma = 0.12$. The variation of the masses is characterized by the parameter $\varepsilon = 0.01$ and a set $\delta = \{0, 1, 1, 0, -1, -1, 0, 1, 1, 0, -1, -1\}$. Switches of the pump frequencies between $\omega_1 = 2.297$ and $\omega_2 = 3.677$ take place after each $N_1 = 85$ and $N_2 = 136$ periods of the oscillations of the suspension, the parameters of the pump intensity are $\kappa_1 = \kappa_2 = 0.6$.

Figure 1b shows a diagram illustrating the transformation of the spatial phase of the standing waves during the pump modulation period. The spatial phase is calculated at the moments when the pump frequency is switched from ω_1 to ω_2 , through the instantaneous angles of deviation of the zero and third pendulums in the chain. This diagram is the main evidence that the Smale-Williams type attractor is implemented in the system, since it shows that one round of the full circle of the angular variable for the pre-image corresponds to three rounds for the image. In this case, the Smale-Williams solenoid is an object in the state space of the Poincaré map of dimension $2N = 24$. Fig. 1c shows the view of this attractor in a two-dimensional projection. The enlarged fragment in the center makes it possible to resolve the transverse structure of the filaments characteristic for the solenoid.

The work is supported by Russian Science Foundation, Grant No. 15-12-20035.

References

- [1] Shilnikov L. *Mathematical Problems of Nonlinear Dynamics: A Tutorial* // *International Journal of Bifurcation and Chaos*, 1997, vol. 7, No 9, pp. 1353-2001.
- [2] Kuptsov P.V., Kuznetsov S.P., Pikovsky A. *Hyperbolic Chaos of Turing Patterns* // *Phys. Rev. Lett.*, 2012, vol. 108, 194101.
- [3] Cuevas-Maraver J., Kevrekidis P. G., Williams F. (ed.). *The sine-Gordon model and its applications: From pendula and Josephson Junctions to Gravity and High-Energy Physics*. Springer, 2014. 263 p.

Theory of hidden oscillations

Nikolay V. Kuznetsov^{1,2,3}, Timur N. Mokaev¹

¹ *Saint-Petersburg State University, Russia*

² *Institute for Problems in Mechanical Engineering RAS, St.-Petersburg, Russia*

³ *University of Jyväskylä, Finland*

The development of mathematics and the emergence of such directions as the theory of absolute stability, the theory of bifurcations, the theory of chaos, and new computational technologies made it possible to take a fresh look at a number of well-known scientific problems and practical problems of analyzing multidimensional dynamical systems and led to the emergence of *the theory of hidden oscillations* which represents the genesis of the modern era of Andronov's theory of oscillations [1].

The basis for the theory of hidden oscillations become a new classification of attractors of dynamical systems: *an attractor is called hidden if its basin of attraction does not intersect with a neighborhood of all equilibria; otherwise, it is called a self-excited attractor* [2–5].

While trivial attractors (stable equilibrium points) can be easily found analytically or numerically, the search of periodic and chaotic attractors can turn out to be a challenging problem (see, e.g. famous 16th Hilbert problem on the number of coexisting periodic attractors in two-dimensional polynomial systems, which was formulated in 1900 and is still unsolved, and its generalization for multidimensional systems with chaotic attractors [6]). For numerical localization of an attractor, one needs to choose an initial point in the basin of attraction and observe how the trajectory, starting from this initial point, after a transient process visualizes the attractor. Nowadays *self-excited attractors*, even coexisting in the case of multistability [7], can be revealed numerically by the integration of trajectories, started in small neighbourhoods of unstable equilibria, while *hidden attractors* have the basins of attraction, which are not connected with equilibria and are “hidden somewhere” in the phase space. Thus, the search and visualization of hidden attractors in the phase space may be a challenging task.

For the engineering dynamical models the importance of identifying hidden attractors is related with the classical problems of determining the exact boundaries of global stability and identifying classes of models for which the necessary and sufficient conditions for global stability coincide. In practice, the transition of the state of the system to a hidden attractor, caused by external disturbances, results in undesirable modes of operation and is often the

cause of accidents and catastrophes. The suggested classification, not only demonstrated difficulties of fundamental problems and applied systems analysis, but also triggered the discovery of new hidden attractors in well-known engineering and physical models (see [8–13] and others).

This lecture is based on recent surveys [14, 15] and is devoted to theoretical and engineering problems in which hidden attractors (their absence or presence and disposition) play an important role: Keldysh's problem of nonlinear analysis of flutter suppression systems, Aizerman and Kalman conjectures on absolute stability of control systems, 16th Hilbert's problem, Sommerfeld effect, Chua circuit, phase-locked loops, drilling systems and others.

We acknowledge support from the Leading Scientific Schools of Russia (project NSh-2858.2018.1) and Russian Scientific Foundation (project 19-41-02002).

References

- [1] Andronov A., Vitt E., Khaikin S. Theory of Oscillators (in Russian), ONTI NKTP SSSR, 1937, [English transl.: 1966, Pergamon Press].
- [2] Leonov G., Kuznetsov N. Hidden attractors in dynamical systems. From hidden oscillations in Hilbert-Kolmogorov, Aizerman, and Kalman problems to hidden chaotic attractors in Chua circuits, International Journal of Bifurcation and Chaos in Applied Sciences and Engineering 23 (1), art. no. 1330002.
- [3] Bragin V., Vagaitsev V., Kuznetsov N., Leonov G. Algorithms for finding hidden oscillations in nonlinear systems. The Aizerman and Kalman conjectures and Chua's circuits, Journal of Computer and Systems Sciences International 50 (4) (2011) 511–543.
- [4] Leonov G., Kuznetsov N., Mokaev T. Homoclinic orbits, and self-excited and hidden attractors in a Lorenz-like system describing convective fluid motion, The European Physical Journal Special Topics 224 (8) (2015) 1421–1458.
- [5] Kuznetsov N. V. Analytical-numerical methods for the study of hidden oscillations (Habilitation thesis, in Russian), Saint-Petersburg State University, 2016.
- [6] Leonov G., Kuznetsov N. On differences and similarities in the analysis of Lorenz, Chen, and Lu systems, Applied Mathematics and Computation 256 (2015) 334–343.
- [7] Pisarchik A. N., Feudel U. Control of multistability, Physics Reports 540 (4) (2014) 167–218.
- [8] Kuznetsov N. Hidden attractors in fundamental problems and engineering models. A short survey, Lecture Notes in Electrical Engineering 371 (2016) 13–25,

(Plenary lecture at International Conference on Advanced Engineering Theory and Applications 2015).

- [9] Dudkowski D., Jafari S., Kapitaniak T., Kuznetsov N., Leonov G., Prasad G. Hidden attractors in dynamical systems, *Physics Reports* 637 (2016) 1–50.
- [10] Chen G., Kuznetsov N., Leonov G., Mokaev T. Hidden attractors on one path: Glukhovskiy–Dolzhansky, Lorenz, and Rabinovich systems, *International Journal of Bifurcation and Chaos in Applied Sciences and Engineering* 27 (8), art. num. 1750115.
- [11] Stankevich N., Kuznetsov N., Leonov G., Chua G. Scenario of the birth of hidden attractors in the Chua circuit, *International Journal of Bifurcation and Chaos in Applied Sciences and Engineering* 27 (12), art. num. 1730038.
- [12] Dudkowski G., Kuznetsov G., Mokaev G. Chimera states and hidden attractors, *Physics of Life Reviews* <https://doi.org/10.1016/j.plrev.2019.02.005>.
- [13] Kuznetsov N., Leonov G., Mokaev T., Prasad T., Shrimali T. Finite-time Lyapunov dimension and hidden attractor of the Rabinovich system, *Nonlinear Dynamics* 92 (2) (2018) 267–285.
- [14] Kuznetsov N. Theory of hidden oscillations (plenary lecture), in: 5th IFAC Conference on Analysis and Control of Chaotic Systems, 2018.
- [15] Kuznetsov N. Theory of hidden oscillations and stability of control systems, *Journal of Computer and Systems Sciences International* (in press).

On Pauli's theorem in Clifford algebra $R_{p,q}$

Sergey P. Kuznetsov¹, Vladimir V. Mochalov¹, Vasiliy P. Chuev¹

¹ *Chuvash State University, Cheboksary, Russia*

In this article, in the Clifford algebra $R_{p,q}$, we investigated Pauli's theorem. An algorithm for constructing Pauli's operator is given. It is shown that the problem of constructing Pauli's operator is related to the problem of zero divisor in Clifford algebras.

Let $R_{p,q}$ a real Clifford algebra dimension $m = 2^n$ ($n=p+q$) with a basis $e_\alpha = e_{i_1} \cdots e_{i_k}$, $1 \leq i_1 < \dots < i_k \leq n$, where the multi-index $\alpha = i_1 \dots i_k$ runs through all subsets of the set $1, \dots, n$, the set of which is denoted by Γ_n . Let $e_0 = 1$ unit of algebra, e_1, \dots, e_n -generating basis $e_\tau = e_1 e_2 \cdots e_n$. Product in $R_{p,q}$ determined by the relation

$$e_i e_j + e_j e_i = 2\delta_{ij} \varepsilon_i, \tag{1}$$

where $\varepsilon_i = e_i^2 = 1, i = 1, \dots, p, \varepsilon_i = e_i^2 = -1, i = p + 1, \dots, p + q$.

Algebra $R_{p,q}$ is called even (odd), if n - is even (odd) number. Let us denote by $R_{p,q}^{(k)}$ $k = 0, \dots, n$ vector subspaces $R_{p,q}$ strung on the basic elements $e_\alpha = e_{i_1} \cdots e_{i_k}$ numbered by ordered indeces of length k . Elements of $R_{p,q}^{(k)}$ are called elements of rank k . We have [1]:

$$R_{p,q} = R_{p,q}^{(0)} \oplus R_{p,q}^{(1)} \oplus \dots \oplus R_{p,q}^{(n)}.$$

Arbitrary and Clifford conjugated elements of the algebra can be written as follows:

$$w = \sum_{\alpha \in \Gamma_n} x_\alpha e_\alpha = \sum_{k=0}^n \sum_{\alpha \in \Gamma_n}^k x_\alpha e_\alpha, \quad \hat{w} = \sum_{\alpha \in \Gamma_n} x_\alpha \hat{e}_\alpha = \sum_{k=0}^n (-1)^{\frac{k(k+1)}{2}} \sum_{\alpha \in \Gamma_n}^k x_\alpha e_\alpha,$$

where x_α are real number, \hat{w} - elements of rank k . Operations \hat{w} have the following properties [2, p. 95–97]: $\hat{\hat{w}} = w, (\hat{uv}) = \hat{v} \cdot \hat{u}, (u + v) = \hat{u} + \hat{v}$.

Let $R_{p,q}$ a even Clifford algebra. Consider another generating basis $\{e_{\gamma_i}\}_{i=1}^n$, formed by the elements of the space $R_{p,q}^{(1)}$:

$$e_{\gamma_i} = \sum_{k=1}^4 \alpha_k^{(i)} e_k, \tag{2}$$

for which the conditions are fulfilled (1). From (2) it follows that $\hat{e}_{\gamma_i} = -e_{\gamma_i}$.

Let us find Pauli's operator T , which has an inverse T^{-1} and satisfies the equations $Te_i = e_{\gamma_i}T$.

We will find the operator T as: $T = \sum_{\alpha \in \Gamma_4} a_\alpha e_\alpha$. Basis $\{e_\alpha\}_{\alpha \in \Gamma_4}$ consists of 2^n elements. Element e_1 commutes with half of the elements of a basis and anticommutes with the other half of it. Denote $w_1 = \sum a_\alpha e_\alpha$, $v_1 = \sum a_\alpha e_\alpha$ elements $R_{p,q}$ which commute with e_1 and anticommute with it respectively. We choose the coefficients a_α so that the equation $Te_1 = e_{\gamma_1}T$. We have

$$(e_1 - e_{\gamma_1})w_1 = (e_1 + e_{\gamma_1})v_1 \quad (3)$$

We multiply the equation (3) on the left by $(e_1 + e_{\gamma_1})\widehat{}$ and we obtain

$$(e_1 + e_{\gamma_1})(e_1 - e_{\gamma_1})w_1 = (e_1 + e_{\gamma_1})(e_1 + e_{\gamma_1})v_1.$$

Expression $(e_1 + e_{\gamma_1})\widehat{}(e_1 + e_{\gamma_1}) = -2\varepsilon_1(1 + \alpha_1^{(1)})e_0$. If a $\alpha_1^{(1)} = -1$, the $(e_1 + e_{\gamma_1})\widehat{}$ is a divisor of zero for $(e_1 + e_{\gamma_1})$, then $(e_1 - e_{\gamma_1})\widehat{} = -(e_1 - e_{\gamma_1})$ is not a zero divisor, since $(e_1 - e_{\gamma_1})\widehat{}(e_1 - e_{\gamma_1}) = -4\varepsilon_1 e_0$.

First, let us assume that $\alpha_1^{(1)} \neq -1$, then we have

$$v_1 = \frac{(e_1 + e_{\gamma_1})(e_1 - e_{\gamma_1})}{(e_1 + e_{\gamma_1})^2}w_1, \quad T = \frac{T_1}{(1 + \alpha_1^{(1)})}w_1, \quad T_1 = e_0 + e_{\gamma_1}e_1.$$

If $\alpha_1^{(1)} = -1$, then let us multiply the equation (3) on the left by $(e_1 - e_{\gamma_1})\widehat{} = -(e_1 - e_{\gamma_1})$, and we obtain

$$T = \frac{e_0 - e_{\gamma_1}e_1}{2\varepsilon_1}v_1.$$

The results of these studies can be formulated as a theorem.

Theorem 1. *Let in a Clifford algebra $R_{p,q}$, elements of a new basis be represented as follows from (2). Then there exists an unique (up to multiplication by a real number) element of a Clifford algebra T , such that $e_{\gamma_i} = Te_iT^{-1}$, $i = 1, \dots, n$. Operator Pauli is iterative formula $T = T_n$, where*

$$T_1 = e_0 \pm \varepsilon_1 e_{\gamma_1} e_1, \quad T_i = T_{i-1} \pm \varepsilon_i e_{\gamma_i} T_{i-1} e_i, \quad i = 2, 3, \dots, n,$$

where $\varepsilon_i = e_i^2 = e_{\gamma_i}^2$, the plus sign is taken if there are no zero divisors at the stage, minus sign if there are zero divisors at the stag.

References

- [1] Marchuk N. G. Demonstration performance and tensor products of Clifford algebra. Proceedings of the Steklov Institute of Mathematics. VA Steklov, 2015, Vol. 290, 154–165.
- [2] Marchuk N. G., Shirokov D. S. Introduction to the theory of Clifford algebras. Phasis. Moscow, 2012. 590.
- [3] Shirokov D. S. The generalization of the Pauli theorem to the case of Clifford algebras. DAN, 2011, 440 (5), 1–4.

Analysis of bifurcations at varying boundary conditions in a logistic equation with delay and diffusion

Dmitry S. Loginov

P. G. Demidov Yaroslavl State University, Yaroslavl, Russia

The logistic equation with delay and diffusion

$$\frac{\partial u}{\partial t} = d \frac{\partial^2 u}{\partial x^2} - ru(x, t - \tau)(1 + u), \quad 0 \leq x \leq 1 \quad (1)$$

and with boundary conditions

$$\left. \frac{\partial u}{\partial x} \right|_{x=0} = 0, \quad \left. \frac{\partial u}{\partial x} \right|_{x=1} = \gamma u \Big|_{x=1} \quad (2)$$

is one of the basic models of mathematical ecology. The coefficients of d , r and τ in (1) are positive. The boundary problem (1), (2) has a clear biological meaning. It describes, for example, a change in population size in the case when migration is possible through one of the borders. This migration is determined by the magnitude of the deviation of the number from its average value with the coefficient γ .

The paper shows that the negative values of the γ parameter expand the range of variation of the r parameter values at which the equilibrium state in (1), (2) is stable, and the positive γ — is narrowed.

In cases close to critical in the problem of the stability of the zero solution, an analysis of the local dynamics of the boundary value problem (1), (2) is given.

The proposed approach can be extended to more general boundary value problems, including equations with the dimension of the phase variable greater than 1.

The research was carried out with the financial support of the Russian Foundation for Basic Research in the framework of the research project No. 18-29-10043.

References

- [1] Gourley S. A., Sou J. W.-H., Wu J. H. *Nonlocality of Reaction-Diffusion Equations Induced by Delay: Biological Modeling and Nonlinear Dynamics*. Journal of Mathematical Sciences, 2004, vol. 124, no. 4, pp. 5119–5153.

- [2] Kaschenko S. A. *Local dynamics of a spatially distributed logistic equation with a delay and a high transfer coefficient* (in Russian)// *Differencialnie uravneniya*, 2014, vol. 50, no. 1, pp. 73–78.
- [3] Marsden J. E., McCracken M. F. *The Hopf Bifurcation and Its Applications*. New-York: Springer, 1976.
- [4] Kaschenko S. A. *On complex periodic solutions of a system of differential-difference equations with low diffusion* (in Russian)// *Dokladi Akademii Nauk SSSR*, 1989, vol. 306, no. 1, pp. 35–38.
- [5] Kaschenko S. A. *Normalization in the systems with small diffusion*// *International Journal of Bifurcation and Chaos in Applied Sciences and Engineering*, 1996, vol. 6, no. 6., pp. 1093–1109.
- [6] Kaschenko S. A. *Bifurcational Features in Systems of Nonlinear Parabolic Equations with Weak Diffusion*// *International Journal of Bifurcation and Chaos in Applied Sciences and Engineering*, 2005, vol. 15, no. 11, pp. 3595–3606.

Integrability analysis of constrained Euler equation on six dimensional Lie algebras

Andrzej J. Maciejewski¹, Maria Przybylska¹

¹ *University of Zielona Góra, Poland*

We consider several examples of Euler equations on six dimensional Lie algebra. A linear constraints was imposed on the vector fields defining these systems. Integrability analysis of obtained differential equations allows to identify integrable cases which are analogous to the Suslov and Kozlov cases. Non-integrability of several multi-parameter families of such systems was proved.

Dynamics of a Chaplygin sleigh with an unbalanced rotor

Ivan S. Mamaev¹, Ivan A. Bizyaev², Alexey V. Borisov²

¹ *M. T. Kalashnikov Izhevsk State Technical University, ul. Stencheskaya 7, Izhevsk, 426069 Russia*

² *Moscow Institute of Physics and Technology, Institutskii per. 9, Dolgoprudnyi, 141700 Russia*

Consider a system moving on a horizontal plane and consisting of two bodies. One of them is the carrying body — a platform (Chaplygin sleigh) which slides on a horizontal plane. The point P fixed on the platform cannot slide in some direction \mathbf{n} fixed relative to the platform:

$$(\mathbf{v}_P, \mathbf{n}) = 0, \quad (1)$$

where \mathbf{v}_P is the velocity of point P . The constraint (1) can be realized by means of the knife edge or the wheel pair, in which there is no slipping at the points of contact of the wheels with the plane. The other body is an unbalanced rotor. It is fixed on the platform at some point R and rotates freely in the horizontal plane (see Fig. 1).

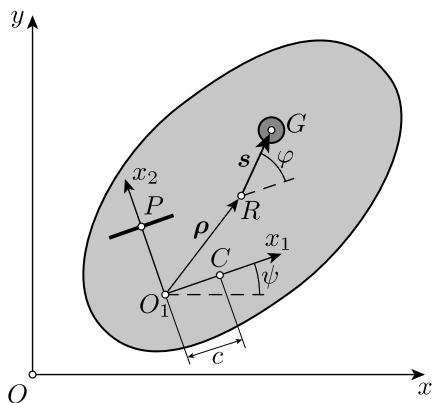


Fig. 1. A Chaplygin sleigh with a free rotor.

Let us introduce generalized coordinates. Let $\mathbf{r} = (x, y)$ be the radius vector of point O_1 in the fixed coordinate system Oxy . We specify the orientation of the platform by angle ψ between the axes Ox and O_1x_1 , and

the orientation of the rotor by angle φ between the axis O_1x_1 and the radius vector s directed from point R to the center of mass of the rotor G .

Thus, the configuration space \mathcal{N} is

$$\mathcal{N} = \{(x, y, \psi, \varphi), \psi, \varphi \bmod 2\pi\} \approx R^2 \times T^2.$$

In this case, instead of the generalized velocities $\dot{\mathbf{q}} = (\dot{x}, \dot{y}, \dot{\psi}, \dot{\varphi})$ it is more convenient to parameterize the tangent space $T_q\mathcal{N}$ using the quasi-velocities $\mathbf{v} = (v_1, v_2)$ — the projection of the velocity of point O_1 onto the axes of the moving coordinate system $O_1x_1x_2$, and ω_s, ω_r — the absolute angular velocities of the Chaplygin sleigh and the rotor:

$$v_1 = \dot{x} \cos \psi + \dot{y} \sin \psi, \quad v_2 = -\dot{x} \sin \psi + \dot{y} \cos \psi, \quad \omega_s = \dot{\psi}, \quad \omega_r = \dot{\psi} + \dot{\varphi}. \quad (2)$$

In this case, the constraint equation can be represented in the simplest form

$$f = v_2 = 0. \quad (3)$$

Equations of motion on $\mathcal{M}^7 = \{v_1, \omega_s, \omega_r, \varphi, \psi, x, y\}$, which we represent as

$$\begin{aligned} & \left[\begin{pmatrix} m_s + m_r & -m_r b & -m_r s \sin \varphi \\ -m_r b & J_s & m_r s (a \cos \varphi + b \sin \varphi) \\ -m_r s \sin \varphi & m_r s (a \cos \varphi + b \sin \varphi) & J_r \end{pmatrix} \begin{pmatrix} v_1 \\ \omega_s \\ \omega_r \end{pmatrix} \right] = \\ & = \begin{pmatrix} \omega_s (m_r s \omega_r \cos \varphi + (m_r a + m_s c) \omega_s) \\ \omega_s (m_r s (a \sin \varphi - b \cos \varphi) \omega_r - (m_r a + m_s c) v_1) \\ -\omega_r (m_r s (a \sin \varphi - b \cos \varphi) \omega_s + m_r s v_1 \cos \varphi) \end{pmatrix}, \\ & \quad \dot{\varphi} = \omega_r - \omega_s, \\ & \quad \dot{\psi} = \omega_s, \quad \dot{x} = v_1 \cos \psi, \quad \dot{y} = v_1 \sin \psi. \end{aligned} \quad (4)$$

The parameters of this system are contained in Table 1.

Suppose that the center of mass of the sleigh C and the point R of attachment of the rotor lie on the axis O_1x_2 , that is, $a = 0, c = 0$. In this case, there exists an additional integral

$$F = m_s b v_1 + I_s \omega_s, \quad I_s = J_s - m_r b^2. \quad (5)$$

Consequently, the reduced system defines the flow on the two-dimensional manifold. We examine this flow in more detail.

In this paper, the problem of the motion of a sleigh with a free rotor has been discussed. It is shown that three types of motion can be distinguished for an unbalanced sleigh:

Table 1. Description of the system parameters

Parameter	Description
I_s, m_s	the mass and the moment of inertia of the sleigh
I_r, m_r	the mass and the moment of inertia of the rotor
(a, b)	the coordinates of point R of attachment of the rotor in the coordinate system $O_1x_1y_1$
s	the distance from point R to the center of mass of the rotor G
c	the abscissa of the center of mass of the sleigh in the coordinate system $O_1x_1y_1$
J_s, J_r	auxiliary parameters

- 1) Asymptotically stable equilibrium points in which there is no rotation of the rotor relative to the platform. These motion regimes are generalizations of the motion of a usual sleigh (without a rotor).
- 2) The rotor undergoes periodic oscillations, and the trajectory of the point of contact of the sleigh traces out a quasi-periodic curve on the plane.
- 3) The rotor undergoes chaotic oscillations, and the trajectory of the point of contact of the sleigh traces out an unbounded curve on the plane.

The work was supported by the RNF under grant No. 18-71-00110.

The motion of foils in a fluid due to periodical excitations

Ivan S. Mamaev¹, Evgeny V. Vetchanin²

¹ *Kalashnikov Izhevsk State Technical University, Izhevsk, Russia*

² *Udmurt State University, Izhevsk, Russia*

This paper is concerned with plane-parallel motion of smooth foil (see Fig. 1a) and Zhukovskii foil (see Fig. 1b) in a fluid.

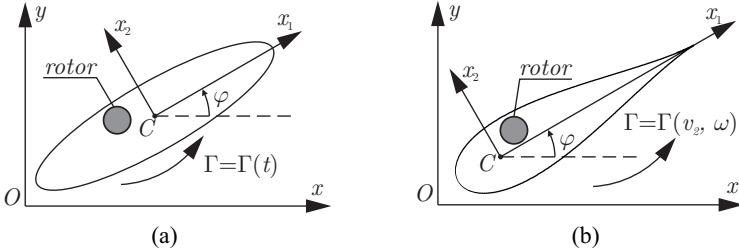


Fig. 1. Foils considered and coordinate system: a fixed frame, Oxy , and a moving frame, Cx_1x_2 , attached to the foil

The motion of the smooth foil is governed by the following equations [1]:

$$\begin{aligned}
 \dot{p}_1 &= p_2\omega - \Gamma v_2 - \mu_1 v_1, & \dot{p}_2 &= -p_1\omega + \Gamma v_1 - \mu_2 v_2, \\
 \dot{M} &= p_1 v_2 - p_2 v_1 - \mu_3 \omega, \\
 p_1 &= Av_1 - c_2\omega, & p_2 &= Bv_2 + c_1\omega, & M &= -c_2 v_1 + c_1 v_2 + I\omega + k(t), \\
 k(t) &= \varepsilon_k \sin \Omega t, & \Gamma &= \Gamma_0 + \varepsilon_\Gamma \sin(\Omega t + \delta).
 \end{aligned} \tag{1}$$

Here v_1 and v_2 are the components of linear velocity vector, ω is the angular velocity, p_1 and p_2 are the components of linear momentum, M is the angular momentum, μ_1 , μ_2 and μ_3 are the drag coefficients, c_1 and c_2 are the components of radius vector of the center of mass of entire system, coefficient A and B include mass of the foil with the rotor and added masses, coefficient I includes moment of inertia of the foil with the rotor and added moment inertial, and Ω is the angular frequency of oscillation of rotor and circulation.

For the smooth foil we can't determine circulation without additional assumptions. Within the framework of this paper we consider that circulation

is a periodic function of time. For the model (1) we investigate possibilities of speed-up, rectilinear motion and appearance of regular and chaotic attractors. More detailed description of results is presented in [1].

The motion of the Zhukovskii foil is governed by the following equations [2]:

$$\begin{aligned} \dot{p}_1 &= p_2\omega - a_1\rho_f\Gamma(v_2 - x_0\omega) - \mu_1v_1|v_1|, \\ \dot{p}_2 &= -p_1\omega + a_2\rho_f\Gamma v_1 - \mu_2v_2|v_2|, \\ \dot{M} &= p_1v_2 - p_2v_1 + a_2\rho_f\Gamma v_1\Delta - \mu_3\omega|\omega|, \end{aligned} \quad (2)$$

Here x_0 is conformal center of gravity, a_1 , a_2 and Δ are the coefficient obtained in [3], and ρ_f is the density of a fluid. Other symbols have meaning similar to above mentioned ones. For the Zhukovskii foil we should determine circulation due to Kutta-Chaplygin condition. So that in this case circulation is a function of linear velocity and angular velocity. An expression for circulation has been taken from PhD Dissertation [4]:

$$\Gamma = 2\pi s(1 - \zeta_c)(2v_2 + \beta\omega), \quad \beta = s(2 + \zeta_c), \quad (3)$$

where ζ_c is the parameter of the foil, and s is the scale factor.

For equations (2), three limit cycles have been found numerically. One of these solutions corresponds to rectilinear motion, two others correspond to the motion near circle. In the framework of the model (2), the rectilinear motion disappears when frequency Ω increases. The computer experiments show that strange attractors may appear in the system (2). More detailed description of results is presented in [3].

This work is supported by the Russian Science Foundation under grant 18-71-00111.

References

- [1] Borisov A. V., Mamaev I. S., Vetchanin E. V., *Self-propulsion of a Smooth Body in a Viscous Fluid Under Periodic Oscillations of a Rotor and Circulation*, Regular and Chaotic Dynamics, 2018, vol. 23, no. 7-8, pp. 850-874
- [2] Mamaev I. S., Vetchanin E. V., *The Self-propulsion of a Foil with a Sharp Edge in a Viscous Fluid Under the Action of a Periodically Oscillating Rotor*, Regular and Chaotic Dynamics, 2018, vol. 23, no. 7-8, pp. 875-886
- [3] Mamaev I. S., Tenenev V. A., Vetchanin E. V., *Dynamics of a Body with a Sharp Edge in a Viscous Fluid*, Russian Journal of Nonlinear Dynamics, 2018, vol. 14, no. 4, pp. 473-494
- [4] Mason R. J., *Fluid Locomotion and Trajectory Planning for Shape-Changing Robots*, PhD Dissertation, Pasadena, Calif.: California Institute of Technology, 2003, 264 pp.

On periodic motions of sympathetic pendulums at resonance in forced oscillations

Anatoly P. Markeev

Ishlinsky Institute for Problems in Mechanics, RAS, Moscow, Russia
Moscow Aviation Institute (National Research University), Moscow, Russia

Two mathematical pendulums of mass m and length ℓ move in a uniform gravity field. The suspension points O_1 and O_2 of the pendulums are located on a fixed horizontal line L at a constant distance $d = O_1O_2$ from one another. The pendulums are connected by a linear elastic spring of stiffness k . The distances of the attachment points of the springs to the pendulums from their suspension points are equal to b . In the relaxed state, the length of the spring is equal to d . Such pendulums are called sympathetic; their small linear oscillations are well studied [1].

The report assumes that the suspension points of the pendulums make periodic oscillations along the straight line L :

$$OO_1 = a \cos \omega t, \quad OO_2 = d + a \cos \omega t.$$

Here O is a fixed point of a straight line L , a is a constant quantity, $\omega = \sqrt{g/\ell}$ is the partial frequency of small linear oscillations of each of the pendulums.

Assuming that the amplitude of the oscillations of the suspension points is small, as well as the spring stiffness, the nonlinear problem of the existence and stability in the first approximation of periodic pendulum motions with a frequency equal to the oscillation frequency of the suspension points is solved. The formulated problem is characterized by the fact that it implements a 1: 1: 1 resonance, when the frequency of an external periodic action on the system is equal to its two frequencies of small natural oscillations.

Let us denote by ϕ_1 and ϕ_2 the angles of deflection of the pendulums from the vertical. Let $q_1 = 1/2(\phi_1 + \phi_2)$, $q_2 = 1/2(\phi_1 - \phi_2)$ be the generalized coordinates, p_1, p_2 be the corresponding impulses dimensionless with the help of the multiplier $m\ell\sqrt{g\ell}$, and $\tau = \omega t$ be the dimensionless time. Set

$$a = \varepsilon^3 \ell, \quad kb^2 = \varepsilon^2 mgl s, \quad q_i = \varepsilon Q_i, \quad p_i = \varepsilon P_i \quad (i = 1, 2),$$

where ε is a small parameter, s is a dimensionless parameter of the problem of the order of unity. Hamiltonian function is represented by a series of

powers ε as follows:

$$\begin{aligned} H &= H_0 + \varepsilon H_2 + \varepsilon^4 H_4 + \dots, \\ H_0 &= \frac{1}{2}(Q_1^2 + Q_2^2 + P_1^2 + P_2^2), \\ H_2 &= \sin \tau P_1 + s Q_2^2 - \frac{1}{24}(Q_1^4 + Q_2^4) - \frac{1}{4} Q_1^2 Q_2^2. \end{aligned}$$

Using Poincare and Lyapunov methods, and the perturbation theory of Hamiltonian systems [2], the following results have been obtained.

There are periodic motions of three types. For the motion of the first type (when $\phi_1 = \phi_2$; such motion in the considered problem always exists, regardless of the values of the parameters ε and s) we have

$$q_1 = -2\varepsilon \cos \tau + O(\varepsilon^3), \quad q_2 = 0.$$

For small values of ε , the motion of the first type is stable in the first (linear) approximation if $0 < s < 1/4$ or $s > 3/4$; they are unstable in Lyapunov if $1/4 < s < 3/4$.

For motions of the second type

$$q_1 = -\frac{\varepsilon}{2s} \cos \tau + O(\varepsilon^3), \quad q_2 = \pm \varepsilon \frac{\sqrt{64s^3 - 1}}{2s} \sin \tau + O(\varepsilon^3).$$

They exist only if $s > 1/4$, and are stable in the first approximation.

The motions of the third type are represented as

$$q_1 = \varepsilon \left(z - \frac{z^3 + 8}{16s} \right) \cos \tau + O(\varepsilon^3), \quad q_2 = \varepsilon \frac{z^3 + 8}{16s} \cos \tau + O(\varepsilon^3),$$

where z is the root of a polynomial $f(z, s)$ of the sixth degree of the form

$$f(z, s) = z^6 - 24sz^4 + 16z^3 + 192s^2z^2 - 192sz - 1024s^3 + 64.$$

In the plane z, s on the curve $f(z, s) = 0$, seven points $P_j(z_j, s_j)$ have been found with the coordinates

$$\begin{aligned} z_1 &= -2.57, & s_1 &= 0.31; & z_2 &= -2, & s_2 &= 0.75; \\ z_3 &= 0.98, & s_3 &= 0.31; & z_4 &= -2.51, & s_4 &= 0.50; \\ z_5 &= -2.43, & s_5 &= 0.64; & z_6 &= -1.19, & s_6 &= 0.64; \\ z_7 &= -0.54, & s_7 &= 0.50. \end{aligned}$$

The values $s = s_1$ and $s = s_2$ are bifurcation. For $s < s_1$, motions of the third type do not exist, for $s_1 < s < s_2$, there are four, and for $s > s_2$,

two periodic motions of the third type. Only those periodic motions that correspond to the values of z and s lying inside the segments P_1P_4 , $P_5P_2P_6$ and P_7P_3 of the curve $f(z, s) = 0$ are stable. Outside these segments, periodic motions of the third type are unstable.

The report was supported by state contract no. AAAA-A17-117021310382-5 and RFBR (project no. 17-01-00123) in Ishlinsky Institute for Problems in Mechanics RAS and Moscow Aviation Institute (National Research University).

References

- [1] Sommerfeld A. *Mechanik*. Zweite, revidierte auflage, 1944.
- [2] Arnold V.I. Kozlov V. V., and Neyshtadt A. I. *Mathematical Aspects of Classical and Celestial Mechanics*. 3rd ed. Encyclopedia Math. Sci. vol.3. Berlin: Springer, 2006. 526 p.

Local dynamics of a pair of Hutchinson equations with competitive and diffusion interaction

Elena A. Marushkina

P. G. Demidov Yaroslavl State University, Yaroslavl, Russia

The Hutchinson equation, first proposed in [1], is the simplest way to account for age structure in the population dynamics problem of individuals fighting for common food. We consider a system of two coupled Hutchinson equations describing the dynamics of weak competitive interaction between two populations:

$$\begin{aligned}\dot{N}_1 &= r(1 - N_1(t-1) + \alpha N_2)N_1 + d(N_2 - N_1), \\ \dot{N}_2 &= r(1 - N_2(t-1) + \alpha N_1)N_2 + d(N_1 - N_2).\end{aligned}\tag{1}$$

Here $N_1(t)$, $N_2(t)$ are the densities of populations, r is the Malthusian linear growth factor. The communication parameter α is responsible for species competition, and d is the coefficient of diffusion interaction.

Assume that parameter r is close to the critical value $r = \frac{\pi}{2} + \varepsilon$, and the coupling coefficients $d > 0$ and $\alpha > 0$ are proportional to the small parameter $0 < \varepsilon \ll 1$. Note that at $\varepsilon = 0$ in the stability spectrum of the equilibrium state $(1, 1)^T$ of the system (1) there is a pair of purely imaginary eigenvalues $\lambda = \pm i\frac{\pi}{2}$ of multiplicity 2, which correspond to two linearly independent eigenfunctions. In this case, this problem has a stable local four-dimensional integral manifold.

To find a system of ordinary differential equations responsible for the dynamics of the system (1) on this manifold, the standard replacement of the normal form method was used (see, for example, [2-4]):

$$N_j(t) = 1 + \sqrt{\varepsilon}(z_j(\tau)e^{i\frac{\pi}{2}t} + \bar{z}_j(\tau)e^{-i\frac{\pi}{2}t}) + \varepsilon u_{j1}(t, \tau) + \varepsilon^{3/2}u_{j2}(t, \tau) + \dots,\tag{2}$$

where $z_j(\tau)$ are the complex-valued functions of slow time $\tau = \varepsilon t$, ($j = 1, 2$).

On the third step of the algorithm from the conditions of solvability of problems for $u_{j2}(t, \tau)$ in the class of 4-periodic by t functions the following normal form was obtained:

$$\begin{aligned}\left(1 + i\frac{\pi}{2}\right)z_1' &= iz_1 + \frac{(1-3i)\pi}{10}z_1|z_1|^2 - \frac{\pi}{2}\alpha z_2 + d(z_2 - z_1), \\ \left(1 + i\frac{\pi}{2}\right)z_2' &= iz_2 + \frac{(1-3i)\pi}{10}z_2|z_2|^2 - \frac{\pi}{2}\alpha z_1 + d(z_1 - z_2).\end{aligned}\tag{3}$$

The dynamics of system (3) is studied. In particular, the conditions under which the homogeneous regime ($z_1 \equiv z_2$) of the problem loses stability in a divergent and oscillatory way are found. This allows us to find out the local dynamics of the system (1) at sufficiently small ε .

The work was supported by RFBR (project No. 18-29-10043).

References

- [1] Hutchinson G.E. *Circular causal system in ecology*// Ann. N.-Y. Acad. Sci., 1948, vol. 50, pp. 221–246.
- [2] Glyzin S.D. *Dynamical properties of the simplest finite-difference approximations of the “reaction-diffusion” boundary value problem* // Differential Equations, 1997, vol. 33, no. 6, pp. 808–814.
- [3] Glyzin S.D. *A registration of age groups for the Hutchinson’s equation*// Model. Anal. Inform. Syst., 2007, vol. 14, no. 3, pp. 29–42.
- [4] Glyzin S.D., Kolesov A. Yu. *Lokalnye metody analiza dinamicheskikh sistem*. Yaroslavl: Yaroslavl State University, 2006, 92 p. (in Russian)

Sub-Riemannian Geometry in Image Processing and Modelling of Human Visual System

Alexey R. Mashtakov

Ailamazyan Program Systems Institute of RAS, Pereslavl-Zalessky, Russia

The talk is devoted to usage of sub-Riemannian (SR) geometry in image processing and modelling of human visual system. In recent research in psychology of vision it was shown (J. Petitot, G. Citti, A. Sarti) that SR geodesics appear as natural curves that model a mechanism of the primary visual cortex V1 of a human brain for completion of contours that are partially corrupted or hidden from observation. We extend the model by including data adaptivity via a suitable external cost in the SR metric. We show that data-driven SR geodesics are useful in real image analysis applications and provide a refined model of V1 that takes into account a presence of visual stimulus.

We start from explanation of basic concepts of SR geometry and then show how they provide brain inspired methods in computer vision. We discuss how considering of SR structures on 2D and 3D images (or more precisely on their lift to the extended space of positions and directions) helps to detect some features, e.g. salient curves. We consider several particular examples: tracking of blood vessels in planar and spherical images of human retina, tracking of neural fibers in MRI images of human brain. Afterwards we show how a proper choice of the external cost based on a response of simple cells to the visual stimulus provide a model for geometrical optical illusions.

The talk is based on joint works [1–5].

References

- [1] Bekkers E., Duits R., Mashtakov A., Sanguinetti G. *A PDE approach to data-driven sub-Riemannian geodesics in $SE(2)$* // SIAM Journal on Imaging Sciences, 2015, vol. 8, no. 4, pp. 2740–2770.
- [2] Duits R., Ghosh A., Dela Haije T., Mashtakov A. *On sub-Riemannian geodesics in $SE(3)$ whose spatial projections do not have cusps* // Journal of Dynamical and Control Systems, 2016, vol. 22, no. 4, pp. 771–805.
- [3] Mashtakov A.P., Popov A. Yu. *Extremal controls in the sub-Riemannian problem on the group of motions of Euclidean space* // Regular and Chaotic Dynamics, 2017, vol. 22, no. 8, pp. 952–957.

- [4] Mashtakov A., Duits R., Sachkov Yu., Bekkers E., Beschastnyi I. *Tracking of lines in spherical images via sub-Riemannian geodesics on $SO(3)$* // Journal of Mathematical Imaging and Vision, 2017, vol. 58, no. 2, pp. 239–264.
- [5] Franceschiello B., Mashtakov A., Citti G., Sarti A. *Geometrical optical illusion via sub-Riemannian geodesics in the roto-translation Group* // Differential Geometry and its Applications, 2019, vol. 65, pp. 55–77.

The solution of dynamic problems of filtration consolidation in a rectangular area and the area representing the band, in the formulation of V. A. Florin

Evgenia A. Mikishanina

Cheboksary, Russia

The porous fully water-saturated flat region with the given coefficients of lateral pressure ξ_0 , the coefficient of relative compressibility of the medium m_v , the filtration coefficient k , the density of the medium ρ_T is considered. The medium is linear isotropic and obeys Hooke's law. Filtration of water in this environment is subject to the law of Darcy. External pressure applied to the water-saturated medium is transferred to the water. Thus, the proposed task below is relevant for clay soils.

The differential equation of plane filtration consolidation in the formulation of V. A. Florin [1] has the form

$$\frac{\partial H}{\partial t} = \frac{1}{2\gamma_m} \frac{\partial \Theta}{\partial t} + c_v \Delta H,$$

where H – the function of pressure, $\Theta = \sigma_{1,1} + \sigma_{2,2}$ – the sum of the main stresses from the external load, $c_v = \frac{k(1+\xi_0)}{2\gamma_w m_v}$ – the coefficient of consolidation for the plane problem, γ_w – the volumetric weight of water, $\Delta = \frac{\partial^2}{\partial x_1^2} + \frac{\partial^2}{\partial x_2^2}$ – the Laplace operator. The coefficient ξ_0 of side pressure of the soil of subjects is higher, than the elasticity of the soil is higher. Therefore, for sufficiently elastic media, the coefficient can be considered equal to 1.

Taking into account the inertial forces that arise during non-stationary deformation in the medium of zero shear stiffness ($\sigma_{i,i} = \sigma$, $\sigma_{i,j} = 0$), the system of equations relating the stresses σ , the velocity vector \mathbf{v} and the displacements \mathbf{u} will take the form [1, 2]

$$\begin{cases} \frac{\partial \sigma}{\partial x_i} + \rho_T \mathbf{f} = \rho_T \ddot{\mathbf{u}}, \\ \dot{\sigma} = \rho_T c_p^2 (\nabla \cdot \mathbf{v}), \\ \rho_T \ddot{\mathbf{u}} = \rho_T \mathbf{f} + (\lambda + \mu) \nabla (\nabla \cdot \mathbf{u}) + \mu \Delta \mathbf{u} \end{cases}$$

Thus, to solve the dynamic problem of consolidation theory, we can proceed to the boundary value problem for the system of differential equations

$$\begin{cases} \ddot{\sigma} = \frac{(\lambda + 2\mu)}{\rho_T} \Delta \sigma + \rho_T c_p^2 \nabla \cdot \mathbf{f}, \\ \dot{H} = \frac{1}{\gamma_w} \dot{\sigma} + c_v \Delta H. \end{cases}$$

Boundary conditions are determined by the features of the simulated scenario and depend on the shape of the region.

The problem is solved in a rectangular region by the method of separating variables, as well as in the region representing the band in the class of almost-periodic functions using the generalized discrete Fourier transform [3, 4].

References

- [1] Tsytoich N. A. Soil mechanics. Higher School, 1979, 272 p.
- [2] Terentiev A. G. Theory of elasticity with elements of resistance of materials and plasticity. Chuvash State Publ., 2016, 264 p.
- [3] Kulagina M. F., Mikishanina E. A. Construction of almost-periodic solutions of some differential equation systems // Mathematical notes of NEFU, vol. 22, no. 3, pp. 11–19.
- [4] Mikishanina E. A. Construction of almost-periodical solutions of some differential equation systems in the problems of filtration theory, UGATU publ., 2016, pp. 138–141.

Superposition method in computer simulation of multi-agent systems and its supercomputer implementation

Alexander A. Nazarov

Chuvash State University, Cheboksary, Russia

The study is based on the works of Russian scientists Makarov V.L., Bakhtizina A.R. and others, in which quite a lot of attention is paid to the construction of multi-agent systems [1]. The study proposes an approach to efficiently allocation of the counting core of multi-agent models on the architecture of a modern supercomputer, the use of more efficient low-level tools, the use of inter-node interaction, and the study of the possibility of common use of the central and graphics processor. The developed algorithm and software is based on new numerical algorithms and methods for multi-agent modeling problems and is designed to produce comprehensive, science-based estimates. The software package will realize for an intuitive dialogue between the decision maker and the mathematical model expressed as a system of simultaneous nonlinear equations (recursive functions and lag variables are possible) for solving which the theory of superposition of laws distributions and methods of numerical integration with a pre-determined degree of accuracy will be used.

Funding

The reported study was funded by RFBR and Chuvash Republic according to the research project No. 19-410-210012.

References

- [1] Application of Supercomputer Technologies for Simulation of Socio-Economic Systems / V.V.Okrepilov, V.L.Makarov, A.R.Bakhtizin, S.N.Kuzmina // R-Economy. 2015. Vol. 1, Iss. 2. P. 340–350.

Cloning of chimera states in a multiplex network of relaxation bistable oscillators

Vladimir I. Nekorkin

Institute of Applied Physics of Russian Academy of Science

A new phenomenon of the chimera states cloning in a large two-layer multiplex network with short-term couplings has been discovered and studied. For certain values of strength and time of multiplex interaction, in the initially disordered layer, a state of chimera is formed with the same characteristics (the same average frequency and amplitude distributions in coherent and incoherent parts, as well as an identical phase distribution in coherent part), as in the chimera which was set in the other layer. The mechanism of the chimera states cloning is examined. It is shown that the cloning is not related with synchronization, but arises from the competition of oscillations in pairs of oscillators from different layers.

Topological invariants for the Chaplygin–Goryachev integrable case with non-compact Liouville foliations

Stanislav S. Nikolaienko

*Lomonosov Moscow State University, Moscow Institute of Physics and Technology,
Moscow, Russia*

The Chaplygin–Goryachev case of integrability [1,2] can be considered as a one-parameter family of Hamiltonian systems on the dual space of the Lie algebra $e(3)$ given (in standard coordinates s_i, r_i) by the Hamiltonian function

$$H = \frac{1}{2} \left(s_1^2 + s_2^2 + 2s_3^2 + r_1^2 - r_2^2 + \frac{b}{r_3} \right), \quad b \in R.$$

On the symplectic leaf given by $r_1^2 + r_2^2 + r_3^2 = a^2$, $a > 0$, and $s_1r_1 + s_2r_2 + s_3r_3 = 0$, these systems are Liouville integrable with two degrees of freedom. For the case $b \geq 0$ their Liouville foliations were investigated in terms of Fomenko and Fomenko–Zieschang invariants (rough molecule, marked molecule) by O. Orel, P. Ryabov, and the author.

In the case $b < 0$ all the leaves of the corresponding Liouville foliations turn out to be non-compact: regular leaves are diffeomorphic to a cylinder $S^1 \times R$ and all 3D-bifurcations on regular energy levels have the type of a direct product [3]. To study the topology of the Chaplygin–Goryachev systems in this case, we use an analogue of the Fomenko–Zieschang invariant which completely classifies them on regular energy levels up to the Liouville equivalence.

References

- [1] Chaplygin S. A. *A new particular solution of the problem of motion of a rigid body in a fluid* // Tr. Otdel. Fiz. Nauk Obshch. Lubitelei Estestvozn., 1903, vol. 11, no. 2, pp. 7–10. (Russian)
- [2] Goryachev D. N. *New integrability cases of Euler's dynamic equations* // Varsh. Univ. Izv., 1916, no. 3, pp. 1–13. (Russian)
- [3] Nikolaenko S. S. *Topological Classification of the Goryachev Integrable Systems in the Rigid Body Dynamics: Non-Compact Case* // Lobachevskii Journal of Mathematics, 2017, vol. 38, no. 6, pp. 1050–1060.

Design features and control of a Spherical Robot of pendulum-type

Alexey V. Nozdrin¹, Yury L. Karavaev^{1,2,3}, Sergey V. Sokolov¹

¹ *Moscow Institute of Physics and Technology (State University), Dolgoprudny, Moscow Region, 141701, Russian Federation*

² *M. T. Kalashnikov Izhevsk State Technical University, 7 Studencheskaya str., Izhevsk 426069, Russian Federation*

³ *Center for Technologies in Robotics and Mechatronics Components, Innopolis University*

This paper is concerned with the design and control features of a spherical robot of pendulum-type, the scheme and dynamics of which are described in studies [1, 2]. Interest in spherical robots due to their structural features, which greatly expand the scope of their application, using fairly simple design concepts. Sealed spherical shell provides absolute protection of the spherical robot from aggressive environmental conditions (humidity, dust, temperature). The complete geometric symmetry of the spherical robot allows to realize omnidirectional motion, which for some modifications can be performed without additional energy costs.

Experimental studies of a spherical robot of combined type as an internal wheeled platform with a rotor placed inside the sphere are presented in studies [3, 4]. In this paper, we consider a spherical robot with a two-stage internal pendulum mechanism with the possibility of additional installation of mechanisms providing small periodic displacements of the center of mass and small changes of the kinetic moment is considered. Consider the equations of motion of a spherical equations of pendulum type rolling without slipping on an inclined absolutely rough plane. Based on the equations describing the dynamics, a control algorithm for the implementation of rectilinear motion and rotations is developed. A prototype of a spherical robot was created for experimental evaluation of the developed algorithms. In this paper, we consider the design features of the prototype, including the adjustment of regulators to ensure the specified rotational speeds of DC control motors. For each engine, we provide a feedback in the form of two potentiometers installed on one engine. These two precision potentiometers allow to get rid of the “dead zone” and significantly increase the accuracy of determining the angles of rotation of the pendulum.

References

- [1] Kilin A. A., Pivovarova E. N., Ivanova T. B. Spherical Robot of Combined Type: Dynamics and Control // *Regular and Chaotic Dynamics*, 2015, vol. 20, no. 6, pp. 716–728.
- [2] Ivanova T. B., Kilin A. A., Pivovarova E. N. Controlled Motion of a Spherical Robot with Feedback // *Journal of Dynamical and Control Systems*, 2018, 24, pp. 497–510.
- [3] Borisov A. V., Kilin A. A., Karavaev Yu. L., Klekovkin A. V. Stabilization of the motion of a spherical robot using feedbacks // *Applied Mathematical Modelling*, 2019, 69, pp. 583–592.
- [4] Kilin A. A., Karavaev Yu. L. Experimental research of dynamic of spherical robot of combined type // *Russian Journal of Nonlinear Dynamics*, 2015, vol. 11, no. 4, pp. 721–734.

Saturation free numerical scheme for computing the flow past a lattice of airfoils with sharp edge

Alexander G. Petrov

IPMech RAS

The Zhukovskiy–Chaplygin condition, which allows us to determine the circulation of the flow past contour with sharp edge — this is one of the most important achievements of S. A. Chaplygin, whose 150 birthday is celebrated this year. This research is devoted to this problem.

We consider the flow past of a lattice of airfoils by a potential fluid flow (Fig. 1).

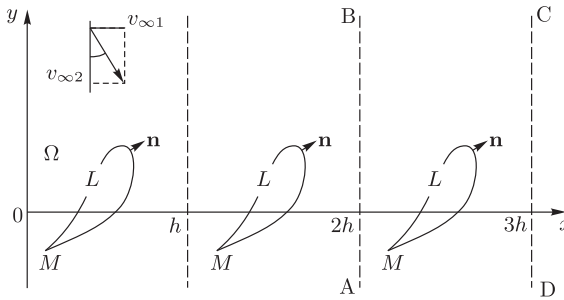


Fig. 1.

The profile line is determined parametrically by a equation in the form of two dependences of the Cartesian coordinates on parameter. For a smooth closed loop the Cartesian coordinates are periodic analytical functions $x(s)$ and $y(s)$. Their Fourier series coefficients decrease exponentially depending on the harmonic number. In the meantime, for a sharp edge loop they decrease much slower — inverse proportional to the square of the harmonic number. A substantial improvement of the Fourier series coefficients convergence may be obtained as follows. Let the digitized profile be given by the Cartesian coordinates $x_n, y_n, n = 1, 2, \dots, N$ so that the sharp edge corresponds to the coordinates origin (Fig. 1).

Then, if we continue by symmetry the profile curve, we will obtain a self-intersecting line at the coordinates origin in the shape of eight, shown in Fig. 2. The points of this curve are defined as follows: $\bar{x}_n = x_n, \bar{x}_{N+n} = -x_{N-n}; \bar{y}_n = y_n, \bar{y}_{N+n} = -y_{N-n}; n = 1, 2, \dots, N$. The

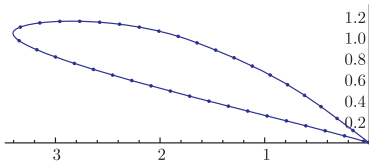


Fig. 2.

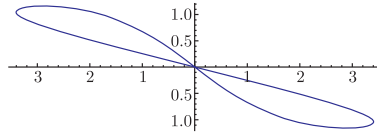


Fig. 3.

advantage of this curve compared to the initial one consists in the fact that on a double period $0, 2l$ it is determined by smooth infinitely differentiable functions $\bar{x}(s)$ and $\bar{y}(s)$. On a double period they can be calculated using quickly converging Fourier series. Furthermore, symmetry considerations imply that they will contain only sines

$$x = \sum_{n=1}^m a_n \sin n\gamma, \quad y = \sum_{n=1}^m b_n \sin n\gamma,$$

$$a_n = \frac{1}{N} \sum_{n=1}^{2N} \bar{x}_n \sin \frac{2\pi ni}{2N}, \quad b_n = \frac{1}{N} \sum_{n=1}^{2N} \bar{y}_n \sin \frac{2\pi ni}{2N}.$$

The velocity distribution at the boundary of the profile is found from the integral equation. With the help of quadrature formulae with no saturation, it is reduced to a linear system of equations. Checking the accuracy of calculations is carried out using generalized Zhukovsky profiles. They are built as follows. Equation $\frac{z-z_0 e^{i\varphi}}{z+z_0 e^{i\varphi}} = \left(\frac{Z-Z_0 e^{i\varphi}}{Z+Z_0 e^{i\varphi}} \right)^{z_0/Z_0}$ implies that the complex variable z can be expressed through Z : $z(Z) = z_0 e^{i\varphi} \frac{1+\sigma(Z)}{1-\sigma(Z)}$, $\sigma(Z) = \left(\frac{Z e^{-i\varphi} - Z_0}{Z e^{-i\varphi} + Z_0} \right)^{z_0/Z_0}$.

The complex variable Z is expressed through Z'' : $Z = (Z_0 - a e^{-i\beta} + Z'') e^{i\varphi}$.

The boundary points on the plane z correspond to a circle of radius a on the plane Z'' . The form and the position of the profile on plane z are determined by five parameters $Z_0, z_0, \beta, a, \varphi$. The angle of the sharp edge equals $\tau = \pi(2 - z_0/Z_0)$. The circulation is found from the condition that the velocity at the sharp edge equals zero: $\Gamma = -4\pi U a \sin(\theta + \beta)$. It is convenient to test use this exact solution for testing the numerical scheme. For the comparison let us take the profile from fig. 2, that is, the parameters of the profile are $Z_0 = 0.95$, $\tau = 0.4$, $\beta = 0.1$, $a = 1$, $\varphi = 0$. For angle $\theta = 0$ $\theta = 0$ and unit flow velocity $U = 1$ we obtain the exact value of

circulation $\Gamma = -1.2545437$, and for $\theta = 0.5$ we obtain $\Gamma = -7.09550658$. The results of calculus are presented in the array. In the first and second lines are presented the values of circulation errors for $N = 32; 48; 64$ and 80 .

	N	32	48	64	80
$\theta = 0$	$\Delta\Gamma$	-6×10^{-4}	-1×10^{-4}	-7×10^{-5}	-1×10^{-5}
$\theta = 0.5$	$\Delta\Gamma$	9×10^{-4}	7.7×10^{-5}	7×10^{-5}	6.7×10^{-5}

Acknowledgments

The research was carried out within the state assignment of FASO of Russia (state registration No. AAAA-A17-117021310382-5), supported in part by RFBR (project No. 17-01-00901).

References

- [1] Petrov A. G. Saturation Free Numerical Scheme for Computing the Flow Past a Lattice of Airfoils and the Determination of Separation Points in a Viscous Fluid // Computational Mathematics and Mathematical Physics, 2011, Vol. 51, No. 7, pp. 1239–1250.
- [2] Babenko K. I. Foundations of numerical analysis. Izhevsk, RCD. 2002, 848 p.
- [3] Loytzyansky L. G. Mechanics of liquid and gas. Moscow, Nauka, 1973. 848 p.

Modeling and analysis of dynamic systems in robotics polygon meshes

Vladimir N. Pichugin

Chuvash State University, Cheboksary, Russia

Three types of dynamic systems modeling are used in practice: on the basis of inhomogeneous rational bézier splines, on the basis of polygonal grids and on the basis of surfaces with hierarchical partitioning [1]. When modeling dynamic systems an important issue is the detail of the object, scene, and other visualization time (Fig. 1).

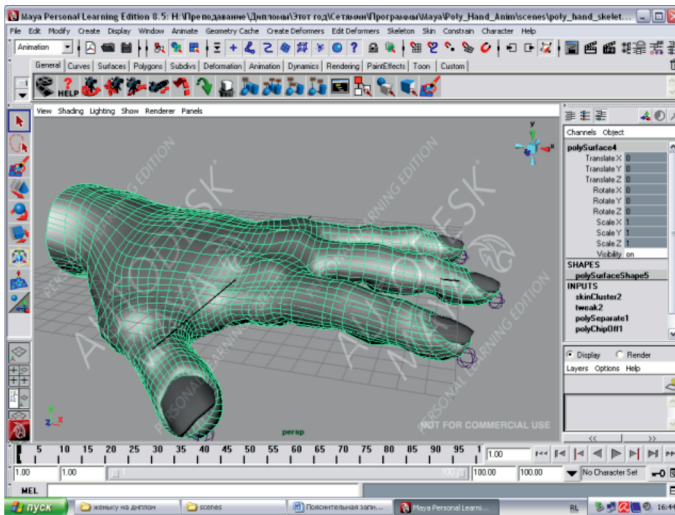


Fig. 1. Final polygon model with textures

The methodological recommendation for detailing the dynamic system, confirmed by a number of experiments, is the choice of values of the number of points of the polygon grid from the range 10...30 [1]. The use of adaptive decimation does not have much influence on the speed of the modeling algorithm, but significantly accelerates the calculation in the analysis of dynamic systems [2].

References

- [1] Kononykhin A. A. Modeling, visualization and analysis of volume bodies based on radial basis functions // Dis. kand. Techn. sciences. Moscow, 2007. 215 p.
- [2] Pichugin V. N. Computer graphics / V. N. Pichugin, R. V. Fedorov, M. P. Nemcova, A. A. Soldatov // International journal of experimental education. 2017. No. 2. P. 95–96.

Symmetric extremal trajectories in left-invariant optimal control problems

Alexey V. Podobryaev

A. K. Ailamazyan Program Systems Institute of RAS, Pereslavl-Zalesskiy, Russia

Geometric control theory (see for example [1]) deals with left-invariant optimal control problems on a Lie group G . Consider a family of left-invariant vector fields F_u that depend analytically on $u \in U \subset \mathbb{R}^n$. Consider also a left-invariant analytic function $\varphi : G \times U \rightarrow \mathbb{R}$, a point $q_1 \in G$, and a fixed time $t_1 > 0$. The problem is to find a control $u \in L^\infty([0, t_1], U)$ and a Lipschitz curve $q_u : [0, t_1] \rightarrow G$ such that

$$\int_0^{t_1} \varphi(q_u(t), u(t)) dt \rightarrow \min, \quad (1)$$

$$\dot{q}_u(t) = F_{u(t)}(q_u(t)), \quad q_u(0) = \text{id}, \quad q_u(t_1) = q_1 \in G.$$

The Pontryagin maximum principle [1, 2] gives us the necessary conditions for optimality. We obtain a Hamiltonian vector field $\vec{H} = \text{sgrad}H$ on the cotangent bundle T^*G , where H is the maximised Hamiltonian of the Pontryagin maximum principle. The projections of the trajectories of the vector field \vec{H} are called *the extremal trajectories*.

Definition 1. *A Maxwell point for an optimal control problem (1) is a point where two distinct extremal trajectories meet one another with the same value of the cost functional and the time. This time is called a Maxwell time.*

It is well known (see for example [3]), that an extremal trajectory can not be optimal after a Maxwell point. That is why description of Maxwell points plays an important role in investigation of optimality of extremal trajectories. In particular, the first Maxwell time is an upper bound for the time of loss of optimality (*the cut time*). A natural reason of appearance of Maxwell points is a symmetry of extremal trajectories. Let us give corresponding definitions.

Definition 2. *The exponential map of problem (1) is the map*

$$\text{Exp} : \mathfrak{g}^* \times \mathbb{R}_+ \rightarrow G, \quad \text{Exp}(p, t) = \pi \circ e^{t\vec{H}}(\text{id}, p), \quad (p, t) \in \mathfrak{g}^* \times \mathbb{R}_+,$$

where \mathfrak{g} is the Lie algebra of the Lie group G , and $e^{t\vec{H}}$ is the flow of the Hamiltonian vector field \vec{H} .

Definition 3. A symmetry of the exponential map is a pair of diffeomorphisms

$$s : \mathcal{W} \times \mathbb{R}_+ \rightarrow \mathcal{W} \times \mathbb{R}_+, \quad S : G \rightarrow G \quad \text{such that} \quad \text{Exp} \circ s = S \circ \text{Exp},$$

where $\mathcal{W} \subset \mathfrak{g}^*$ is an open dense subset.

Consider the trivialization of the cotangent bundle via left shifts:

$$\begin{aligned} \tau : G \times \mathfrak{g}^* &\rightarrow T^*G, & \lambda &= \tau(g, p) = dL_{g^{-1}}^*(p) \in T_g^*G, \\ g &\in G, & p &\in \mathfrak{g}^* = T_{\text{id}}^*G. \end{aligned}$$

where $L_g : G \rightarrow G$ is the left shift by the element $g \in G$.

The Hamiltonian H is left-invariant, so we assume that $H \in C^\infty(\mathfrak{g}^*)$. A Hamiltonian vector field is a sum of *the horizontal* and *the vertical parts* [1]:

$$\begin{aligned} \vec{H}(\tau(g, p)) &= d_{(g,p)}\tau(\vec{H}_{\text{hor}}(g, p) + \vec{H}_{\text{vert}}(p)), \\ \vec{H}_{\text{hor}}(g, p) &= dL_g d_p H, & \vec{H}_{\text{vert}}(p) &= (\text{ad}^* d_p H)p, \end{aligned}$$

where $d_p H \in T_p^* \mathfrak{g}^* \simeq \mathfrak{g}$ is the differential of H at a point p .

We see that due to the left-invariance of the problem the Hamiltonian system $\dot{\lambda} = \vec{H}(\lambda)$ is triangular (its vertical part is independent of state variables). So, one can naturally consider symmetries of the exponential map induced by symmetries of the vertical part of the Hamiltonian system.

We introduce sufficient conditions for existence of extension of symmetries of the vertical subsystem to symmetries of the exponential map. Also we give a construction of such extension.

Theorem 1. Let G be a connected Lie group, such that generic stabilizer of the coadjoint action is connected and has dimension not more than 1. Assume that $H : T^*G \rightarrow \mathbb{R}$ is a left-invariant Hamiltonian, and an operator $\sigma^* : \mathfrak{g}^* \rightarrow \mathfrak{g}^*$ is such that σ^* preserves the Hamiltonian H and there holds one of the two conditions:

- (a) $\sigma^*(\vec{H}_{\text{vert}}) = \vec{H}_{\text{vert}}$ and σ is an automorphism of the Lie algebra \mathfrak{g} ;
 - (b) $\sigma^*(\vec{H}_{\text{vert}}) = -\vec{H}_{\text{vert}}$ and σ is an anti-automorphism of the Lie algebra \mathfrak{g} .
- Then the pair of diffeomorphisms (s, S^{-1}) is a symmetry of the exponential map, where

$$s(p, t) = \begin{cases} (\sigma^* p, t), & \text{in case (a),} \\ (\sigma^* e^{t\vec{H}_{\text{vert}}} p, t), & \text{in case (b),} \end{cases}$$

and $S : G \rightarrow G$ is the (anti-)automorphism of the Lie group such that $d_{\text{id}} S = \sigma$.

Acknowledgment. This work is supported by the Russian Science Foundation under grant 17-11-01387 and performed in A. K. Ailamazyan Program Systems Institute of Russian Academy of Sciences.

References

- [1] Agrachev A. A., Sachkov Yu. L. *Control theory from the geometric viewpoint*. Springer, 2004.
- [2] Pontryagin L. S., Boltyanskii V. G., Gamkrelidze R. V., Mishchenko E. F. *The Mathematical Theory of Optimal Processes*. Oxford: Pergamon Press, 1964.
- [3] Sachkov Yu. L. *The Maxwell set in the generalized Dido problem*// Sbornik: Mathematics, 2006, vol. 197, no. 4, pp. 595–621.

Precession of the Kovalevskaya and Goryachev-Chaplygin tops

Ivan Yu. Polekhin

Steklov Mathematical Institute, Moscow, Russia

Let us consider a Liouville integrable Hamiltonian system and suppose that the level sets of the first integrals are compact. The motion in such a system is always a periodic or quasi periodic winding of the invariant torus. In special action-angle variables, the equations of motion have the following simple form:

$$\dot{I} = 0, \quad \dot{\varphi} = f(I). \quad (1)$$

These equations are in some sense convenient since their solutions can be presented explicitly in coordinates I, φ . At the same time, the simple form of the system and its integrability do not directly lead to the understanding of dynamics in original variables that have clear mechanical or geometrical interpretation. Many classical mechanical systems, especially integrable tops, can be considered as examples of such situations. Therefore, it would be useful to have various interpretations of motion in these integrable cases for an in-between view on the dynamics of the systems that is less complex than the ‘explicit’ quadratures and more detailed than the general statement of the Liouville-Arnold theorem.

One of the possible approaches to the description of motion of the Kovalevskaya top in the absolute space is provided by the result by V.V. Kozlov stating that the line of nodes has a mean motion Λ (provided some mild conditions are satisfied). To be more precise, the result means that the change of the precession angle ψ as a function of time has the form

$$\psi(t) = \psi_0 + \Lambda t + f(\varphi_1^0 + \omega_1 t, \varphi_2^0 + \omega_2 t) - f(\varphi_1^0, \varphi_2^0), \quad (2)$$

where f is a continuous function on a two-dimensional torus. Therefore, from the theorem, we obtain that the motion of the radius-vector of the axis of dynamical symmetry in the absolute space is a composition of two motions. First, if we put $\Lambda = 0$, then the radius-vector moves on the unit sphere. If $\Lambda \neq 0$ then the final motion is the composition of the motion on the sphere and the rotation around the vertical axis with the angular velocity Λ . This interpretation of motion is close to the classical picture of motion in the Lagrange case. Taking into account the result on the existence of a mean motion in the Kovalevskaya case, it is natural to try to find the dependence

of Λ on the initial data. For instance, we can try to find the initial data for which the mean motion of the precession angle is zero.

In the talk I will present some results concerning the change of the precession angle for two classical integrable tops: the Kovalevskaya top and the Goryachev–Chaplygin top. Based on the known results on the topology of Liouville foliations for these systems, we find initial conditions for which the average change of the precession angle is zero or can be estimated asymptotically. Some more difficult cases are studied numerically. In particular, we show that the average change of the precession angle for the Kovalevskaya top can be non-zero even in the case of zero area integral.

Dynamics of rolling and sliding rigid bodies

Maria Przybylska¹, Stefan Rauch-Wojciechowski²

¹ *Institute of Physics, University of Zielona Góra, Licealna 9, PL-65-417 Zielona Góra, Poland*

² *Department of Mathematics, Linköping University, 581 83 Linköping, Sweden*

Rigid bodies rolling and sliding in a horizontal plane belong to famous examples of nonholonomic mechanics. We will present results concerning dynamics of a rolling and sliding disk, a rolling rattleback and a rolling and sliding Jellett's egg. Dynamics of these systems is very complicated and hard for analysis because they are described by high-dimensional systems of non-integrable differential equations. In our analysis we use analytical and numerical calculations. Analytical studies are restricted to determination of asymptotic solutions: vertical spinning solutions, tumbling solutions and straight rolling solutions (only for disc) and analysis of their linear stability. These results are complemented with numerical simulations which provide a basis for better understanding of the behaviour of the investigated systems.

References

- [1] Przybylska M., Rauch-Wojciechowski S. *Dynamics of a rolling and sliding disk in a plane. Asymptotic solutions, stability and numerical simulations*// Regul. Chaotic Dyn., 2016, vol. 21, no. 2, pp. 204–231.
- [2] Rauch-Wojciechowski S., Przybylska M. *Understanding reversals of a rattleback*// Regul. Chaotic Dyn., 2017, vol. 22, no. 4, pp. 368–385.
- [3] Rauch-Wojciechowski S., Przybylska M. *On dynamics of Jellett egg*// Regul. Chaotic Dyn., 2019, in preparation.

Symplectic classification of spherical 2-atoms

Aleksandrina Yu. Rembovskaya

Lomonosov Moscow State University, Moscow, Russia

A Hamiltonian system with one degree of freedom is given by a function (Hamiltonian) on a two-dimensional symplectic manifold. If the Hamiltonian is a Morse function, then the neighborhood of its critical level containing saddle critical points is a two-dimensional surface P with a symplectic form on which a function having exactly one saddle critical value is given. This surface with a function on it is called a 2-atom (or simply an atom). Atoms are called symplectic equivalent if there is a symplectomorphism from one atom to another that translates levels of one function into levels of another. It is known that two symplectic equivalent atoms have the same variables of action. However, for arbitrary atoms, the coincidence of the action variables is not enough to state that they are symplectically equivalent.

Theorem. *Two topological equivalent spherical atoms with one atom's circle symplectically equivalent if corresponding period functions equal.*

References

- [1] Bolsinov A. V., Fomenko A. T. *Integrable Hamiltonian systems: geometry, topology, classification* // CHAPMAN & HALL/CRC. A CRC Press Company Boca Raton, London, New York, Washington, D.C. USA, 2004, 724 p.

Bifurcation Diagram and its Visualization in the One Generalized Integrable Model of Vortex Dynamics

Pavel E. Ryabov^{1,2,3}, Artemiy A. Shadrin¹

¹ *Financial University under the Government of the Russian Federation, Moscow, Russia*

² *Institute of Machines Science, Russian Academy of Sciences, Moscow, Russia*

³ *Udmurt State University, Izhevsk, Russia*

The report is devoted to results of phase topology research on a generalized mathematical model which covers such two problems as dynamics of two point vortices enclosed in a harmonic trap in a Bose-Einstein condensate and dynamics of two point vortices bounded by a circular region in an ideal fluid.

The generalized mathematical model is described by a Hamiltonian system of differential equations

$$\Gamma_k \dot{x}_k = \frac{\partial H}{\partial y_k}(z_1, z_2), \quad \Gamma_k \dot{y}_k = -\frac{\partial H}{\partial x_k}(z_1, z_2), \quad k = 1, 2, \quad (1)$$

where the Hamiltonian H has the form

$$H = \frac{1}{2} \left[\Gamma_1^2 \ln(1 - |z_1|^2) + \Gamma_2^2 \ln(1 - |z_2|^2) + \Gamma_1 \Gamma_2 \ln \left(\frac{[|z_1 - z_2|^2 + (1 - |z_1|^2)(1 - |z_2|^2)]^\varepsilon}{|z_1 - z_2|^{2(c+\varepsilon)}} \right) \right].$$

Here, the Cartesian coordinates of k -th vortex ($k = 1, 2$) with intensities Γ_k are denoted by $z_k = x_k + iy_k$. Physical parameter “ c ” expresses the extent of the vortices’ interaction, ε is a parameter of deformation, which determines two limiting cases, namely, a model of two enclosed in a harmonic trap point vortices in a Bose-Einstein condensate ($\varepsilon = 0$) [1] and a model of two bounded by a circular region point vortices in an ideal fluid ($c = 0, \varepsilon = 1$) [2].

The phase space \mathcal{P} is defined as a direct product of two open disks of radius 1 with the exception of vortices’ collision points. The Poisson structure on the phase space \mathcal{P} is given in the standard form $\{z_k, \bar{z}_j\} = -\frac{2i}{\Gamma_k} \delta_{kj}$, where δ_{kj} is the Kronecker delta. System (1) admits an additional first integral of motion, *the angular momentum of vorticity*, $F = \Gamma_1 |z_1|^2 + \Gamma_2 |z_2|^2$.

The function F together with the Hamiltonian H forms on \mathcal{P} a complete involutive set of integrals of system (1). According to the Liouville-Arnold theorem, a regular level surface of the first integrals is a nonconnected union of two-dimensional tori filled with conditionally periodic trajectories. The *momentum mapping* $\mathcal{F} : \mathcal{P} \rightarrow \mathbb{R}^2$ is defined by setting $\mathcal{F}(\mathbf{x}) = (F(\mathbf{x}), H(\mathbf{x}))$. Let \mathcal{C} denote the set of all critical points of the momentum mapping, i.e., points at which $\text{rank } d\mathcal{F}(\mathbf{x}) < 2$. The set of critical values $\Sigma = \mathcal{F}(\mathcal{C} \cap \mathcal{P})$ is called a *bifurcation diagram*.

In works [3] and [4] the bifurcation diagram was analytically investigated at $c = 1$ and $\varepsilon = 0$. In [5] and [6] a reduction to a system with one degree of freedom was performed and a bifurcation of three tori into one was found at $c > 3$ and $\varepsilon = 0$. This bifurcation was observed earlier by Kharlamov [7] while studying a phase topology of the Goryachev-Chaplygin-Sretensky integrable case in rigid body dynamics. In Fomenko, Bolsinov, and Matveev's work [8] it was found as a singularity in a 2-atom form of a Liouville foliation's singular layer. In Oshemkov and Tuzhilin's work [9] devoted to the splitting of saddle singularities, such a bifurcation was found to be unstable and its perturbed foliations were presented. In the situation where the physical parameter of vortices' intensity ratio is experiencing integrable perturbation, said bifurcation comes down to the bifurcation of two tori into one and vice versa [5]. In another limiting case ($c = 0, \varepsilon = 1$), the bifurcation analysis of dynamics of two point vortices bounded by a circular domain in an ideal fluid is performed [2]. In these limiting cases completely different bifurcation diagrams were obtained. In the case of a positive vortex pair [10] a new bifurcation diagram is obtained for which the bifurcation of four tori into one is indicated. The presence of three-into-one and four-into-one tori bifurcations in the integrable model of vortex dynamics with positive intensities indicates a complex transition and connection between two bifurcation diagrams in both limiting cases.

The report proposes an algorithm for an interactive visualization of the bifurcation diagram Σ and the bifurcations of Liouville tori for the generalized mathematical model described by (1) using *Python* and *Jupyter Notebook* capabilities.

The work of P.E. Ryabov was supported by RFBR grant 17-01-00846 and was carried out within the framework of the state assignment of the Ministry of Education and Science of Russia (1.2404.2017/4.6).

References

- [1] Koukouloyannis V., Voyatzis G., Kevrekidis P.G. *Dynamics of three noncorotating vortices in Bose–Einstein condensates*// Phys. Rev. E., 2014, vol. 89, no. 4, pp. 042905-1–14.
- [2] Kilin A. A., Borisov A. V., Mamaev I. S. *The Dynamics of Point Vortices Inside and Outside a Circular Domain*// in *Basic and Applied Problems of the Theory of Vortices* Borisov A. V. and Mamaev I. S. and Sokolovskiy M. A. (Eds.), Izhevsk: Regular and Chaotic Dynamics, Institute of Computer Science, 2003, pp. 414–440 (Russian).
- [3] Sokolov S. V., Ryabov P.E. *Bifurcation Analysis of the Dynamics of Two Vortices in a Bose-Einstein Condensate. The Case of Intensities of Opposite Signs* // Regular and Chaotic Dynamics, 2017, vol. 22, no. 8, pp. 979–998.
- [4] Sokolov S. V., Ryabov P.E. *Bifurcation Diagram of the Two Vortices in a Bose-Einstein Condensate with Intensities of the Same Signs* // Doklady Mathematics, 2018, vol. 97, no. 3, pp. 1–5.
- [5] Ryabov P.E. *Bifurcations of Liouville Tori in a System of Two Vortices of Positive Intensity in a Bose-Einstein Condensate* // Doklady Mathematics, 2019, vol. 99, no. 2, pp. 1–5.
- [6] Ryabov P.E., Sokolov S.V. *Phase Topology of Two Vortices of Identical Intensities in a Bose-Einstein Condensate*// Rus. J. Nonlin. Dyn., 2019, vol. 15, no. 1, pp. 59–66.
- [7] Kharlamov M.P. *Topological Analysis of Integrable Problems of Rigid Body Dynamics*, Leningrad: Leningr. Gos. Univ., 1988 (Russian).
- [8] Bolsinov A. V., Matveev S.V., Fomenko A.T. *Topological classification of integrable Hamiltonian systems with two degrees of freedom. List of systems of small complexity*// Russian Mathematical Surveys, 1990, vol. 45, no. 2, pp. 59–94.
- [9] Oshemkov A. A., Tuzhilin M.A. *Integrable perturbations of saddle singularities of rank 0 of integrable Hamiltonian systems* // Sbornik: Mathematics, 2018, vol. 209, no. 9, pp. 1351–1375.
- [10] Ryabov P.E. *On bifurcation of the four Liouville tori in one generalized integrable model of the vortex dynamics* // <https://arxiv.org/abs/1903.09945> (Russian).

Abnormal extremals in $(2, 3, 5, 8)$ sub-Riemannian problem

Yury L. Sachkov¹, Elena F. Sachkova¹

¹ *Program Systems Institute of RAS, Pereslavl-Zalessky, Russia*

We consider the left-invariant sub-Riemannian problem with the growth vector $(2, 3, 5, 8)$. The Hamiltonian flow for normal extremals for this problem is not Liouville integrable [1].

Instead, we study abnormal extremals for this problem. We show that abnormal extremals are obtained as the intersection of the symplectic foliation on the Lie coalgebra with the annihilator of square of the underlying distribution. Further, we describe qualitative types of abnormal extremals (including non-smooth ones). We characterize strictly abnormal and non-strictly abnormal geodesics. Further, we show that projections of abnormal extremals to the plane of underlying distribution are curves of the second and first order. Finally, we obtain bounds for corank of abnormal geodesics [2].

References

- [1] Lokutsievsky L.V., Sachkov Yu. L. *On Liouville integrability of sub-Riemannian problems on Carnot groups of step 4 and more*// Sbornik mathematics, 2018, vol. 209, no. 5, pp. 74–119.
- [2] Sachkov Yu. L., Sachkova E.F. *Structure of abnormal extremals in sub-Riemannian problem with the growth vector $(2, 3, 5, 8)$* , submitted.

Dynamics of a point in the axisymmetric potential of a massive fixed ring and center

Aleksandr V. Sakharov

Moscow Institute of Physics and Technology, Dolgoprudny, Russia

We consider a problem of three-dimensional motion of the passively gravitating point A in the potential created by a homogeneous thin ring and a massive point O , located in the center of the ring (fig. 1). The ring and center O are assumed to be fixed. Is such formulation potential is described by the expression [1–3]:

$$\Pi = -\frac{1-\mu}{r} - \frac{2\mu K(k)}{\pi p},$$

where $1-\mu$ – mass of the center O ($0 < \mu < 1$), μ – mass of the ring, r – distance from the center O to the point A , $K(k)$ – complete elliptic integral of the first kind with the module $k = \sqrt{1-q^2/p^2}$, q and p – minimum and maximum distance from the point A to the ring respectively ($0 \leq k < 1$).

Because of the axisymmetric symmetry of the problem it is convenient to consider cylindrical coordinate system ρ, φ, z . Then the potential doesn't depend on the angle φ . Defining the effective potential (fig. 2) it is possible to decrease the equations of motion by two orders of magnitude:

$$\ddot{\rho} = -\frac{\partial \tilde{\Pi}}{\partial \rho}, \quad \ddot{z} = -\frac{\partial \tilde{\Pi}}{\partial z}, \quad \tilde{\Pi}(\rho, z) = \Pi(\rho, z) + \frac{c^2}{2\rho^2}, \quad c = \rho^2 \dot{\varphi} = \text{const.}$$

The system also admit the integral of energy $h = (\dot{\rho}^2 + \dot{z}^2) / 2 + \tilde{\Pi}(\rho, z)$, which allows reduce order of the system.

In the study, invariant manifolds of the phase space of the system were found, some partial motions were described and classified, and phase portraits were constructed. Using the Poincare section, a stochastic layer was found. It was showed that in comparison with the work [3] some particular motions are preserved.

References

- [1] Duboshin G.N. *The theory of attraction*. Moscow, 1961, 288 p. (In Russian)
- [2] Lass H., Blitzer L. *The gravitational potential due to uniform disks and rings* // *Celestial Mechanics*, 1983, vol. 30, pp. 225–228.

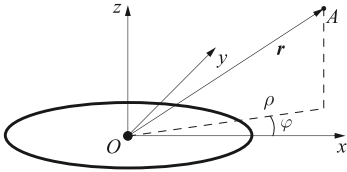


Fig. 1. Massive center O , ring and point A

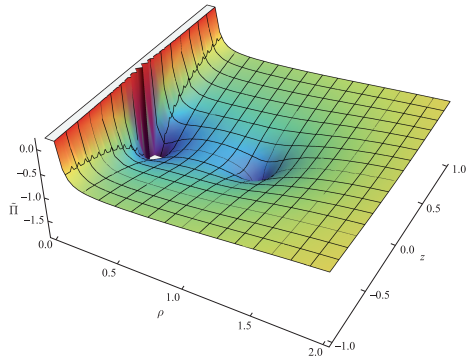


Fig. 2. Effective potential $\tilde{\Pi}(\rho, z)$

- [3] Broucke R. A., Elipe A. *The Dynamics of Orbits in a Potential Field of a solid Circular Ring* // Regular and Chaotic Dynamics, 2005, vol. 10, no. 2, pp. 129–143.
- [4] Tresaco E., Elipe A., Riaguas A. *Dynamics of a particle under the gravitational potential of a massive annulus: properties and equilibrium description* // Celestial Mechanics and Dynamical Astronomy, 2011, vol. 111, no. 4, pp. 431–447.
- [5] Alberti A., Vidal C. *Dynamics of a particle in a gravitational field of a homogeneous annulus disk* // Celestial Mechanics and Dynamical Astronomy, 2007, vol. 98, no. 2, pp. 75–93.

Hamiltonian systems and Lagrangian manifolds, corresponding to linearized equations of relativistic hydrodynamics

Andrei I. Shafarevich

Moscow State University, Moscow, Russia

We study short-wave asymptotic solutions of the linearized equations of relativistic hydrodynamics. These solutions are expressed in terms of conical Lagrangian manifolds in the cotangent bundle to the Minkowsky space. We discuss modes, corresponding different types of characteristics, and geometric phase — connection in the line bundle over Lagrangian surface, which govern the evolution of the wave amplitude.

Experimental investigations of the control algorithm of a mobile manipulation robot on a highly maneuverable platform with omniwheels

Vyacheslav A. Shestakov¹, Kirill S. Efremov¹, Yury L. Karavaev¹

¹ *Kalashnikov Izhevsk State Technical University, Izhevsk, Russia*

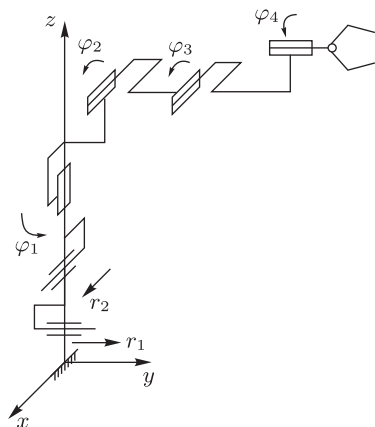
The mobile manipulation robot is a mobile platform on which manipulation and gripping mechanisms are placed. The design of a mobile platform with omniwheels is the most promising from the point of view of practical application due to the possibility of omnidirectional movement. Previously, management task of a highly mobile platform were discussed in works [1, 2, 3], and theoretical studies of the mobile manipulation robot were conducted, during which design was analyzed and the influence of center mass's position on the trajectory of motion was determined [4, 5, 6].

This paper presents experimental investigations of the control algorithm of a mobile manipulation robot on a highly maneuverable platform with omniwheels. During the execution of the algorithm, the following tasks are solved: recognition of a object of manipulation, determination of the distance to it; solution of the inverse positional problem for the mobile manipulation robot taking into account the minimization of energy consumption per movement. The result of the algorithm is the capture and loading of the object of manipulation, inaccessible to capture without the movement of the mobile platform.

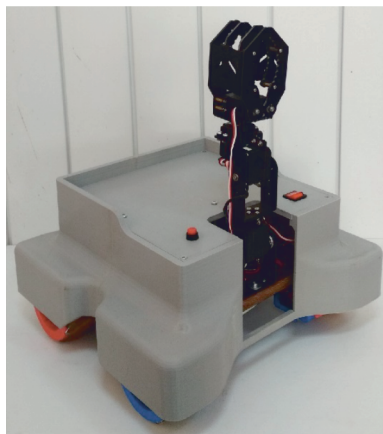
The reported research was funded by Russian Foundation for Basic Research and the government of the region of the Russian Federation, grant No. 18-48-183004 r_mol_a.

References

- [1] Borisov A. V., Kilin A. A., Mamaev I. S. An omni-wheel vehicle on a plane and a sphere // Russian Journal of Nonlinear Dynamics, 2011, vol. 7, no. 4, pp. 785–801.
- [2] Kilin A. A., Bobykin A. D. Control of a Vehicle with Omniwheels on a Plane // Russian Journal of Nonlinear Dynamics, 2014, vol. 10, no. 4, pp. 473–481.
- [3] Kilin A., Bozek P., Karavaev Y., Klekovkin A., Shestakov V. Experimental investigations of a highly maneuverable mobile omniwheel robot // International Journal of Advanced Robotic Systems, 2017, vol. 14, no. 6, pp. 1–9.



(a)



(b)

Fig. 1. Structural scheme a) and a prototype b) of a mobile manipulation robot on a highly maneuverable platform with omniwheels

- [4] Shestakov V., Karavaev Y., Klekovkin A. Development of a mobile omniwheel robot with a manipulator // The collection of materials of the Republican exhibition of the XXV sessions of innovative student projects, 2018, pp. 76–79.
- [5] Karavaev Y., Shestakov V., Building service area of a highly maneuverable mobile omniwheel robot // Intelligent systems in manufacturing, 2018, vol. 16, no. 3, pp. 90–96.
- [6] Shestakov V., Karavaev Y., Klekovkin A., Evaluation of the effect of position of center of mass of a highly maneuverable mobile omniwheel robot // XXX International Innovation Conference of Young Scientists and Students IICYSS-2018, 2018, pp. 516–520.

Estimation of azimuthal instabilities under the joint action of laser radiation and a magnetic field on a plasma

Vyacheslav V. Shumaaev

Bauman Moscow State Technical University, Moscow, Russia

One of the main obstacles to the uniform laser compression of a fusion target is the plasma formation instability (the Rayleigh–Taylor instability is the most dangerous). In all the considered schemes, the impulsive character is important [1–14]. In this case, not all possible plasma instabilities are dangerous, but only those of them that most rapidly increase with time (for example, Rayleigh-Taylor instability).

Let us estimate the value of azimuthal instabilities of the Rayleigh–Taylor type in the combined effect of laser radiation and a magnetic field on the plasma, using separate results of [15, 16]. Let us turn to the coordinate system associated with the spatially averaged position of the contact boundary. In this case, the volume forces acting on the contact boundary will either accelerate its movement (at the first two stages: $d^2r/dt^2 = a > 0$), or slow down (at the third stage: $a < 0$). The speed of azimuthal disturbances development in time is determined by the relation:

$$\omega^2 \approx \left| \frac{dV}{dt} \right| k \approx \left| \frac{dV}{dt} \right| \frac{\ell}{r}, \quad \frac{d\vec{V}}{dt} = \frac{d^2\vec{r}}{dt^2}, \quad (1)$$

where the wave number k is determined by the condition $\lambda\ell = 2\pi r$, $\ell = 1, 2, 3, \dots$; $\lambda = 2\pi/k$ is the length of the azimuth wave. On the contact boundary between the solid wall of the target and the environment, the following boundary condition can be set:

$$k_m \frac{\partial T_s}{\partial r} = q - D\rho_0\Omega. \quad (2)$$

Assuming that the relationship (2) is satisfied, it is possible to determine the speed of movement D and acceleration dD/dt of the contact boundary in a relative coordinate system:

$$D = \frac{q(t)}{\rho_0\Omega}, \quad a = \frac{dD}{dt} = \frac{dq/dt}{\rho_0\Omega}, \quad (3)$$

where ρ_0 is the density of the target substance, Ω is the specific heat of evaporation (phase transition) of the target substance, $q(t)$ is the flux density of broadband radiation on the target.

The magnitude of the acceleration of the contact boundary can be estimated using an approximate ratio of the form:

$$\frac{dV}{dt} = \frac{dD}{dt} + \frac{\frac{P}{\rho_0} \pm \frac{H^2}{2\rho_0\pi} - V^2/2}{\delta},$$

where δ is the target wall thickness, $\rho_c = \frac{m_0 m_e}{4\pi e^2} \left(\frac{2\pi c}{\lambda}\right)^2 = 1,83 \times 10^{-3} \frac{A\lambda}{z}$ is the critical plasma density, m_0 is the mass of one particle of a substance (molecule, atom or ion), A is the atomic weight of plasma nuclei, λ is the laser radiation wavelength, z is the average ion charge, $P \approx q^{2/3} \rho_c^{1/3}$ is the value of the maximum pressure that can be achieved in the plasma.

Then the maximum time $1/\omega$ for the development of the Rayleigh–Taylor instability:

$$\frac{1}{\omega} \approx \sqrt{\frac{r}{|d\vec{V}/dt| \ell}}. \quad (4)$$

From relation (4) it follows that in the process of compression ($r \rightarrow 0$), the probability of instability increases. It also follows that an increase in the rate of heating of the target ($dq/dt \rightarrow \infty$) can have a negative role on the development of instability. However, by the time instant t_1 target material vapors form, near the contact boundary, a very dense layer of vapor that does not pass laser radiation $q(t)$ through it. The screening process is also facilitated by the compression of the plasma vapor layer using an external magnetic field.

This research is supported by the Russian Ministry of Science and Higher Education (Project No. 13.5240.2017/8.9) and Bauman Moscow State Technical University Target Program for 2018–2020.

References

- [1] Varaksin A. Yu. Concentrated Air and Fire Vortices: Physical Modeling // High Temperature, 2016, 54.
- [2] Ryzhkov S. V., Chirkov A. Y. and Ivanov A. A. // Fusion Sci. Technol. 1013, 63, pp. 135–138.
- [3] Varaksin A. Yu. Air Tornado-like Vortices: Mathematical Modeling // High Temperature, 2017, 55, 286.
- [4] Kuzenov V. V., Polozova T. N., Ryzhkov S. V. Numerical simulation of pulsed plasma thruster with a preionization helicon discharge // Problems of Atomic Science and Technology, 2015, 4(98), pp. 49.

- [5] Zarubin V. S., Kuvyrkin G. N., Savel'eva I. Y. Radiative-conductive heat transfer in a spherical cavity // *High Temperature*, 2015, vol. 53, pp. 234–239.
- [6] Kuzenov V. V., Ryzhkov S. V., Shumaev V. V. Numerical thermodynamic analysis of alloys for plasma electronics and advanced technologies // *Probl. At. Sci. Technol.* 2015. No. 4 (98). P. 53–56.
- [7] Kuzenov V. V., Ryzhkov S. V., Shumaev V. V. Application of Thomas-Fermi model to evaluation of thermodynamic properties of magnetized plasma // *Probl. At. Sci. Technol.* 2015. No. 1 (95). P. 97–99.
- [8] Ryzhkov S. V., Kuzenov V. V. Analysis of the ideal gas flow over body of basic geometrical shape // *International Journal of Heat and Mass Transfer*, 2019, vol. 132, pp. 587–592.
- [9] Kuzenov V. V., Ryzhkov S. V., Gavrilova A. Yu. et al. Computer simulation of plasmadynamic processes in capillary discharges // *High Temperature Material Processes*, 2014, 18, 119.
- [10] Kuzenov V. V., Ryzhkov S. V. Numerical Modeling of Laser Target Compression in an External Magnetic Field // *Mathematical Models and Computer Simulations*, 2018, vol. 10, pp. 255–264.
- [11] Kuzenov V. V., Ryzhkov S. V. Approximate method for calculating convective heat flux on the surface of bodies of simple geometric shapes // *J. Physics: Conference Series*, 2017, vol. 815, 012024.
- [12] Ryzhkov S. V., Kuzenov V. V. New realization method for calculating convective heat transfer near the hypersonic aircraft surface // *ZAMP*, 2019, vol. 70, p. 46.
- [13] Kuzenov V. V., Ryzhkov S. V. // *Applied Physics*, 2015, no. 2, pp. 37–44.
- [14] Kuzenov V. V., Ryzhkov S. V. Radiation-hydrodynamic modeling of the contact boundary of the plasma target placed in an external magnetic field // *Applied Physics*, 2014, no. 3, pp. 26–30.
- [15] Caldirola P., Knoepfel H. (eds.) *Physics of High Energy Density*. Academic Press, 1971. 418 p.
- [16] Knoepfel H. *Pulsed High Magnetic Fields*. North-Holland Publishing Company, 1970.

On the Influence of the Pressure Gradient on the Electron Concentration in the Wake of Descent Spacecraft

Nikolai I. Sidnyaev¹, Vladimir U. Loginov¹

¹ *Bauman Moscow State Technical University (BMSTU), Moscow*

A characteristic feature of the problems of aerodynamics and heat transfer of high supersonic velocities is the need for joint account of dissipative processes due to viscosity, thermal conductivity and diffusion, as well as physical and chemical processes in the “trace” (see Fig. 1), which can lead to qualitatively new effects in comparison with the flows of perfect gas [1–3]. In such tasks, it is necessary to take into account the multicomponent, high temperature, chemically reacting mixture in a high-speed flow, in which various gas-dynamic processes can occur. In the case of non-equilibrium flow it is necessary to take into account a number of new processes of chemical energy transfer, which are not taken into account in equilibrium flows or in the flow of an ideal gas. In particular, the interaction of the surface of the spacecraft (SC) with the atmosphere is essential to its catalytic properties. On the flight path in the atmosphere flow regimes in the Wake of spacecraft vary from subsonic to molecule O_2 and N_2 , however, the model of perfect gas can be used only in the field of supersonic velocities. Air dissociation is observed in the hypersonic region and it is necessary to use a 5-component model to describe it (O_2 , N_2 , NO , O , N) [1, 7]. At Mach numbers greater than 12, ionization is observed and in this case it is necessary to take into account 7 components, and at Mach more than 17–11 components. In comparison with the kinetics of homogeneous reactions, the mechanism and rates of processes determining the interaction of gas with the surface are much less studied and expressed quantitatively [1]. The coefficients characterizing the processes on the surface depend both on the surface properties and on the conditions in the gas phase [7]. Therefore, both in experiments and in flight conditions, when studying the electron concentration in the “trace”, it is required to apply very accurate theoretical models of the flow and methods for calculating heat transfer with the corresponding gas-phase reactions on the surface.

References

- [1] Sidnyaev N.I. Flow around hypersonic aircraft in the conditions of surface destruction. — M.: FIZMATLIT, 2017. — 304 p.

- [2] Sidnyaev N. I. Study of heat and mass transfer for hypersonic flow past a complex body of revolution // *Thermophysics and Aeromechanics*, 2006, Vol. 13. No. 1. P. 2–16.
- [3] Sidnyaev N. I. Pressure distribution along the surface of combined bodies streamlined by a hypersonic flow // *Technical Physics Letters*, 2006, Vol. 32. No. 7. P. 564–566.
- [4] Sidnyaev N. I. Aerodynamic Performances of Hypersonic Aircrafts with Surface Mass Transfer // *Mathematical Models and Computer Simulations*, 2009, Vol. 1. No. 3. P. 343–352.
- [5] Prokopenko E. A., Pirogov S. Yu. Study of reflection of radio waves from the plasma region in the Wake of an axisymmetric body moving in the earth's atmosphere // *Space research*, 2018, Vol. 56. No. 3. P. 218–227.
- [6] Sidnyaev N. I., Gordeeva N. M. Asymptotic theory of flows for the near wake of an axisymmetric body // *Journal of Applied and Industrial Mathematics*, 2015, Vol. 9, No. 1, pp. 110–118.
- [7] Sidnyaev N. I. and Gordeeva N. M. Study of the influence of energy and mass transfer on the flow in the “trace” of supersonic models of conical bodies/ *Mathematical modeling and numerical methods*. 2015. Vol. 5. No. 5 (5). P. 31–49.

Численные исследования предельного сопротивления остроугольного анизотропного клина сдвигу и отрыву

Марина Е. Сироткина¹, Елена Г. Ефимова¹, Евгения В. Володина¹

¹ ЧГУ имени И. Н. Ульянова, Чебоксары, Россия

Предлагается обобщение исследований предельного напряженного состояния остроугольного клина с учетом анизотропных свойств материала и его разрывной в силу составного материала клина неоднородности. По разные стороны от линии разрыва свойств анизотропный материал клина обладает различными пределами текучести [1]. Условия предельного сопротивления деформациям сдвига имеют вид $\tau_n(\gamma) = C_1(\gamma)$, $\tau'_n(\gamma) = C'_1(\gamma)$ в зоне, примыкающей к нагруженной грани, $\tau_n(\gamma) = C_2(\gamma)$, $\tau'_n(\gamma) = C'_2(\gamma)$ в зоне, примыкающей к свободной от нагрузки грани. $C_1(\gamma)$, $C_2(\gamma)$ – предельные касательные напряжения на площадках, составляющих угол γ с осью Ox . Условия сопротивления отрыву в зоне растягивающих напряжений имеют вид $\sigma_n(\gamma) = d(\gamma - \lambda_d)$, $\sigma'_n(\gamma) = d'(\gamma - \lambda_d)$, где $d(\gamma)$ – предел сопротивления анизотропного материала отрыву [2].

Из условий равновесия элементов клина на линии разрыва и в зоне отрыва составлена и решена система нелинейных уравнений для нахождения геометрических параметров составного остроугольного клина и предельной нагрузки.

Список литературы

- [1] Григорьева М. Е., Григорьев Е. А. Задача об изгибе клина при разрывном условии анизотропной пластичности // Актуальные задачи математики и механики. Сб. статей. Чебоксары, ЧувГУ, 1995. С. 44–50.
- [2] Сироткина М. Е., Артемьев И. Т. К численному решению нелинейных дифференциальных уравнений с частными производными и условиями состояния методом характеристик // Вестник ЧувГУ, № 3–4, 2001. С. 56–59.

Bifurcation Diagram For Two Vortices of Opposite Signs in Trapped Bose–Einstein Condensate

Sergei V. Sokolov

Moscow Institute of Physics and Technology, Moscow, Russia

Dynamics of the vortex filaments is traditional object of interest for mathematicians and physicists. At recent three decades a lot of experimental and theoretical results were obtained for the new physical object – Bose-Einstein condensate, in which vortex filaments also can be observed.

This report will be concerned on the dynamics of two vortex filaments in a Bose-Einstein condensate confined into the trap. We introduce new results of topological analysis of corresponding dynamical system. Work based on our previous results [1–3]. Mentioned above dynamical system is a completely Liouville integrable Hamiltonian system with two degrees of freedom. Here we introduce the bifurcation diagram of momentum map and corresponding bifurcations of Liouville tori. With comparison of the [3] we discuss vortices with intensities of the opposite signs.

The work of S. V. Sokolov was carried out at MIPT under project 5–100 for state support for leading universities of the Russian Federation and also partially support by RFBR grant 18-01-00335.

References

- [1] S. V. Sokolov and P. E. Ryabov, Bifurcation Analysis of the Dynamics of Two Vortices in a Bose–Einstein Condensate. The Case of Intensities of Opposite Signs, *Regular and Chaotic Dynamic*, 2017, vol. 22, no. 8, p. 976–995.
- [2] S. V. Sokolov, and P. E. Ryabov, Bifurcation Diagram of the Two Vortices in a Bose-Einstein Condensate with Intensities of the Same Signs, *Doklady Mathematics*, 2018, vol. 97, no. 3, pp. 1–5.
- [3] P. E. Ryabov, and S. V. Sokolov, Phase Topology of Two Vortices of Identical Intensities in a Bose – Einstein Condensate, *Russian Journal of Nonlinear Dynamics*, 2019, vol. 15, no. 1, pp. 59–66.

The investigation of whirlwind in stability of the plasmoid above the water surface

Gennady M. Sorokin¹, Tatiana G. Terekhova¹

¹ *Chuvash State University, Cheboksary, Russia*

With the help of an optical Tyopler device the processes of origin, formation and decay of the plasmoid of 10–12 cm in diameter were investigated. The experimental setup for obtaining such plasmoids as a result of the high-voltage discharge in the steam–and–air area is described in [1]. The working area of the interferential shadow device of AIB–458 type represents a circle in diameter of 20 cm that allows to observe the streams of gas and plasma near the object under study. The process of injection of an electron beam in the steam–and–air area was recorded. By means of the digital system of registration the video pictures showing the formation of spherical plasmoids and its decay are obtained. The authors believe that the warming of the bottom surface of the plasmoid from the side of the not cooled down electrode corresponds to the process of decay of the plasmoid. The difference of the temperatures from above and from below the spherical shell leads to disruption of the thermodynamic equilibrium inside the plasmoid, which decomposes, turning into a turbulent ring whirlwind. The paper discusses, that time of life of a ring whirlwind is approximately equal to time of life of a spherical plasmoid.

References

- [1] Sorokin G. M., Ruzan L. L., Germanov I. N. The Research of the high-voltage category over a water surface // Optics of the at-mosphere and the ocean. 2010. Vol. 23. No. 12. P. 1127–1131.

Bifurcation analysis of periodic motions originating from hyperboloidal precession of a dynamically symmetric satellite

George A. Sukhov

Moscow aviation institute, Moscow, Russia

We deal with periodic motions of a symmetric satellite originating from its Hyperboloidal precession. The satellite is considered to be a dynamically symmetric rigid body with principal moments of inertia J_1 , J_2 and J_3 ($J_1 = J_2$). Its center of mass O moves in a circular orbit in central Newtonian gravitational field at angular velocity ω_0 . To describe the satellite's motion around its center of mass we introduce an orbital reference frame $OXYZ$ and a mobile reference frame $Oxyz$. Axes OX , OY and OZ are aligned with transversal and normal vectors to the orbit and with the radius-vector of the satellite's center of mass, respectively. Axes Ox , Oy and Oz are aligned with the satellite's principal axes of inertia. Relative position of these reference frames is defined by Euler's angles ψ , θ , ϕ . Following [1] the equations of motion of a dynamically symmetric satellite can be written in a canonical form with the following Hamiltonian:

$$\begin{aligned}
 H = & \frac{p_\psi^2}{2 \sin^2 \theta} + \frac{p_\theta^2}{2} - \left(\frac{\gamma \cos \theta}{\sin^2 \theta} + \cos \psi \cot \theta \right) p_\psi - \\
 & - \sin \psi p_\phi + \frac{1}{2} \gamma^2 \cot^2 \theta + \gamma \frac{\cos \psi}{\sin \theta} + \frac{1}{2} \delta \cos^2 \theta,
 \end{aligned} \tag{1}$$

where p_ψ and p_θ are dimensionless impulses corresponding to ψ and θ , $\gamma = \frac{J_3}{J_1} \frac{r_0}{\omega_0}$ and $\delta = 3(J_3/J_1 - 1)$ are dimensionless parameters and r_0 is projection of satellite's absolute angular velocity along its principal axis Oz . The independent variable is true anomaly $\nu = \omega_0 t$. The system possesses a cyclical coordinate ϕ and its respective impulse p_ϕ retains constant value.

Equations of motions with Hamiltonian (1) possess a particular solution $\theta_0 = \frac{\pi}{2}$, $\cos \psi_0 = -\gamma$, $p_{\theta_0} = \sin \psi_0$, $p_{\psi_0} = 0$ known as Hyperboloidal precession. If $\delta > 0$ the Hyperboloidal precession is Lyapunov stable and two types of periodic motions exist in its neighbourhood: short-periodic motions with period close to $2\pi/\omega_2$ and long-periodic motions with period close to $2\pi/\omega_1$, respectively, where $\omega_{1,2} = \sqrt{1/2 \left(\delta + 1 \mp \sqrt{(\delta - 1)^2 + 4\gamma^2 \delta} \right)}$ are the frequencies of the linearized system. In [2–4] the aforementioned periodic motions were obtained analytically in form of power series. Analytical

representation is only valid for small deviations Δh of energy integral constant h from its value for Hyperboloidal precession. For non-small values of Δh a numerical method was used [3–5].

In this work a numerical bifurcation analysis was carried out for families of periodic motions originating from Hyperboloidal precession of a symmetric satellite in a non-resonant case and in case of third ($\omega_2 = 2\omega_1$) and fourth ($\omega_2 = 3\omega_1$) order resonances. Fig. 1. shows the existence domains of these families for $\delta = 1.0$. For small values of Δh ($h \lesssim 0.005$) in a non-resonant case there exist one family of long-periodic motions Γ_1, Γ_2 or Γ_4 and one family of short-periodic motions Γ_S . In the neighborhood of third-order resonance there exist two families of long-periodic motions Γ_1 and Γ_2 and the family Γ_S . In the neighborhood of fourth-order resonance there exist three families of long-periodic motions Γ_2, Γ_3 and Γ_4 and the family of short-periodic motions Γ_S . B_1 – B_5 are bifurcation points of said families for $h = 0.001, \delta = 1.0$. To the left of the point B_1 there exist two families of periodic motions originating from Hyperboloidal precession – Γ_S and Γ_1 . Family Γ_2 detaches from Γ_1 in point B_1 . In point B_2 family Γ_1 coincides with Γ_S . Between points B_2 and B_3 there exist families Γ_2 and Γ_S . In B_3 families Γ_3 and Γ_4 appear. Γ_2 and Γ_3 coincide with Γ_S in point B_4 . In B_5 family Γ_4 coincides with Γ_S . Fig. 2. shows evolution of a Poincare map near the point B_1 where family Γ_2 detaches from Γ_1 .

This work was carried out at the Moscow Aviation Institute (National Research University) within the framework of the state assignment (project No. 3.3858.2017/4.6)

References

- [1] Markeev A. P. Linear Hamiltonian systems and certain problems of stability of motion of a satellite in relation to its center of mass. — Moscow, Izhevsk: Regular and Chaotic Dynamics, Institute of Computer Research, 2009.
- [2] Sokolskiy A.G., Khovanskiy S.A. Periodic motions close to hyperboloidal precession of a satellite in circular orbit // Cosmic Research. 1979. Vol. 17, no. 2. P. 208–217.
- [3] Sukhov E.A., Bardin B.S. Numerical and analytical construction and stability study of periodic motions of a symmetric satellite // Engineering Journal: Science and Innovation. 2017, no. 11.
- [4] Sukhov E. Analytical and Numerical Computation and Study of Long-periodic motions Originating from Hyperboloidal Precession of a Symmetric Satellite // AIP Conference Proceedings. — 2018. Vol. 1959, no. 040021.
- [5] Sokolskiy A. G., Khovanskiy S. A.. On numerical continuation of periodic motions of a Lagrangian system with two degrees of freedom // Cosmic Research. 1983. Vol. 21, no. 6. P. 851–860.

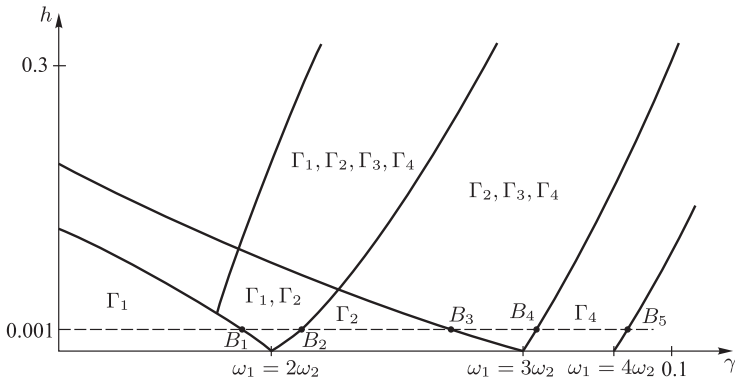


Fig. 1. Existence domains of periodic motions originating from Hyperboloidal precession of a satellite for $\delta = 1.0$. $\Gamma_1, \Gamma_2, \Gamma_3, \Gamma_4$ are families of long-periodic motions, B_1-B_5 are bifurcation points

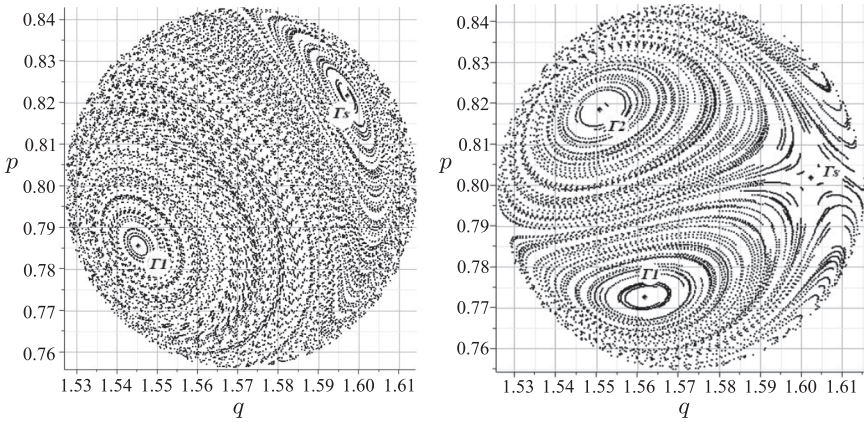


Fig. 2. Poincaré maps computed in the neighborhood of a bifurcation point B_1 . The left map shows motions belonging to Γ_S and Γ_1 before bifurcation where both motions are linear orbital stable. The right map shows motions belonging to Γ_S, Γ_1 and Γ_2 where Γ_S becomes orbital unstable

Modeling and Motion Analysis of a Fluid Actuated Spherical Rolling Robot

Seyed Amir Tafrishi¹, Mikhail Svinin²,
Esmaeil Esmaeilzadeh³, Motoji Yamamoto¹

¹ *Mechanical Engineering Department, Kyushu University, Fukuoka, Japan*

² *College of Information Science and Engineering, Ritsumeikan University, Kusatsu, Japan*

³ *Mechanical Engineering Department, Tabriz University, Tabriz, Iran*

Recently, rolling-based locomotion systems are receiving considerable attention in the literature on robotics [1]. In this paper, we propose and analyze a novel spherical mobile robot (see Fig. 1) based on the mass imbalance driving principle. The design features two spherical masses moving

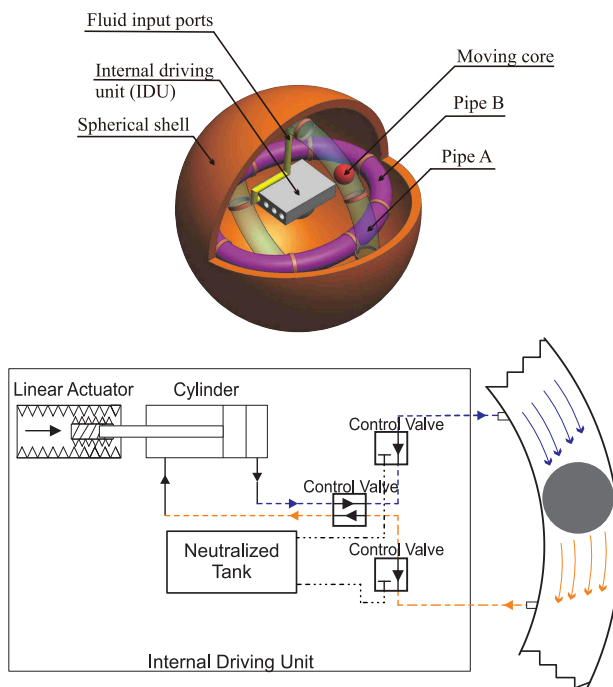


Fig. 1. Fluid-actuated spherical robot (up) and schematic of the driving unit (down)

inside two perpendicular circular pipes, which creates mass imbalance and results in the robot locomotion. The driving force is generated by the internal driving unit (IDU) which circulates the incompressible fluid via a moving pneumatic cylinder that works as a pump actuator to create a continuous flow. The flow is circulated through the circular pipes and neutralized tank via relatively small rectilinear injection pipes. The cylinder provides the flow of the fluid while control valves manipulate the flow direction. The cylinder is connected to a linear actuator for controlling the pressure of the injected fluid.

First, we describe the structure of the robot and derive its nonholonomic dynamics by using the D'Alembert principle. Next, we model the internal driving unit that actuates the driven masses inside the circular pipes. The viscous force (decomposed to the head loss and the drag) and the buoyancy force, acting on the moving masses within the pipe, are also taken into account. The driving force is proportional to the fluid pressure which is obtained by solving algebraic Bernoulli equations together with the states variables of the dynamic model of the linear actuator. The driving unit is studied with respect to three parameters—the input motor torque, the actuator size and the fluid properties—and the design constraints are formulated. The overall model of the robot is then used for analyzing motion patterns of the rolling robot under simulations. The simulation results show the performance and verify the feasibility of the robot actuation system.

References

- [1] Borisov A. V., Mamaev I. S., Karavaev Yu. L. *Mobile robots: robot-wheel and robot-ball*. Izhevsk, RCD Publishers, 2013, 532 p.

Numerical solution of the problem of flow around flexible arcs

Alexey G. Terentyev¹, Nikolay A. Fedorov¹

¹ *Chuvash State University, Cheboksary, Russia*

Because of the great practical importance of the problem of flow around the periodic cascade was considered by many authors (Kochin N.E., Sedov L.I., Stepanov G. Yu., Terentyev A.G., Kuznetsov Yu. V., etc.), and the shape of the profile was considered to be given. The first two authors obtained an exact analytical solution that serves as a benchmark for comparing exact and numerical methods. In contrast to the isolated profile, the flow rates before and after the periodic flow are different ($\nu_1^{-i\alpha_1}$, $\nu_2^{-i\alpha_2}$). If Γ is the circulation around the foil, $le^{i\beta}$ is the period of the cascade, then in accordance with the theorem on the change of momentum one obtains the equality

$$\nu_2 e^{-i\alpha_2} - \nu_1 e^{-i\alpha_1} = \frac{\Gamma}{l} e^{-i\beta}. \quad (1)$$

The vector of the resultant force is

$$X - iY = i\rho \frac{\Gamma}{2} (\nu_1 e^{-i\alpha_1} + \nu_2 e^{-i\alpha_2}). \quad (2)$$

Of the seven parameters that characterize the flow of around through the periodic cascade, only four can be set, for example, $\nu_1^{-i\alpha_1}$ and $le^{i\beta}$, and the flow velocity behind the periodic cascade $\nu_2^{-i\alpha_2}$ and circulation are to be determined. Since the vector of the resulting force of the isolated profile and the profile in the periodic cascade differ both in magnitude and direction, it is therefore necessary to compare their projections to any direction, for example, to the direction of the period $e^{i\beta}$

$$K = \frac{\text{Im}((X - iY) e^{i\beta})}{\text{Im}((X_0 - iY_0) e^{i\beta})} = \frac{\Gamma \text{Im} \left(\frac{\nu_1 e^{-i\alpha_1} + \nu_2 e^{-i\alpha_2}}{2} e^{i\beta} \right)}{\Gamma_0 \text{Im}(\nu_1 e^{-i\alpha_1})}. \quad (3)$$

The dependence is shown in Fig. 1. There's also shows the dependence of the monograph by L. I. Sedov [1]. It can be seen that the curves are very different from each other.

In the case of arcs with fixed edges on the deformable arc, the Dirichlet condition (current function $\psi = \text{const}$) and the Laplace condition must be satisfied

$$\frac{p^- - p^+}{2} = -T \cdot \frac{\partial \theta}{\partial s}, \quad (4)$$

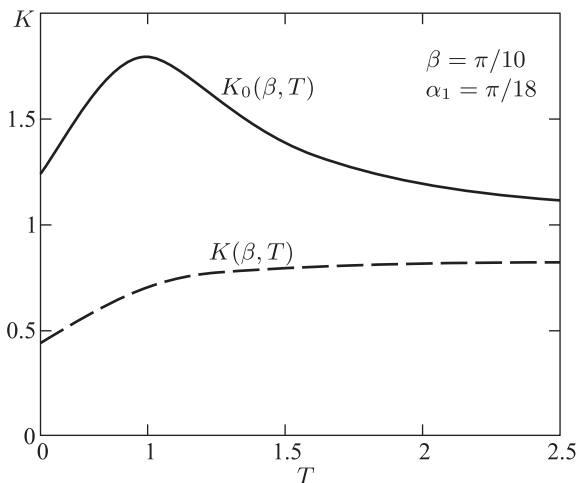


Fig. 1. $K(\beta, T)$ – periodic cascade effect, $K_0(\beta, T)$ – the effect of cascade [1]

where T is the tension, $p^- - p^+$, the pressure difference above and below the curved arc is a curvilinear coordinate, θ – is a tangent angle.

A numerical algorithm for studying the flow through a periodic flow with flexible arcs on the basis of an iterative process is proposed. At each stage, the boundary element method numerically solves the problem of the flow around the arc periodic cascade with a given configuration [2], and then the arc shape is corrected using the condition (1). The process is repeated until the specified accuracy is achieved

$$\frac{\sum_k \left(y_k^{(n)} - y_k^{(n-1)} \right)}{\sum_k y_k^{(n)}} \leq \varepsilon. \quad (5)$$

An analytical solution for the isolated arc in the case of small angles α_1 , α_2 and large tension T is also obtained. In Fig. 2 comparison of numerical results by iterative method and analytical formulas is shown.

A detailed numerical analysis of the cascades of arbitrary foils including soft arcs is given. It is shown that flexible blades allow obtaining sufficiently high hydrodynamic characteristics

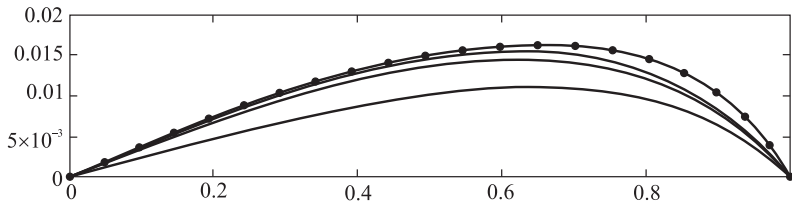


Fig. 2. —●— analytical formulas is shown, ——— iterative method

References

- [1] Sedov L.I., Two-Dimensional Problems of Hydrodynamics and Aerodynamics, Nauka, Moscow (1966).
- [2] Terentiev A. G., Kirschner I.N., Uhlman J. S. The Hydrodynamics of Cavitating Flows. Backbone Publishing Company, USA, 2011, 598S.

AI Driving Olympics challenge: reinforcement learning approach solving line following task

Stepan S. Troeshestov^{1,3}, Vladimir A. Aliev¹,
Anton E. Mashikhin¹, Sergey I. Nikolenko^{1,2}

¹ Samsung AI Center, Moscow, Russia

² Neuromation OU, Tallinn, Estonia

³ Chuvash State University, Cheboksary, Russia

Abstract: We are a team from Samsung AI Center Moscow and we participated in AI Driving Olympics Challenge. The problem was to learn how to control the car called *Duckiebot* on a simple track. It was encouraged by organizers to do this with Reinforcement Learning approach.

Tracks and scoring: To train our agent we used the simulator provided by the organizers. To avoid overfitting our agent to a specific track, we created own one, complicated, with different objects, intersections, and turns. Scoring consists of the following things:

- How many track tiles the *Duckiebot* drove (maximum episode length is 16.6 secs)
- How much time passed before the *Duckiebot* drove off the road
- How far the *Duckiebot* drove from the center of its lane
- Penalty for driving in the wrong lane

The default reward in the simulator was a linear combination of all 4 parts.

Our approaches: At the very beginning, we decided to try the state-of-the-art reinforcement learning algorithms from scratch. The default input for the task was a picture from the simulator. We took 3 consecutive pictures, grayscaled them and fed into CNN as different channels. The default output was continuous actions: velocity and steering. Technically, there are 2 wheels (left and right) on the *Duckiebot* and it was possible to control them separately from -1 to 1. We tried 4 algorithms that can provide continuous actions:

- Soft Actor-Critic (SAC)
- Deep Deterministic Policy Gradient (DDPG)
- Twin Delayed Deep Deterministic Policy Gradient (TD3)
- Proximal Policy Optimization (PPO)

but they all worked much worse than we expected.

Actions: The main problem with continuous actions was poor local minimas. Without any modifications, the agent learns to stay still. Disappointed with continuous actions, we tried to train the algorithm on discrete ones. We chose 5 discrete actions: full forward, forward-left, forward-right, turn left without moving forward, turn right without moving forward. We removed driving backward because we didn't need it at all. As RL algorithms that can provide discrete actions, we tried different Deep Q-networks (DQN). After some reward engineering, we choose Rainbow DQN and made it to the 5th place.

Controller: We decided to make a manual proportional controller and train RL agent with it. Our controller was pretty simple. We compute the current step destination point and the angle between where we need to go and where the *Duckiebot* looks now. Then we give the command to motors based on this angle.

Final solution: As a result, the controller only needs one angle to calculate the action. We decided to use noisy controllers as an exploration strategy. So, we had workers-controllers who drove in the simulator and put their experience in the replay buffer. TD3 optimizer sampled from this buffer and made a gradient update. The resulting T3 agent also drove in the simulator and put his own experience in the replay buffer. Initially, the replay buffer was 90 percent of the controller-workers and 10 percent of the RL agents, but over time the number of the agents increased until it became 100 percent.

Artificial neural networks for creation of energetic materials genome

Daria A. Troeshestova¹, Victor S. Abrukov¹, Michael V. Kiselev¹,
Nichith Chandrasekaran²

¹ *Chuvash State University, Cheboksary, Russia*

² *Indian Institute of Science, Bangalore, India*

The results of usage of data science methods, in particular artificial neural networks, for the creation of new multifactor computational models of the energetic materials (EM) combustion that solve the direct and inverse tasks are presented. The analytical platform Loginom was used for the models creation. The models of combustion of double based EM with such nano additives as metals, metal oxides, metal salts, metal composite materials, organic metallic compounds, termites and carbon nano materials were created by means of experimental data published in scientific literature. The goal function of the models were burning rate (direct tasks) as well as propellants composition (inverse tasks). The basis (script) of a creation of Data Warehouse of EM combustion was developed. The Data Warehouse can be supplemented by new data in automated mode and serve as a basis for creating generalized combustion models of EM and thus the beginning of work in a new direction of combustion science, which the authors propose to call “Advanced Energetic Materials Genome” (by analogy with a very famous Materials Genome Initiative, USA). The usage of such modern methods of Data Science as deep learning neural networks, multiple adaptive regression splines, modern decision trees, etc could make the possibilities of multifactor modelling of EM combustion most wide. “Advanced Energetic Materials Genome” opens new possibilities for accelerate the advanced energetic materials development.

Illustrations of our previous work deal with this abstract are presented on the Web-site: <http://www.wcrc.ru/Indo-Russian-JRP.html>. Also it has an example of autonomous computer module of a multifactor computational model of the EM combustion. Anyone can download the module and execute research on their own and obtain all graphs which depict relationship between variables of the object.

We are ready to help to any researcher to create a multifactor computational model of his own experiment. If you have a data base (a table) of experimental measurements we will be able to create yours multifactor computational model.

This work is jointly supported and funded by the Department of Science and Technology (DST), India and the Russian Foundation for Basic Research (RFBR), Russia (Research Project No. 16-53-48010) under the DST-RFBR inter-disciplinary scientific cooperation programme under Grant INT/RUS/RFBR/IDIR/P-3/2016.

Integrable systems with algebraic first integrals

Andrey V. Tsiganov

Saint Petersburg State University, Saint Petersburg, Russia

According to Abel's theorem set of points moving along a plane curve can be subjected to a finite number of algebraic constraints in such a way that a sum of the corresponding indefinite algebraic integrals can be expressed in terms of elementary functions of the coordinates of the moving points.

In 1863 Clebsch proposed geometric approach to construction of algebraic constraints, closely interwoven with the intersection theory, which was continued by Brill and Noether in 1857 and formalized by Poincaré in 1901 and Severy in 1914. According to this interpretation algebraic constraints are coordinates of the fixed points on the curve and, therefore, system of Abel's differential equations is described a motion of the k points around m fixed points on the plane curve.

In classical mechanics movable points describe evolution of dynamical system in term of variables of separation, whereas coordinates of the fixed points play the role algebraic integrals of motion or parameters of discretization. In this talk we discuss some examples of such algebraic integrals and the corresponding closed algebraic trajectories for dynamical systems on the plane, n -dimensional sphere, etc.

Viscous fluid burning particles

Olga V. Vasilyeva¹, Sergey I. Ksenofontov², Alexander N. Lepaev³

¹ *Chuvash State University, Cheboksary, Russia*

² *Chuvash State Pedagogical University named after I. Ya. Yakovlev*

³ *Cheboksary Institute (branch) of the Moscow Polytechnic University, Cheboksary, Russia*

Particles of light metals in a flame of the condensed systems burn in the vapor-phase mode, forming spherical bright is ardent, exceeding diameter 2–3 times in size of the burning particle. The flame around the particles has brightness irregularities. The burning particle is surrounded only by a spherical halo, while the contours of the actively burning particle through the flame are not visible. Between a surface of the condensed particle and a flame there is a space where concentration of disperse particles is minimum or equal to zero.

The temperature distribution of the burning particle was determined by photopyrometry. Temperature of a flame exceeds temperature of a surface of the particle. Combustion products are condensed from the vapor phase and form a cloud of daughter particles. The maximum concentration of these particles in the spherical layer reaches 10^9 cm^{-3} .

the speed of the particle can be determined when the particle moves in the flow of combustion products or when it burns out outside the main flow. The speed of the particle soaring is small, because the interaction of the particle with the environment occurs on the outer surface of the flame with an effective viscosity that is commensurate with the viscosity of the liquid. A trail is formed behind the moving particle, populated by the daughter particles carried away from the flame. The concentration of particles in the wake is constant. It was determined in a dynamic mode, both in terms of absorption and scattering of light by daughter particles. The boundary layer between the spherical flame and the environment is a two-phase flow with a decreasing concentration of daughter particles according to the quadratic law.

The dynamics of rigid bodies with internal mechanisms

Evgeny V. Vetchanin¹, Evgenia A. Mikishanina²

¹ *Udmurt State University, Izhevsk, Russia*

² *Chuvash State University, Cheboksary, Russia*

This paper is concerned with studying the dynamics of rigid bodies controlled by internal mechanisms and under the action of external periodic forces. One of the systems considers

Данная работа посвящена исследованию динамики твердых тел, управляемых внутренними механизмами и подверженных влиянию внешних периодических сил. Одна из рассмотренных систем описывает вращение вокруг неподвижной точки твердого тела с переменными моментами инерции и колеблющимися роторами. Уравнения движения такой системы могут быть записаны в следующей форме:

$$\dot{\mathbf{M}} = \mathbf{M} \times \boldsymbol{\omega}, \quad (1)$$

где $\mathbf{M} = \mathbf{I}(t)\boldsymbol{\omega} + \mathbf{k}(t)$ — момент импульса системы, $\boldsymbol{\omega}$ — вектор угловой скорости тела, $\mathbf{I}(t) = \text{diag}(I_1, I_2, I_3)$ — тензор инерции тела, $\mathbf{k}(t) = (k_1, k_2, k_3)^T \sin \Omega t$ — гиостатический момент, создаваемый роторами. Уравнения (1) допускают первый интеграл:

$$F = \mathbf{M}^2 = \text{const}. \quad (2)$$

Для системы (1) компоненты тензора инерции задавались следующим образом:

$$I_k = i_k + \sum_{n \neq k} (j_n + \Delta j_n \sin \Omega t).$$

Известно, что рассматриваемая система может демонстрировать хаотическое поведение [1]. Для компьютерного анализа динамики системы (1) на фиксированном уровне интеграла (2) была выполнена следующая замена переменных:

$$M_1 = F_0 \cos \varphi \sqrt{1 - z^2}, \quad M_2 = F_0 \sin \varphi \sqrt{1 - z^2}, \quad M_3 = F_0 z. \quad (3)$$

Отображения за период для рассматриваемой системы приведены на рис. 1.

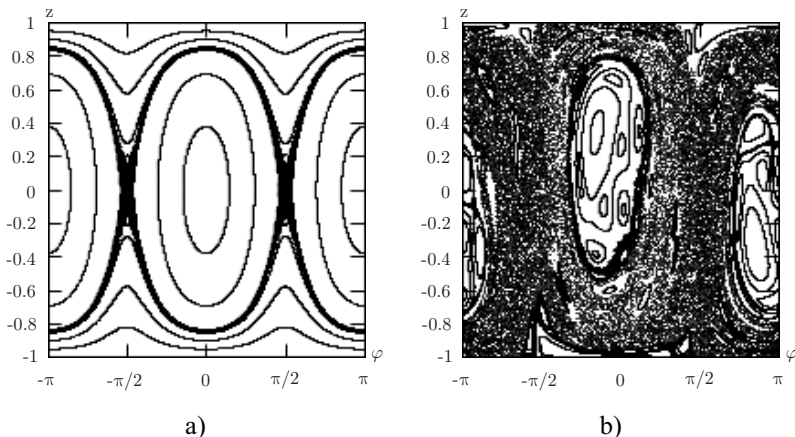


Рис. 1. Отображения за период для системы. а) $i_1 = 2, i_2 = 3, i_3 = 4, j_1 = j_2 = j_3 = 0, \Delta j_1 = 0.6, \Delta j_2 = 0.2, \Delta j_3 = 0.3, k_1 = k_2 = k_3 = 0, \Omega = 3, F_0 = 10$. б) $i_1 = 2, i_2 = 6, i_3 = 7, j_1 = j_2 = j_3 = 0, \Delta j_1 = 0.6, \Delta j_2 = 0.2, \Delta j_3 = 0.3, k_1 = 0.2, k_2 = 0.6, k_3 = 1, \Omega = 1, F_0 = 3$

В работе [2] было показано, что в системах подобных (1) при добавлении диссипации и накачки энергии могут быть возникать различные странные аттракторы, обнаруженные в системах Lorenz, Rössler, Newton-Leipnik, Sprott. В рамках данной работы, нами была рассмотрена система с параметрическим возбуждением, подобная (1) и описанная в работе [2]:

$$\begin{aligned} \dot{x} &= \frac{-\sigma(x-y)}{1-\varepsilon \sin \Omega t}, & \dot{y} &= \frac{rx-y-(1-3\varepsilon \sin \Omega t)xy}{1+\varepsilon \sin \Omega t}, \\ \dot{z} &= \frac{(1-3\varepsilon \sin \Omega t)xy-bz}{1+\varepsilon \sin \Omega t}. \end{aligned} \quad (4)$$

При $\sigma = 10, r = 28, b = 8/3$ и $\varepsilon = 0$ уравнения (4) переходят в известную систему Лоренца. При построении отображения через период для системы (4) обнаруживаются неподвижные точки и странные аттракторы. Одним из механизмов возникновения аттракторов в системе (4) является каскад бифуркаций удвоения периода. Фрагмент однопараметрической бифуркационной диаграммы для неподвижной точки () периода 2 показан на рис. 2.

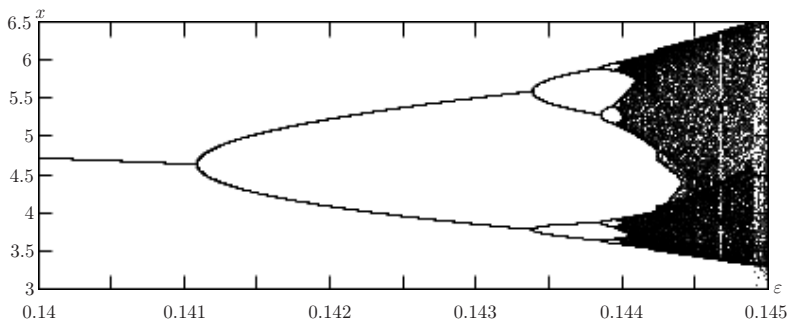


Рис. 2. Фрагмент однопараметрической бифуркационной диаграммы для системы (4) при значениях параметров $\sigma = 10$, $r = 28$, $b = 8/3$, $\Omega = 13$.

Список литературы

- [1] Borisov A. V. *On the Liouville Problem* // Numerical Modelling in the Problems of Mechanics, Moscow: Izd. Mosk. Uiver., 1991, pp. 110–118
- [2] Doroshin A. V. *Modeling of chaotic motion of gyrostats in resistant environment on the base of dynamical systems with strange attractors* // Commun Nonlinear Sci Numer Simulat, 2011, vol. 16, pp. 3188–3202.

An approach moving over obstacles for a wheeled jumping robot

Lyudmila Yu. Vorochaeva¹, Sergei I. Savin², Andrey V. Malchikov¹

¹ Southwest State University, Kursk, Russian Federation

² Innopolis University, Innopolis, Russian Federation

The advantage of jumping robots compared to other classes of robotic devices is their high maneuverability when moving over the rough terrain, as well as the ability to overcome various obstacles (fences, stairways) [1–3]. This paper focuses on the task of overcoming a staircase with n steps by a jumping robot described in [4] (Fig. 1).

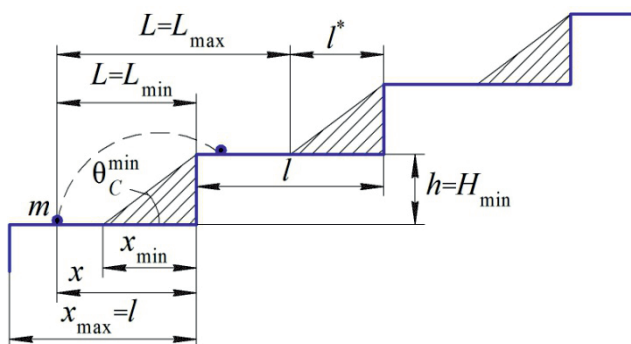


Fig. 1. Diagram of overcoming a staircase span by a jumping robot

Let the length and the height of each step be equal to l and h correspondingly. We will consider the robot a material point of mass m , which, to perform the jump, gains the speed v_C , that is the speed of separation of the device from the surface, the velocity vector direction relative to the horizon is given by angle θ_C . Before jumping, the robot is located at a distance x from the step

$$x \in [l^*, l], \quad (1)$$

where $l^* = h \operatorname{ctg}(\theta_C^{\min})$ defines the distance within which the robot should not be located on the step due to the impossibility of making a jump from there while being limited by the height h of the step and the minimum angle of inclination of the velocity of separation θ_C^{\min} . The characteristics of

the robot's jump will include its length L and height H , calculated by the formulas:

$$L = v_C^2 \sin 2\theta_C / g, \quad L \in [x + (n - 1)l, x + nl - l^*], \quad (2)$$

$$H = v_C^2 \sin^2 \theta_C / 2g, \quad H \in [nh, H_{\max}], \quad (3)$$

where g stands for the free fall acceleration, and the distance H_{\max} is limited by the height of the staircase ceiling. Overcoming the flight of stairs can be implemented using a different number of jumps p from 1 to the amount equaling the number of steps:

$$p \in [p_{\min}, p_{\max}], \quad p_{\min} = 1, \quad p_{\max} = n, \quad (4)$$

The number of steps, herewith, overleaped in one jump:

$$N \in [N_{\min}, N_{\max}], \quad N_{\min} = 1 \text{ at } p_{\max}, \quad N_{\max} = n \text{ at } p_{\min}. \quad (5)$$

The distribution of surmountable steps over jumps can be described as follows:

$$N_1 = (a_{\min} + (k - 1)), \quad k \in [1, k_1^*],$$

...

$$N_p = (a_{\min} + (k - 1)) \quad k \in [N_{p-1}, k_p^*] \text{ with } N_{p-1} \in [N_{(p-1)\min}, N_{(p-1)\max}],$$

...

$$N_{p_{\max}} = n - \sum N_1 \dots N_{p_{\max}-1} \text{ with } N_{p_{\max}} \geq N_{p_{\max}-1}, \quad (6)$$

where $a_{\min} = 1$ denotes the minimum number of steps to be surmounted,

$$k_1^* = \begin{cases} \min(N_{p_{\max}}), & \sum n_1 \dots n_{p_{\max}} \bmod (p_{\max}) = 0, \\ \min(N_{p_{\max}} - 1), & \sum n_1 \dots n_{p_{\max}} \bmod (p_{\max}) \neq 0, \end{cases} \quad (7)$$

$$k_p^* = \begin{cases} \min(N_{p_{\max}}), & \sum n_p \dots n_{p_{\max}} \bmod (p_{\max} - p + 1) = 0, \\ \min(N_{p_{\max}} - 1), & \sum n_p \dots n_{p_{\max}} \bmod (p_{\max} - p + 1) \neq 0, \end{cases} \quad (8)$$

$\min(N_{p_{\max}})$ – the smallest number of steps to be overcome during the last jump. According to the given formula, the number N_1 of the steps jumped over the first leap can vary from 1 to $\min(N_{p_{\max}})$ or $\min(N_{p_{\max}} - 1)$ depending on the fulfillment of the specified condition. The number

N_p of the overleaped in jump p steps can vary from 1 to $\min(N_{p_{\max}})$ or $\min(N_{p_{\max}} - 1)$ at each value N_{p-1} of the steps overleaped in the previous jump. The number $\min(N_{p_{\max}})$ of the steps jumped over in the last jump is always represented as the difference between the number of steps in a flight of stairs and the number of steps already overleaped in previous jumps. And this number cannot be less than the steps jumped over in the previous jump. While determining the optimal way of overcoming the staircase span, the problem of minimizing kinetic energy W of the robot at the moment of separation from the surface can be solved:

$$\min(W) = \min(mv_C^2/2). \quad (9)$$

The concepts and formulas of jumps performed on the steps of the staircase span introduced here will be further made use of to develop an optimal way of overcoming it.

The work was carried out within the RFBR project No. 18-31-00075.

References

- [1] Wehner M. et al. Pneumatic energy sources for autonomous and wearable soft robotics // Soft robotics, 2014, vol. 1, no. 4, pp. 263–274.
- [2] Ackerman E. Boston dynamics sand flea robot demonstrates astonishing jumping skills // IEEE Spectrum Robotics Blog, 2012, vol. 2(1).
- [3] Zhang J., Yang X., Song G., Zhang Y., Fei S., Song A. Structural-parameter-based jumping-height-and-distance adjustment and obstacle sensing of a bio-inspired jumping robot // Intern. J. of Advanced Robotic Systems, 2015, vol. 12, no. 6, pp. 1–14.
- [4] Vorochaeva L., Savin S. Study of the acceleration modes of a jumping robot for two cases of realisation // Dynamics of Systems, Mechanisms and Machines (Dynamics): Proc. IEEE Conf., Omsk, Russia, 2018, pp. 1–6.

until the equality $\varphi = \varphi^{01}$ is true, where φ^{01} — indicates some given value of the rotation angle of the robot link, corresponding to the completion of the first stage. After this, the second stage of the movement begins, point O_2 is fixed on the surface, the drive installed in it generates the torque M . The stage will be terminated when the condition $\varphi = -\varphi^{02}$ is satisfied, where the angle value φ^{02} corresponds to the completion of the second stage. Then the stages are repeated. It should be noted that the values φ^{01} and φ^{02} are determined by the robot control system based on the trajectory along which the object must move, for example, when $\varphi^{01} = \varphi^{02}$ the movement will occur in a straight line, at $\varphi^{01} > \varphi^{02}$ — counterclockwise rotation, at $\varphi^{01} < \varphi^{02}$ — clockwise rotation. More explicitly the gait of the robot is illustrated in Table 1. The differential equation of motion of the robot during each of the stages is written as:

$$J\ddot{\varphi} = M - F_{fr}l, \tag{1}$$

where J — stands for the moment of inertia relative to the fixed support point.

Table 2. Description of the crawling robot gait

	Motion O_1	Motion O_2	f_{O_1}	f_{O_2}	Termination condition
stage 1	—	+	f_{\max}	f_{\min}	$\varphi = \varphi^{01}$
stage 2	+	—	f_{\min}	f_{\max}	$\varphi = -\varphi^{02}$

Simulation of motion of the robot allows for the identification of the impact on the characteristics of movement of mass-dimensional (the length and the mass of the link) and control parameters (the value of the control torques and their change laws), as well as the parameters of the supporting surface (friction coefficient value f_{\min} , friction force model). As an example of the simulation results, Fig. 2 represents the range of values of the coefficient f_{\min} , under which the movement of the robot is possible (area 1) and under which the object is stationary (area 2) depending on the torque M , generated by the drive, for three values of the link mass. The model for this simulation was described using dimensionless parameters.

The graphs show that as the value of M increases, the maximum permissible value of the friction coefficient f_{\min} increases, under which the robot will move along the surface. Moreover, the dependence $f_{\min}(M)$ is linear, the coefficient of inclination of the straight line to the axis of the torques decreases with the increasing mass of the link. These dependencies can be

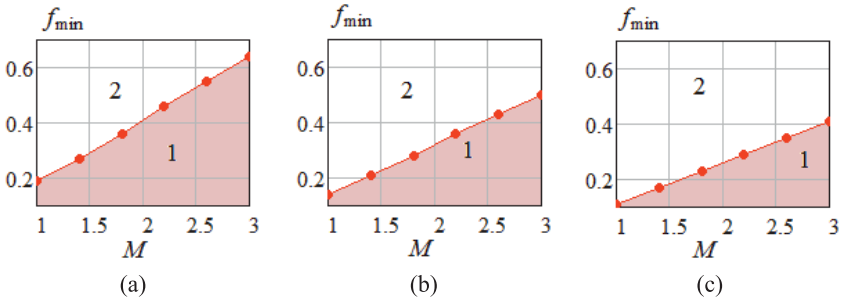


Fig. 2. Diagrams of the areas of $f_{\min}(M)$: a) $m = 0.8$, b) $m = 1$, c) $m = 1.2$, 1 – the range of values when the movement of the robot is possible, 2 – the range of values under which the robot is stationary

made use of in the development of laws for controlling the drives of the device, as well as when selecting materials for support elements.

The work under consideration was carried out within the framework of the Presidential Grant, application number MK-200.2019.1.

References

- [1] Conkur E.S., Gurbuz R. Path Planning Algorithm For Snake-Like Robots // Information Technology and Control, 2008, vol. 37, no. 2, pp. 159–162.
- [2] Lounis D., Spinello D., Gueaieb W., Sarfraz H. Planar kinematics analysis of a snake-like robot // Robotica, 2014, vol. 32, no. 5, pp. 659–675.
- [3] Jatsun S., Vorochaeva L., Yatsun A., Savin S. and Malchikov A. Bio-inspired adaptive control strategy for a snake-like robot // 19th IEEE Intern. Conf. IC-STCC, 2015, pp. 273–278.
- [4] Zhao X., Dou L., Su Z., Liu N. Study of the Navigation Method for a Snake Robot Based on the Kinematics Model with MEMS IMU // Sensors, 2018, vol. 18, no. 3, pp. 879–901.
- [5] Vorochaeva L. Yu., Yatsun A. S., Yatsun S.F. Simulation of the motion of a five-link crawling robot with controlled friction on a surface having obstacles // J. of Computer and Systems Sciences International, 2017, vol. 56, no. 3, pp. 527–552.

Jordan–Kronecker invariants of semidirect sums of Lie algebras

Konstantin S. Vorushilov

Lomonosov Moscow State University, Moscow, Russia

Hamiltonian systems defined by Euler equations on Lie algebras arise in various problems in mathematical physics. In 1978, A. S. Mischenko and A. T. Fomenko presented a so-called argument shift method [2]. This method can be used to construct a family of polynomial functions in involution with respect to a Lie-Poisson bracket on a Lie algebra; these functions are exactly the integrals of such Hamiltonian system. It turns out that these functions commute with respect to another Poisson bracket on a Lie algebra. It is natural to ask whether there exists a complete family of polynomials in involution with respect to both Poisson brackets.

Jordan–Kronecker invariants of a Lie algebra were first introduced by A. V. Bolsinov and P. Zhang in [1]. By definition, these invariants describe the canonical block-diagonal decomposition of a pair of skew-symmetric forms defined by the generic pair of elements of dual Lie algebra with blocks of Jordan and Kronecker types. A pair of skew-symmetric forms corresponds to a pair of Poisson brackets mentioned earlier. It was proved by Bolsinov that the completeness of commutative family of shifts for a Lie algebra is equivalent to the fact that this Lie algebra is of Kronecker type, i.e. the canonical decomposition of two forms contains only Kronecker blocks.

For some types of Lie algebras (for example, for semisimple and low-dimensional Lie algebras), Jordan–Kronecker invariants are known, but for many interesting cases of Lie algebras this question is open.

The talk will cover the recent developments in this area of research. In particular, the methods of calculation of Jordan–Kronecker invariants of semidirect sums of Lie algebras with a commutative ideal will be discussed.

This work was supported by the Russian Science Foundation (project No.17-11-01303).

References

- [1] Bolsinov A. V., Zhang P. *Jordan–Kronecker invariants of finite-dimensional Lie algebras*, *Transform. Groups* **21** (1), 51–86 (2016).
- [2] Mischenko A. S., Fomenko A. T. *Euler equations on finite-dimensional Lie groups*, *Math. USSR Izv.* **12** (2), 371–389 (1978).
- [3] Vorushilov K. *Jordan–Kronecker invariants for semidirect sums defined by standard representation of orthogonal or symplectic Lie algebras*, *Lobachevskii Journal of Mathematics.* **38** (6), 1121–1130 (2017).

On Chaplygin's case of the body in a liquid

Hamad M. Yehia

*Mathematics Department, Faculty of Science,
Mansoura University, Mansoura, Egypt*

Chaplygin discovered this case in 1903 and gave full separation of variables. It was recently studied by several authors, who studied the topology of the iso-energy surfaces, bifurcation diagrams and topological classification of the Liouville tori in its phase space. We give explicit formulas for the Euler-Poisson variables in terms of Jacobian elliptic functions of time and also simulations of different types of trajectories of the vertical apex on the Poisson sphere.

ANS Conference Series

Scientific Heritage of Sergey A. Chaplygin

Nonholonomic Mechanics, Vortex Structures and Hydrodynamics

Book of Abstracts